Positional Effects of Hydroxy Groups on Catalytic Activity of Proton-Responsive Half-Sandwich Cp*Iridium(III) Complexes

Yuki Suna,[†] *Mehmed Z. Ertem*,[‡] *Wan-Hui Wang*,[†,§,#] *Hide Kambayashi*,[†] *Yuichi Manaka*,[†] *James T. Muckerman*,[‡] *Etsuko Fujita*,[‡,*] *and Yuichiro Himeda*[†,§,*]

[†]National Institute of Advanced Industrial Science and Technology, Tsukuba Central 5, 1-1-1 Higashi, Tsukuba, Ibaraki, 305-8565, Japan

[§]Japan Science and Technology Agency, ACT-C, 4-1-8 Honcho, Kawaguchi, Saitama, 332-0012 Japan

[‡] Chemistry Department, Brookhaven National Laboratory, Upton, New York 11973, United States

[#] Current address of W.-H. Wang: School of Petroleum and Chemical Engineering, Dalian University of Technology, Panjin 124221, China

ABSTRACT: Proton-responsive half-sandwich Cp*Ir(III) complexes possessing a bipyridine ligand with two hydroxy groups at the 3,3′-, 4,4′-, 5,5′- or 6,6′-positions (**3DHBP**, **4DHBP**,

5DHBP, or **6DHBP**) were systematically investigated. UV-vis titration data provided average pK_a values of the hydroxy groups on the ligands. Both hydroxy groups were found to deprotonate in the pH 4.6–5.6 range for the **4–6DHBP** complexes. One of the hydroxy groups of the **3DHBP** complex exhibited the low pK_a value of < 0.4 because the deprotonation is facilitated by the strong intramolecular hydrogen bond formed between the generated oxyanion and the remaining hydroxy group, which in turn leads to an elevated pK_a value of ~13.6 for the second deprotonation step. The crystal structures of the **4–** and **6DHBP** complexes obtained from basic aqueous solutions revealed their deprotonated forms. The intramolecular hydrogen bond in the **3DHBP** complex was also observed in the crystal structures. The catalytic activities of these complexes in aqueous phase reactions, at appropriate pH, for hydrogenation of carbon dioxide (pH 8.5), dehydrogenation of formic acid (pH 1.8), transfer hydrogenation reactions using formic acid/formate as a hydrogen source (pH 7.2 and 2.6) were investigated to compare the positional effects of the hydroxy groups. The **4–** and **6DHBP** complexes exhibited remarkably enhanced catalytic activities under basic conditions because of the resonance effect of the strong electron-donating oxyanions, whereas the **5DHBP** complex exhibited negligible activity despite the presence of electron-donating groups. The **3DHBP** complex exhibited relatively high catalytic activity at low pH owing to the one strong electron-donating oxyanion group stabilized by the intramolecular hydrogen bond. DFT calculations were employed to study the mechanism of CO_2 hydrogenation by the **4DHBP** and **6DHBP** complexes, and comparison of the activation free energies of the H_2 heterolysis and CO_2 insertion steps indicated that H_2 heterolysis is the rate-determining step for both complexes. The presence of a pendent base in the **6DHBP** complex was found to facilitate the rate-determining step, and renders **6DHBP** a more effective catalyst for formate production.

INTRODUCTION

The functionalization of ligands is one of the crucial issues for the development of organometallic catalysts[1] because the intrinsic features of the complexes (e.g., electronic properties, steric effects, solubility, etc.) are strongly influenced by the nature of the ligands. Recently, ligands that can tune the properties and function, such as catalytic activity, chemoselectivity and solubility of a transition-metal based catalyst by responding to extrinsic stimuli have received considerable attention because they enable the control of a catalytic process through manipulation of such external factors as pH, light or applied potential.[2-3] In particular, ligands with protic groups, such as hydroxy, amino or carboxylic acid moieties with acid/base equilibria, are classified as "proton-responsive ligands," which are expected to play important roles through second coordination sphere interactions that can facilitate a catalytic process.[4-16] For instance, Hashiguchi et al. reported enhanced C–H activation by a ruthenium (Ru) complex with a protic polydentate ligand in aqueous KOH solution, and proposed that the deprotonated ligand increased the ligand lability and the π-nucleophilicity of the Ru catalyst.[17]

A hydroxy group reversibly deprotonates under basic conditions to generate an oxyanion group (O^-) which is a Lewis base with stronger electron-donating ability than that of its conjugate acid. The deprotonation of hydroxy groups can also cause significant changes in the electronic properties and water solubility of the complex[5, 8-9, 11-13] We have focused on a proton-responsive ligand with hydroxy groups, and developed half-sandwich Cp*Ir (Cp* = C_5Me_5) catalysts possessing a proton-responsive 4,4′-dihydroxy-2,2′-bipyridine (**4DHBP**) ligand (Scheme 1) to employ in aqueous phase reactions. The electron-donating abilities of the hydroxy

and oxyanion groups were found to increase the catalytic activity of CO_2 hydrogenation compared to that with a pristine 2,2′-bipyridine (bpy) ligand.[18-19] Also the acid/base equilibria of the hydroxy groups considerably changed the solubility, electronic nature and catalytic activity of the Ir complexes depending on the pH of the solution,[20-22] as observed for the hydrogenation of CO_2,[10-12, 15, 18-19] dehydrogenation of formic acid (HCO_2H)[20, 23-24] and transfer hydrogenation (TH)[21] of various substrates. Furthermore, we have achieved the recycling of a catalyst complex from the reaction mixture using the pH-dependent differential solubility as the controlling factor for the complexes with 4,7-dihydroxy-1,10-phenanthroline.[25] This is another example of the control of the catalytic activity and direction of a reaction that has been achieved by adjusting reaction solutions to the optimum pH.[20-22]

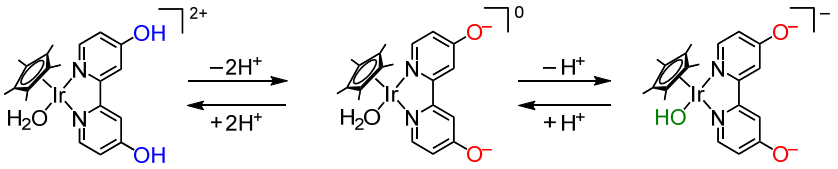

Scheme 1. Acid/base equilibria of the $[Cp^*Ir(\mathbf{4DHBP})(OH_2)]^{2+}$ complex.

To improve the catalytic activity in the CO_2 hydrogenation reaction, we modified the Ir catalyst by changing the position of the hydroxy groups from 4,4′- to 6,6′- positions to mimic the active site of the hydrogenases. A [Fe-Fe]H_2ase has a Lewis base near its metal center, which facilitates the heterolysis of an H_2 molecule.[26-28] Therefore, a Lewis basic oxyanion group adjacent to the metal center was expected to act as a pendent base[26, 29-37] under the basic conditions for CO_2 hydrogenation. The **6DHBP** complex created by the bio-inspired catalytic design achieved an initial TOF that was four times as high as that of the **4DHBP** complex.[38-39]

Our combined experimental and computational analysis demonstrated that a solvent water molecule mediated facile H_2 heterolysis (Scheme 2).[38]

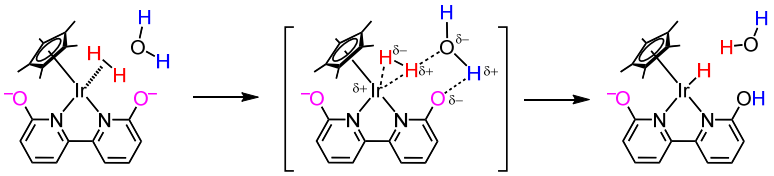

Scheme 2. Proposed mechanism for H_2 heterolysis assisted by a pendent base and proton relay through a water molecule with [Cp*Ir(**6DHBP-2H**$^+$)] (where **6DHBP-2H**$^+$ indicates the doubly deprotonated **6DHBP**).

As mentioned above, we have revealed the positional effects of the hydroxy groups focusing on 4,4′- and 6,6′-positions in the hydrogenation of CO_2. However, the only report on the complex with hydroxy groups at 3,3′-positions was about its low catalytic activity in the hydrogenation of CO_2.[18] As for the complex with hydroxy groups at 5,5′-positions, there has been no report. In this work, we synthesized Ir complexes possessing Cp* and **DHBP** ligands with two hydroxy groups introduced at the 3,3′-, 4,4′-, 5,5′- or 6,6′-positions (see Chart 1), and characterized them spectroscopically and crystallographically as well as with DFT calculations. Furthermore, we have investigated the effects of the hydroxy group positions on the catalytic activity in the aqueous phase for hydrogenation of CO_2 (pH 8.5), dehydrogenation of HCO_2H (pH 1.8) and transfer hydrogenation reactions using HCO_2H/HCO_2^- as a hydrogen source (pH 7.2 and 2.6). We also employed density functional theory (DFT) calculations to gain further insight into the positional effect of hydroxyl groups on the mechanism of hydrogenation of CO_2 by **4DHBP** and **6DHBP** complexes.

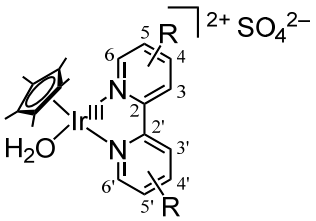

[Cp*Ir(L)(OH$_2$)]SO$_4$

L = **bpy** (R = H)
3DHBP (R = 3,3'-(OH)$_2$)
4DHBP (R = 4,4'-(OH)$_2$)
5DHBP (R = 5,5'-(OH)$_2$)
6DHBP (R = 6,6'-(OH)$_2$)

Chart 1. Structures of Ir complexes.

EXPERIMENTAL SECTION

2,2′-Bipyridine (bpy), 3,3′-dihydroxy-2,2′-bipyridine (**3DHBP**) were purchased from Sigma-Aldrich and 4,4′-dihydroxy-2,2′-bipyridine (**4DHBP**) was purchased from Carbosynth. They were used without further purification. 5,5′-dihydroxy-2,2′-bipyridine (**5DHBP**)[40] and 6,6′-dihydroxy-2,2′-bipyridine (**6DHBP**)[41] were synthesized according to the literature procedures. [Cp*Ir(**4DHBP**)(OH$_2$)]SO$_4$[21] and [Cp*Ir(**6DHBP**)(OH$_2$)]SO$_4$[39] were prepared according to the literature procedure. All the complexes were characterized by NMR spectroscopy, ESI-MS and elemental analysis.

Synthesis of [Cp*Ir(bpy)(OH$_2$)]SO$_4$: A mixture of 2,2′-bipyridine (78 mg, 0.50 mmol), [Cp*Ir(OH$_2$)$_3$]SO$_4$ (268 mg, 0.50 mmol) and water (10 mL) was stirred at room temperature for 18 hours under an argon atmosphere. The resulting solution was filtered to remove any insoluble part, and then the filtrate was evaporated to give a yellow solid quantitatively. ^{1}H NMR (400 MHz, D$_2$O, δ) 9.14 (d, J = 5.4 Hz, 2H, Ar H), 8.56 (d, J = 8.1 Hz, 2H, Ar H), 8.35 (td, J = 7.9, 1.4 Hz, 2H, Ar H), 7.91 (ddd, J = 7.4, 5.6, 1.4 Hz, 2H, Ar H), 1.68 (s, 15H, Cp*). ESI-MS (m/z): [M – SO$_4$ – H$_2$O]$_2^+$ calcd for $C_{20}H_{23}IrN_{22}^+$, 242.08; found, 242.1. [M – SO$_4$ – H$_2$O – H]$^+$ calcd

for $C_{20}H_{22}IrN_2^+$, 483.14; found, 483.1. Anal Calcd for $C_{20}H_{25}IrN_2O_5S+4H_2O$: C, 35.87; H, 4.97, N; 4.18. Found: C; 35.78, H; 4.64, N; 3.84. All values are given as percentage.

Synthesis of [Cp*Ir(3DHBP)(OH$_2$)]SO$_4$: A mixture of 3,3′-dihydroxy-2,2′-bipyridine (50 mg, 0.27 mmol), [Cp*Ir(OH$_2$)$_3$]SO$_4$ (129 mg, 0.27 mmol) and water (6 mL) was stirred at room temperature for 18 hours under an argon atmosphere. The resulting solution was filtered to remove any insoluble part, and then the filtrate was evaporated to give a yellow solid (155 mg, 91 %). ^{1}H NMR(400 MHz, D_2O, δ) 8.52 (d, J = 5.1 Hz, 2H, Ar H), 7.50 (bs, J = 5.9 Hz, 2H, Ar H), 7.38 (bs, 2H, Ar H), 1.60 (s, 15H, Cp*). ESI-MS (*m/z*): [M – SO_4 – H_2O – H]$^+$ calcd for $C_{20}H_{22}IrN_2O_2^+$, 515.13; found, 515.4. Anal. Calcd for $C_{20}H_{25}IrN_2O_7S+2H_2O$: C, 36.08; H, 4.39; N, 4.21. Found: C, 35.90; H, 4.12; N, 3.88. All values are given as percentages.

Synthesis of [Cp*Ir(5DHBP)(OH$_2$)]SO$_4$: A mixture of 5,5′-dihydroxy-2,2′-bipyridine (50 mg, 0.27 mmol), [Cp*Ir(OH$_2$)$_3$]SO$_4$ (129 mg, 0.27 mmol) and water (6 mL) was stirred at room temperature for 18 hours under an argon atmosphere. The resulting solution was filtered to remove any insoluble part, and then the filtrate was evaporated to give a yellow solid, which was purified by recrystallization from water. The purified complex was obtained as a yellow crystal (140 mg, 82 %). ^{1}H NMR (400 MHz, D_2O, δ) 8.64 (d, J = 2.6 Hz, 2H, Ar H), 8.20 (d, J = 9.1 Hz, 2H, Ar H), 7.71 (dd, J = 8.9, 2.6 Hz, 2H, Ar H), 1.67 (s, 15H, Cp*). ESI-MS (*m/z*): [M – SO_4 – H_2O]$_2^+$ calcd for $C_{20}H_{23}IrN_2O_{22}^+$, 258.07; found, 258.1. [M – SO_4 – H_2O – H]$^+$ calcd for $C_{20}H_{22}IrN_2O_2^+$, 515.03; found, 515.0. Anal. Calcd. for $C_{20}H_{25}IrN_2O_7S_2$ + $2H_2O$: C, 36.08; H, 4.39; N, 4.21. Found: C, 35.97; H. 4.29; N, 3.89. All values are given as percentages.

Hydrogenation of CO_2: To a $KHCO_3$ aqueous solution (2.0 M, pH 8.5, 10 mL) was added **4-** and **6DHBP** complexes as a aqueous solution (2.5 mM, 80 μL), the **3-** and **5DHBP** complexes as a solid (3.15 mg, 5.0 μmol) or the bpy complex as a solid (3.0 mg, 5.0 μmol). Then the mixture was degassed by three cycles of Freeze-Pump-Thaw in a flask and was transferred into a stainless autoclave. After 10 min. stabilization at 50 °C under 1.0 MP of H_2/CO_2 (1/1) gas, the reaction was started by stirring (1500 rpm). The stirring was stopped after 1 hour and the pressurized gas was released to measure the concentration of formate in the resulting solution by HPLC.

Dehydrogenation of HCO_2H: A HCO_2H aqueous solution (1.0 M, pH 1.8, 10 mL) was degassed by three cycles of Freeze-Pump-Thaw in a 20 mL pear-shaped flask equipped with a condenser tube. After 10 min of pre-heating at 60 °C, the bpy complex (8.97 mg, 15.0 μmol), the **5DHBP** complex (6.3 mg, 10.0 μmol) or an aqueous solution of the **3-**, **4-** and **6DHBP** complexes (1.0 mM, 200 μL) was added to start the reaction. The flow rate (mL/min) of evolved gas was measured with a soap-film flow meter and the initial TOF was calculated based on the average of the flow rate in the first 10 min. The volume of the gas was also monitored with a gas meter. The reaction was carried out until the gas evolution stopped. The amount of consumed HCO_2H was estimated from the concentration of the residual formate determined by HPLC to calculate the TON.

Transfer hydrogenation of cyclohexanone: Cyclohexanone (2.0 mmol, 207 μL) was added to 20 mL of 1.0 M HCO_2H/HCO_2Na aqueous solution (pH 2.6) degassed by three cycles of Freeze-Pump-Thaw in a 50 mL Schlenk tube. After 10 min of pre-heating at 40 °C, an

aqueous solution of the complex (2.5 mM, 400 μL) was added to start the reaction. Samples of the reaction mixture were extracted with a syringe and monitored by GC. The reaction was performed over a period of 8 hours. The initial TOF was calculated based on the concentration of the generated cyclohexanol in the first 10 min.

Transfer hydrogenation of 2-cyclohexen-1-one: 2-Cyclohexen-1-one (2.0 mmol, 194 μL) was added to 20 mL of 1.0 M HCO_2Na aqueous solution (pH 7.2) degassed by three cycles of Freeze-Pump-Thaw in a 50 mL schlenk tube. After 10 min of pre-heating at 40 °C, the **3**-and **5DHBP** complexes (3.15 mg, 5.0 μmol), the bpy complex (3.00 mg, 5.0 μmol) or an aqueous solution of the **4**-and **6DHBP** complexes (2.5 mM, 200 μL) was added to start the reaction. The reaction was monitored by HPLC during the reaction, and performed until the concentration of the product became constant. The initial TOF was calculated based on the concentration of the cyclohexanol in the first 10 min.

RESULTS AND DISCUSSION

UV-vis Spectroscopic Investigations

The hydroxy groups on the **DHBP** ligand[22, 42-45] and the aqua ligand[46-47] in transition-metal complexes can be reversibly deprotonated and protonated depending on the pH as shown in Scheme 1. UV-vis absorption spectra were collected at varying pH to determine the pK_a of the hydroxy groups and aqua ligands (Figures S1a-S5a). Selected spectra at certain pH values are shown in Figure 1. At the initial pH (pH ~2.0 for the **4**-, **5**- and **6DHBP** complexes, pH 0.3 for

the **3DHBP** complex), at which both of the hydroxy groups and the aqua ligand are fully protonated, the absorption maxima observed in the range of 230–360 nm can be assigned to a metal to ligand charge transfer (MLCT) and/or ligand centered (LC) transitions. The absorption bands of the **3–6DHBP** complexes gradually changed upon increasing the pH, and the absorption maxima were red-shifted by 17–38 nm. A hydroxy group on the **DHBP** ligand is deprotonated to generate a strong electron-donating oxyanion group, which renders the **DHBP** ligand strongly π-basic. A strong π-donor ligand increases the electron density on the metal, and its d(π) orbital is raised in energy to become closer to the π* orbital of the ligand, resulting in a decrease in the MLCT excitation energy.[10, 13, 43, 48] Therefore, a spectral change accompanied by a red-shift can be recognized as reflecting a change in the electronic properties of the complex caused by deprotonation of the hydroxy groups. Figures S1b–S5b show changes in absorbance at a single wavelength as a function of pH. The average of the two hydroxy pK_a values is defined as the inflection point given by a Boltzmann fit of these plots, and these values are summarized in Table 1. The low pK_a value of the **3DHBP** complex reflects the fact that one of the hydroxy groups at the 3 or 3′ positions readily deprotonates, and the remaining hydroxy group forms an intramolecular hydrogen bond to the resulting oxyanion. The proton of the remaining hydroxy group is in a highly electronegative environment as evidenced in the ^{1}H NMR spectrum (δ = 18.2 ppm in DMSO-d_6 in Figure S6). This strong intramolecular hydrogen bond impedes the second deprotonation, and its pK_a is reported as 13.6.[43] Previously, we reported a pK_a value of 9.6 for [Cp*Ir(**4DHBP**)Cl]Cl using a definition in which the pK_a for a two-proton acid-base equilibrium with equal pK_a is twice the pH at the inflection point in the spectrophotometric titration curve.[19] However, owing to the non-intuitive nature of such pK_a values, the average pK_a is often reported as the pH of the inflection point. Accordingly, the previous pK_a value can be regarded as 4.8,

which value is close to the pK_a value of 5.2 for [Cp*Ir(**4DHBP**)(OH_2)]SO_4 reported here. The aqua ligand, if it ~~is~~ remains attached, could also be deprotonated to generate a hydroxo group, which is a negatively charged donor ligand. Spectral changes upon the deprotonation of aqua ligands were found in the high pH region, but they had rather small intensity and wavelength changes compared to those of the hydroxy groups of the DHBP ligands. Their pK_a values were determined in the same way as for the hydroxy groups of the DHBP ligands. The aqua ligand of the **6DHBP** complex exhibited the highest pK_a value of 10.6 within this series, which indicates that the negatively charged oxyanions adjacent to the metal center suppress the generation of a hydroxo possessing a negative charge through electrostatic interactions. Meanwhile, the aqua ligand of the bpy complex showed the lowest pK_a value of 8.5. Previously reported pK_a values are listed in Table 1 for comparison. These values agree with values in the present study, although they were obtained under different experimental conditions.

As mentioned in the computational studies section and the SI, time-dependent density functional theory (TD-DFT) calculations in water were performed to predict the UV-vis spectra of Cp*Ir(**6DHBP**)$(OH_2)^{2+}$, Cp*Ir(**6DHBP-2H$^+$**)(OH_2), and Cp*Ir(**6DHBP-2H$^+$**)$(OH)^-$ (Figure S8). These spectra were found to match very well with the observed experimental spectra.

^{1}H NMR spectra of the Cp*Ir complexes with **bpy** and **DHBP** were obtained in various protonation states to evaluate the electron density on the coordinated proton-responsive ligands. The chemical shifts of the protons of **bpy** and **DHBP** ligands are summarized in Table 2 and the ^{1}H NMR spectra are shown in Figure S7. The pD value of the NMR solvent was determined by shifting the values measured using a pH electrode by 0.4 units.[49] The signals of the **4-**, **5-** and **6DHBP** ligands in their complexes shifted upfield by 0.51–0.86 ppm upon deprotonation of the hydroxy groups of the **DHBP** ligand, indicating an increase in the electron density on the ligands

arising from the generation of oxyanions. On the other hand, the upfield shifts observed in the **bpy** complex owing to deprotonation of the aqua ligand were negligible, in the 0.09–0.11 Δppm range, which indicates that the coordinated hydroxo ion hardly affects the electron density of the bipyridine ligand. In the case of the **3DHBP** complex, the signals shifted upfield by 0.17–0.27 ppm upon the first deprotonation ([Cp*Ir(**3DHBP–H**$^+$)(OH_2)]$^+$, measured at pD 2.0). Here **3DHBP–H**$^+$ indicates the singly-deprotonated **3DHBP**. The shifts did not exceed 0.47 ppm even at high pH ([Cp*Ir(**3DHBP–H**$^+$)(OH)], measured at pD > 12.0), which implies that the deprotonation of the second hydroxy group requires even more basic conditions. Previously reported pK_a values are listed for comparison. These values agree well with values in the present study, although they were obtained under different experimental conditions.

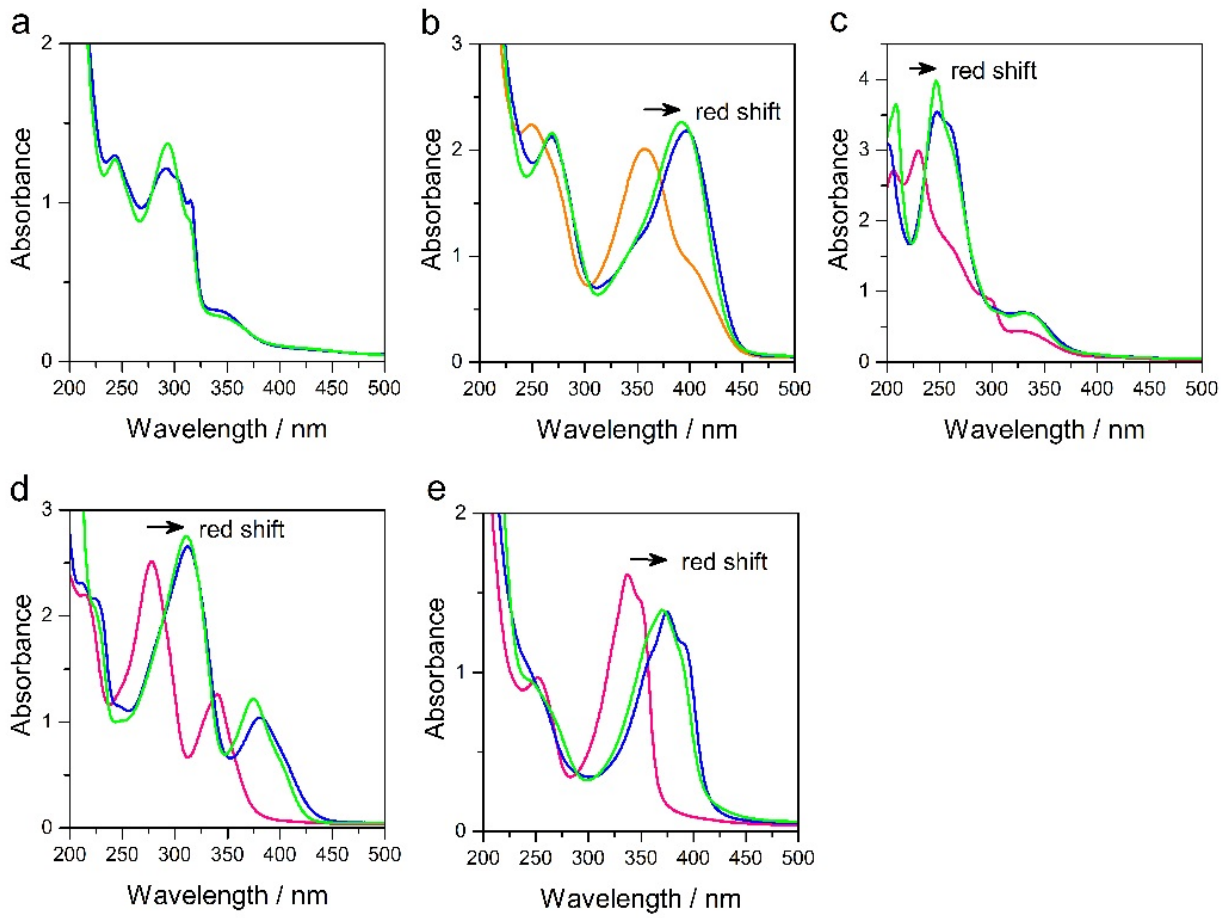

Figure 1. Selected UV-vis absorption spectra for (a) $[Cp^*Ir(bpy)(OH_2)]SO_4$, (b) $[Cp^*Ir(\mathbf{3DHBP})(OH_2)]SO_4$, (c) $[Cp^*Ir(\mathbf{4DHBP})(OH_2)]SO_4$, (d) $[Cp^*Ir(\mathbf{5DHBP})(OH_2)]SO_4$ and (e) $[Cp^*Ir(\mathbf{6DHBP})(OH_2)]SO_4$ in aqueous solution at various pH (orange line: pH 0.3, pink line: pH ~2, blue line: pH ~8, green line: pH ~12).

Table 1. Summary of absorption maxima and the pK_a values.

Complex	λ_{max} [nm]		$\Delta\lambda_{max}$	pK_a		Ref.
	Hydroxy	Oxianion	[nm]	Hydroxy	Aqua	
$[Cp^*Ir(bpy)(OH_2)]SO_4$	–	–	–	–	8.5	Present

[Cp*Ir(bpy)(OH_2)]SO_4	–	–	–	–	8.6 [b]	[50]
[Cp*Ir(**3DHBP**)(OH_2)]SO_4	357	400	43	< 0.4	8.8	Present
[Cp*Ir(**4DHBP**)(OH_2)]SO_4	230	247	17	5.2	9.2	Present
[Cp*Ir(**4DHBP**)(OH_2)]SO_4	–	–	–	5.0	9.1	39
[Cp*Ir(**4DHBP**)(Cl)]Cl [a]	–	–	–	4.4 ± 0.1	–	[51]
[Cp*Ir(**4DHBP**)(Cl)]Cl [a]	–	–	–	9.6 (4.8)	–	19
[Cp*Ir(**5DHBP**)(OH_2)]SO_4	277	312	35	5.6	9.0	Present
[Cp*Ir(**6DHBP**)(OH_2)]SO_4	337	375	38	4.7	10.6	Present
[Cp*Ir(**6DHBP**)(OH_2)]SO_4	–	–	–	4.1	–	39
[Cp*Ir(**6DHBP**)(Cl)]Cl[a]	–	–	–	4.6 ± 0.1	–	[51]

[a] Upon dissolving the Cl complexes in water, they convert to the corresponding aqua complexes. [b] Determined by ^{1}H NMR chemical shifts and corrected by use of the equation $pK_a = 0.929pK_a^* + 0.42$.[52]

Table 2. Chemical shifts of the protons of the bpy and **DHBP** ligands in protonated and deprotonated complex. $\Delta ppm = ppm_{(protonated)} - ppm_{(deprotonated)}$.

Complex	3,3′-position		4,4′-position		5,5′-position		6,6′-position	
	ppm	Δppm	ppm	Δppm	ppm	Δppm	ppm	Δppm
[Cp*Ir(bpy)(OH_2)]$^{2+}$ [a]	8.57	–	8.36	–	7.91	–	9.14	–
[Cp*Ir(bpy)(OH)]$^{+}$ [c]	8.48	0.09	8.25	0.11	7.81	0.10	8.99	0.15
[Cp*Ir(**3DHBP**)(OH_2)]$^{2+}$ [b]	–	–	7.68	–	7.68	–	8.72	–
[Cp*Ir(**3DHBP–H$^+$**)(OH_2)]$^{+}$ [a]	–	–	7.41	0.27	7.51	0.17	8.52	0.20
[Cp*Ir(**3DHBP–H$^+$**)(OH)]^{0} [c]	–	–	7.31	0.47	7.42	0.26	8.37	0.35
[Cp*Ir(**4DHBP**)(OH_2)]$^{2+}$ [a]	7.79	–	–	–	7.25	–	8.77	–
[Cp*Ir(**4DHBP–2H$^+$**)(OH)]$^{-}$ [c]	7.13	0.66	–	–	6.63	0.62	8.25	0.52
[Cp*Ir(**5DHBP**)(OH_2)]$^{2+}$ [a]	8.22	–	7.73	–	–	–	8.67	–
[Cp*Ir(**5DHBP–2H$^+$**)(OH)]$^{-}$ [c]	7.71	0.51	7.13	0.60	–	–	8.11	0.56

[Cp*Ir(**6DHBP**)(OH_2)]$^{2+}$ [a]	7.85	–	8.03	–	7.21	–	–	–
[Cp*Ir(**6DHBP–2H$^+$**)(OH)]$^-$ [c]	6.99	0.86	7.44	0.59	6.41	0.80	–	–

[a] Measured in D_2O/D_2SO_4 (pD 2.0). [b] Measured in D_2O/ D_2SO_4 (pD < 0.1). [c] Measured in D_2O/KOD (pD > 12.0).

Crystallographic Data

X-ray structural analysis of the complexes in various protonation states has been successfully performed and the associated ORTEP diagrams with thermal ellipsoids at a 50% probability are shown in Figure 2. All crystals were grown from their aqueous solutions by slow evaporation at room temperature. Yellow crystals of the complexes with doubly-protonated **4-**, **5-** and **6DHBP** ligands were obtained from aqueous solutions of each complex as [Cp*Ir(**4DHBP**)(OH_2)]$_2$(SO_4)$_2$(H_2O)$_5$, [Cp*Ir(**5DHBP**)(OH_2)](SO_4)(H_2O)$_3$ and [Cp*Ir(**6DHBP**)(OH_2)]$_2$(SO_4)$_2$(H_2O)$_9$, respectively, whereas a crystal of the complex with a doubly-protonated **3DHBP** ligand, [Cp*Ir(**3DHBP**)(OH_2)]$_2$(HSO_4)$_4$(H_2O)$_2$ was obtained from a H_2SO_4 aqueous solution of [Cp*Ir(**3DHBP**)(OH_2)]SO_4. Aqueous solutions containing [Cp*Ir(**3DHBP**)(OH_2)]SO_4 and 10 equivalents of CF_3SO_3Na provided [Cp*Ir(**3DHBP–H$^+$**)(OH_2)](SO_3CF_3) whereas NaOH aqueous solutions yielded [Cp*Ir(**4DHBP–2H$^+$**)(OH_2)](H_2O)$_4$ as a green crystal, [Cp*Ir(**6DHBP–2H$^+$**)(OH_2)](H_2O)$_2$ as a green crystal and [Cp*Ir(**3DHBP–H$^+$**)(OH)](H_2O) as a pale yellow crystal. (Here **DHBP–2H$^+$** indicates doubly-deprotonated **DHBP**.) Unfortunately, we could not obtain a crystal of the complex with a **5DHBP–2H$^+$** ligand despite many attempts. All crystals except [Cp*Ir(**3DHBP–H$^+$**)(OH_2)](SO_3CF_3) contain several non-bonding water molecules which disturb the symmetry of the crystals. Thus their space groups lack mirror-symmetry despite the symmetric structure of the complexes (except for [Cp*Ir(**4DHBP–2H$^+$**)(OH_2)](H_2O)$_4$ and [Cp*Ir(**6DHBP–2H$^+$**)(OH_2)](H_2O)$_2$). However, the R index of all crystals is low enough to rely on the resulting

structure (see SI Table S2–21). In the crystal structure of [Cp*Ir(**3DHBP**)(OH_2)]$_2$(HSO_4)$_4$(H_2O)$_2$ (Figure 2a), hydrogen atoms are intact on both hydroxy groups and point in the same direction to avoid steric crowding, and the co-planarity with the bpy ligand is retained. The two C–O bonds show similar lengths of 1.342(4) and 1.351(4) Å. In contrast, disordered hydrogen atoms are found on the two oxygen atoms with an occupancy factor of 0.5 in the [Cp*Ir(**3DHBP–H$^+$**)(OH_2)](SO_3CF_3) crystal (Figure. 2b). This disorder is also reflected in similar C–O bond lengths of 1.309(3) and 1.320(3) Å, which are too short for C–O single bonds, indicating that one hydroxy group is deprotonated and the remaining hydrogen forms an intramolecular hydrogen bond resulting in a O···H···O structure with an O–O distance of 2.406 Å. The same hydrogen-bonded proton is also observed in [Cp*Ir(**3DHBP–H$^+$**)(OH)](H_2O) (Figure 2c) in which the aqua ligand is deprotonated to become a hydroxo, indicating the difficulty of the deprotonation of the second hydroxy group even at high pH.

The C–O bond lengths in [Cp*Ir(**4DHBP**)(OH_2)]$_2$(SO_4)$_2$(H_2O)$_5$ (Figure 2d) are 1.329(3) and 1.329(3) Å, while those in the [Cp*Ir(**4DHBP–2H$^+$**)(OH_2)](H_2O)$_4$ (Figure 2e) possessing the doubly-deprotonated **4DHBP** ligand are 1.295(4) Å. The shorter C–O bond lengths in the latter imply double-bond character in the C–O bond of the oxyanion groups on the **DHBP** ligand. The C–O bond lengths in [Cp*Ir(**5DHBP**)(OH_2)](SO_4)(H_2O)$_3$ (Figure 2f) are 1.341(3) and 1.342(3) Å and those of [Cp*Ir(**6DHBP**)(OH_2)]$_2$(SO_4)$_2$(H_2O)$_9$ (Figure 2g) are 1.319(3) and 1.321(3) Å, which are long enough to indicate C–O single bond character in the hydroxy groups. The single crystal of the **6DHBP** complex obtained from a NaOH aqueous solution (Cp*Ir(**6DHBP–2H$^+$**)(OH_2)](H_2O)$_2$]) (Figure 2h) reveals its deprotonated state in which two additional water molecules donate a hydrogen bond to the oxyanions while the aqua ligand bound to the Ir center donates hydrogen bonds to the water molecules that donate a hydrogen bond to the oxyanions

(O–O distance; O(1)–O(1S) 2.693 Å and O(1S)–O(2) 2.644 Å). The C–O bond lengths of the deprotonated hydroxy groups (1.272(9) Å) are short enough for a C=O bond.

In both **6DHBP** complexes, the bpy ligand is slightly bent and the average plane of the Cp* ligand is closer to parallel with that of the bpy ligand. (Figure 3c-d) As a result, the dihedral angle between the Cp* ring and N1–C5–C6–N2 plane of the bpy ligand becomes 34.85° in [Cp*Ir(**6DHBP**)$(OH_2)]_2(SO_4)_2(H_2O)_9$ and 24.00° in [Cp*Ir(**6DHBP–2H$^+$**)$(OH_2)](H_2O)_2$. The steric environment around the metal binding site in the **6DHBP** complex is very different from that of the other complexes, and is likely to affect the catalytic activity. Selected bond lengths and dihedral angles between the Cp* and **DHBP** ligands of all crystals are listed in Table 3.

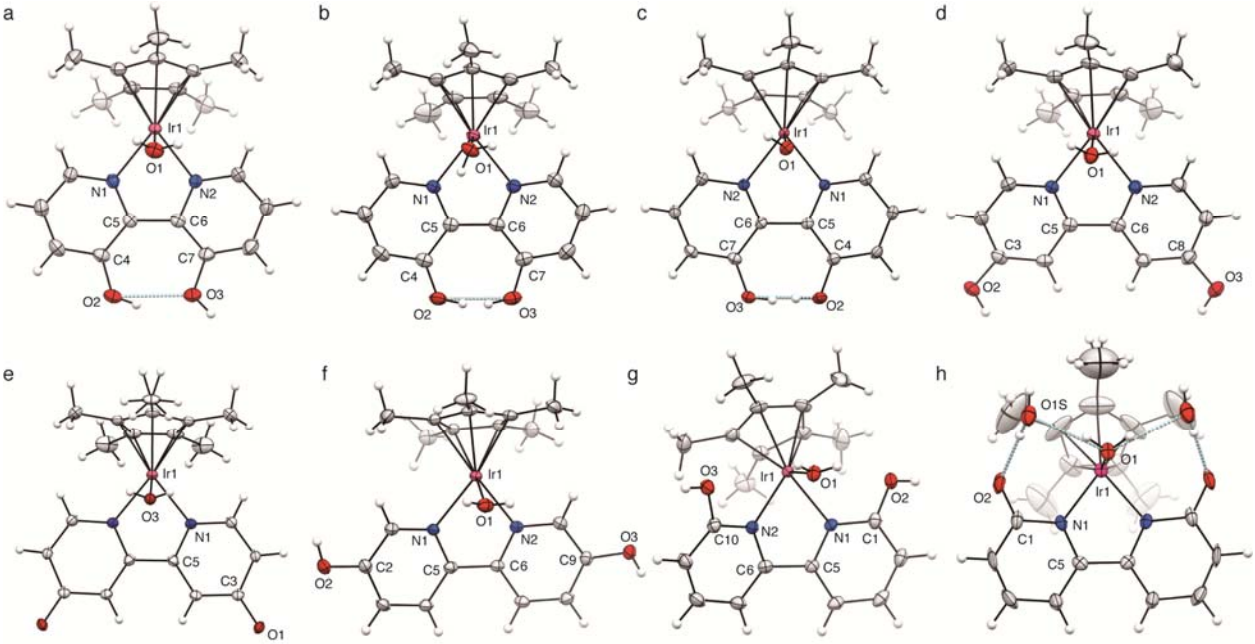

Figure 2. ORTEP diagrams of (a) [Cp*Ir(**3DHBP**)$(OH_2)]_2(HSO_4)_4(H_2O)_2$, (b) [Cp*Ir(**3DHBP–H$^+$**)$(OH_2)]SO_3CF_3$, (c) [Cp*Ir(**3DHBP–H$^+$**)(OH)]$(H_2O)$, (d) [Cp*Ir(**4DHBP**)$(OH_2)]_2(SO_4)_2(H_2O)_5$, (e) [Cp*Ir(**4DHBP–2H$^+$**)$(OH_2)](H_2O)_4$, (f) [Cp*Ir(**5DHBP**)$(OH_2)](SO_4)(H_2O)_3$, (g) [Cp*Ir(**6DHBP**)$(OH_2)]_2(SO_4)_2(H_2O)_9$ and (h) [Cp*Ir(**6DHBP–2H$^+$**)$(OH_2)](H_2O)_2$, with the thermal ellipsoids at a 50% probability. The

counter anions and non-bonding water molecules are omitted for clarity. Hydrogen bonds are indicated by light blue broken lines.

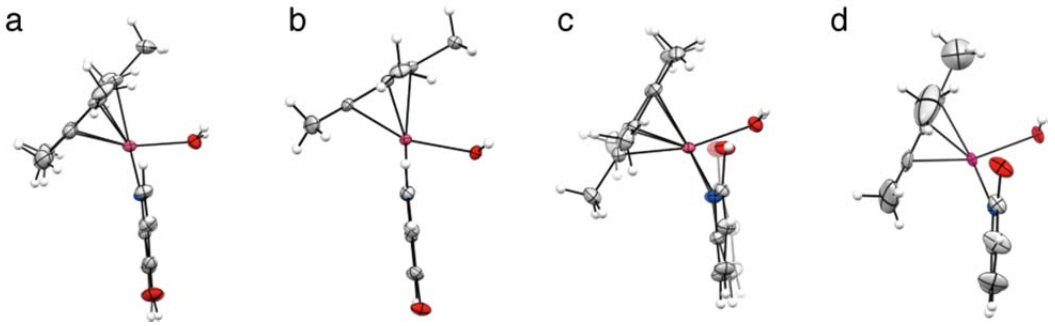

Figure 3. Side views of (a) [Cp*Ir(**4DHBP**)(OH_2)]$_2$(SO_4)$_2$(H_2O)$_5$, (b) [Cp*Ir(**4DHBP–2H**$^+$)(OH_2)](H_2O)$_4$, (c) [Cp*Ir(**6DHBP**)(OH_2)]$_2$(SO_4)$_2$(H_2O)$_9$ and (d) [Cp*Ir(**6DHBP–2H**$^+$)(OH_2)](H_2O)$_2$.

Table 3. Selected bond lengths and dihedral angle between Cp* and **DHBP** ligand in the Ir complexes.

Complex	C–O [Å]	Ir–O [Å]	C5–C6 [Å]	Dihedral angle of Cp* and bipyridine ligand [°]
[Cp*Ir(**3DHBP**)(OH_2)]$_2$(HSO_4)$_4$(H_2O)$_2$	1.342(4), 1.351(4)	2.165(3)	1.487(5)	55.66
[Cp*Ir(**3DHBP–H**$^+$)(OH_2)](SO_3CF_3)	1.309(3), [a] 1.320(3) [a]	2.128(2)	1.482(3)	61.42
[Cp*Ir(**3DHBP–H**$^+$)(OH)](H_2O)	1.318(3), [a] 1.311(3) [a]	2.086(2)	1.485(3)	60.31
[Cp*Ir(**4DHBP**)(OH_2)]$_2$(SO_4)$_2$(H_2O)$_5$	1.329(3), 1.329(3)	2.137(2)	1.483(4)	47.73
[Cp*Ir(**4DHBP–2H**$^+$)(OH_2)](H_2O)$_4$	1.295(4) [b]	2.120(3)	1.473(6) [c]	64.67
[Cp*Ir(**5DHBP**)(OH_2)](SO_4)(H_2O)$_3$	1.341(3), 1.342(3)	2.121(2)	1.465(3)	58.69
[Cp*Ir(**6DHBP**)(OH_2)]$_2$(SO_4)$_2$(H_2O)$_9$	1.319(3), 1.321(3)	2.136(2)	1.474(3)	34.85

[Cp*Ir(**6DHBP–2H**$^+$)(OH_2)](H_2O)$_2$	1.272(9) [d]	2.181(7)	1.457(13) [c]	24.00

[a] Hydrogen-bonded hydroxy group. [b] C(3)–O(1). [c] C(5)–C(5). [d] C(1)–O(2)

Catalytic activities

The UV-vis spectroscopic measurements indicated that remarkable electronic changes were caused by deprotonation of the hydroxy groups and the pK_a values varied according to their positions. Resonance structures of the oxyanion forms are different depending on the position of the hydroxy groups, which leads to different electronic properties even in the same protonation states. Here, we studied the catalytic activities of these complexes for four reactions including: (1) hydrogenation of CO_2 at pH 8.5; (2) dehydrogenation of HCO_2H at pH 1.8; (3) transfer hydrogenations of cyclohexanone at pH 2.6; and (4) transfer hydrogenations of 2-cyclohexen-1-one at pH 7.2. In our previous work using the **4DHBP** complex as a precatalyst for these reactions, significant differences in catalytic activities and in chemoselectivities were observed depending on pH, and the optimum pH was different for each reaction. Therefore, it is of interest to examine the catalytic performance of the complexes in solutions with different pH.

1) Hydrogenation of CO_2

The hydrogenation of CO_2 to HCO_2H or its conjugate base (HCO_2^-)[53-60] in the context of using CO_2 as a C1 fuel source or hydrogen carrier is gathering significant interest lately.[61-68] The results of hydrogenation of CO_2, which are performed in 2.0 M $KHCO_3$ aqueous solution (pH 8.5) at 50 °C for 1 h, under 1.0 MPa H_2/CO_2 (1/1) in the presence of one of the complexes as a precatalyst, are summarized in Table 4. Under these reaction conditions, both hydroxy groups, except for the case of **3DHBP**, on the **DHBP** ligand are deprotonated to become oxyanions.

Initial TOFs of the **4DHBP** (entry 3) and **6DHBP** (entry 6) complexes were far higher, 650 h^{-1} and 1400 h^{-1}, respectively, than that of the bpy complex (0.95 h^{-1}). Based on our previous studies,[18-20] the increased catalytic activity can be attributed to the strong electron-donating oxyanions at the 4,4′- or 6,6′-positions that render the metal center more electron-rich through resonance structures in which the negative charge of the oxygen atom transfers onto the corresponding *para* or *ortho* nitrogen atom.[42] In contrast, the two oxianions at 5,5′-positions did not increase the performance, and the initial TOF of that complex was only 1.1 h^{-1}. The deprotonated **5DHBP** ligand does not possess a resonance structure in which the negative charges are located on nitrogen atoms so that it is not expected to exhibit enhanced catalytic activity. Furthermore, the low solubility of the **3DHBP** and **5DHBP** complexes in the reaction solution also limit the progress of the catalytic reaction. The higher performance of the **6DHBP** complex (entry 6 and 7) over **4DHBP** (entry 3 and 4) can be explained on the basis of a pendent base effect and a proton relay via a water molecule.[38] (See Computational Studies below).

Table 4. Results of hydrogenation of CO_2 catalyzed by $[Cp^*Ir(L)(OH_2)]SO_4$.

Entry	L	Concentration of catalyst [mM]	Reaction time [h]	TOF[c] [h^{-1}]	TON[c]	Ref.
1 [a]	bpy	0.5	1	0.95	0.95	Present
2 [a]	**3DHBP**	0.5	1	0.30	0.30	Present
3 [a]	**4DHBP**	0.02	1	650	650	Present
4 [b]	**4DHBP**	0.02	30	790 [d]	7700	39
5 [a]	**5DHBP**	0.5	1	1.1	1.1	Present
6 [a]	**6DHBP**	0.02	1	1400	1400	Present
7 [b]	**6DHBP**	0.02	9	1650 [d]	5150	39

[a] Carried out in 10 mL of 2.0 M $KHCO_3$ aqueous solution (pH 8.5) at 50 °C under 1.0 MPa H_2/CO_2 (1/1) with stirring (1500 rpm). TOF was determined at 1 h. Under the conditions, the **4-** and **6DHBP**

ligands were doubly-deprotonated and the **3DHBP** ligand was mono-deprotonated. [b] Carried out in 1.0 M $NaHCO_3$ aqueous solution under 1.0 MPa H_2/CO_2 (1/1). [c] Concentration of the generated formate was determined by HPLC. [d] The initial TOF was determined at the first 10 min.

2) Dehydrogenation of formic acid

The dehydrogenation of HCO_2H is an indispensable process for using HCO_2H as a hydrogen source.[69-80] It was previously reported that [Cp*Ir(**4DHBP**)(OH_2)]SO_4 exhibited an excellent ability to dehydrogenate HCO_2H with a high chemoselectivity.[20, 23-24]

The HCO_2H dehydrogenation reactions were performed in 1.0 M aqueous solution of HCO_2H at 60 °C using one of the complexes as a catalyst. The results are summarized in Table 5. The **4DHBP** and **6DHBP** complexes showed high initial TOFs (entry 3: 1800 h^{-1} and entry 6: 2200 h^{-1}, respectively) and all of the HCO_2H contained in the reaction mixture was completely decomposed (TON: 5000, conversion: 100%). Although the TOF values are different within entries 3 and 4, and entries 6 and 7 owing to the different measurement methods, **4DHBP** and **6DHBP** ligands complexed with Ir produce catalysts that can efficiently and entirely dehydrogenate HCO_2H. The moderately electron-donating hydroxy groups at the 3,3′- and 5,5′-positions of the **DHBP** ligand were also found to increase the catalytic activity for the dehydrogenation process. It is noteworthy that the **3DHBP** complex showed a slightly higher initial TOF (entry 2: 440 h^{-1}) than the bpy complex (18 h^{-1}) and the **5DHBP** complex (entry 5: 32 h^{-1}). At pH 1.8, one of the two hydroxy groups on the **3DHBP** ligand remains deprotonated, and the strong electron-donating character of the oxyanion can still increase the catalytic activity.[43]

Table 5. Results of dehydrogenation of HCO_2H catalyzed by $[Cp^*Ir(L)(OH_2)]SO_4$.

Entry	L	Concentration of catalyst [mM]	Reaction time [h]	Initial TOF [h^{-1}]	TON [d]	Ref.
1 [a]	bpy	1.5	8	18	280	Present
2 [a]	**3DHBP**	0.2	8	440	780	Present
3 [a]	**4DHBP**	0.2	4	1800	5000	Present
4 [b]	**4DHBP**	0.2	4	2400	5000	23
5 [a]	**5DHBP**	1.0	8	32	280	Present
6 [a]	**6DHBP**	0.2	3	2200	5000	Present
7 [c]	**6DHBP**	0.1	8	2450	10000	[81]

[a] Carried out in 10 mL of 1.0 M HCO_2H (10 mmol) aqueous solution (pH 1.8) at 60 °C. Initial TOF was calculated based on flow rate (mL/min) of the evolved gas measured with a soap-film flow meter in the first 10 min. Under the conditions, the **3DHBP** ligand was mono-deprotonated. [b] Carried out in 1.0 M HCO_2H aqueous solution, the volume of gas evolution was determined by a wet gas meter (Shinagawa Corp., W-NK-05), the initial TOF was calculated from the initial part of the reaction (typically 30 min). [c] Carried out in 20 mL of 1.0 M HCO_2H aqueous solution, the volume of gas evolution was determined by a wet gas meter. [d] Amount of the consumed formic acid was estimated from concentration of the residual formate determined by HPLC.

3) Transfer hydrogenation

Transition-metal-catalyzed transfer hydrogenation (TH) using HCO_2H or alcohol as a proton source[82-86] is very attractive for the hydrogenation of organic compounds because of its mild reaction conditions compared to hydrogenation using hydrogen gas or metal hydrides.[87-90] Previously, we reported that $[Cp^*Ir(\mathbf{4DHBP})(OH_2)]SO_4$ catalyzes the TH of various α,β-unsaturated carbonyl compounds in aqueous media containing HCO_2H and sodium formate (HCO_2Na). The catalytic activity and chemoselectivity depended on the pH of reaction solutions.[21] At low pH, both C=C and C=O double bonds were reduced with a good conversion yield, whereas only C=C bonds were reduced at high pH.

Here the hydrogenation of cyclohexanone to cyclohexanol was performed under acidic conditions (pH 2.6) at 40 °C. The results are summarized in Table 6. The highest initial TOF was recorded for the **4DHBP** complex (entry 3: 1200 h^{-1}, entry 4: 820 h^{-1}) and the conversion was 90 % after 8 h. Somewhat surprisingly, the **6DHBP** complex exhibited a relatively low initial TOF (740 h^{-1}) despite its two electron-donating hydroxy groups at the 6,6′-positions. This modest activity can be attributed to the steric hindrance between the hydroxy group adjacent to the active site and the substrate. Interestingly, the **3DHBP** complex showed moderately high performance. Its initial TOF was 800 h^{-1}, however, as shown in Figure 4, the TON consistently increased to reach 1700 after 8 h. It can be deduced that the mono-deprotonated **3DHBP** ligand is stable in acidic media owing to the strong intramolecular hydrogen bonds, and generation of one oxyanion is enough to increase the catalytic activity.

Table 6. Results of transfer hydrogenation of cyclohexanone catalyzed by $[Cp^*Ir(L)(OH_2)]SO_4$.[a]

Entry	L	Initial TOF [b] [h^{-1}]	TON in 8 h	Ref.
1	bpy	600	410	Present
2	**3DHBP**	800	1700	Present
3	**4DHBP**	1200	1800	Present
4	**4DHBP**	820 [c]	>2000	21
5	**5DHBP**	530	710	Present
6	**6DHBP**	740	870	Present

[a] All reactions were carried out in 20 mL of 1.0 M HCO_2Na/HCO_2H aqueous solution (pH 2.6) at 40 °C for 8 hours under argon atmosphere with 1.0 μmol of catalyst and 2.0 mmol of substrate (HCO_2H/cyclohexanone/catalyst = 20000/2000/1) and monitored by GC. Under the conditions, the **3DHBP** ligand was mono-deprotonated. [b] Calculated based on the generated cyclohexanol in the first 10 min. [c] Calculated based on the generated cyclohexanol in the first 5 min.

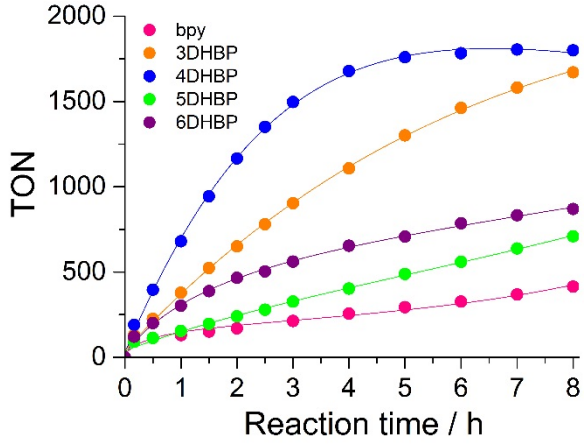

Figure 4. TON values of the transfer hydrogenation of cyclohexanone catalyzed by Ir complexes in 1.0 M HCO_2Na/HCO_2H aqueous solution (pH 2.6) at 40 °C under argon atmosphere.

Although the reduction of α,β–unsaturated carbonyl compounds has been widely studied, and the selective reduction of carbonyl groups has been achieved with relative ease,[46, 90-94] the number of reports regarding the conjugate reduction of α,β-unsaturated carbonyl compounds are still limited.[95-101] We performed TH of 2-cyclohexen-1-one in 1.0 M HCO_2Na aqueous solution (pH 7.2) at 40 °C and achieved the hydrogenation of the C=C bond of 2-cyclohexen-1-one to produce cyclohexanone with a high chemoselectivity. The results are summarized in Table 7. Initial TOFs were as high as 7500 h^{-1} (entry 3) and 4300 h^{-1} (entry 4) for the complex with the **4DHBP** ligand and 4000 h^{-1} with the **6DHBP** ligand. The reaction conditions need to be further optimized because all complexes were drastically deactivated during the course of the reaction and the reactions could not proceed more than 30 min. However, the chemoselectivities were successfully controlled by the pH of the solution. These reactions are very useful because other water-soluble substrates can also be reduced with a high chemoselectivity.[21]

Table 7. Results of transfer hydrogenation of 2-cyclohexen-1-one catalyzed by $[Cp^*Ir(L)(OH_2)]SO_4$.[a]

Entry	L	Concentration of catalyst [mM]	Reaction time [h]	Initial TOF[b] [h^{-1}]	TON	Ref.
1	bpy	0.25	0.5	850	120	Present
2	**3DHBP**	0.25	0.5	240	30	Present
3	**4DHBP**	0.025	0.5	7500	1700	Present
4	**4DHBP**	0.05	2.0	4300 [c]	> 1980	21
5	**5DHBP**	0.25	0.5	500	80	Present
6	**6DHBP**	0.025	0.5	4000	710	Present

[a] All reactions were carried out in 20 mL of 1.0 M HCO_2Na aqueous solution (pH 7.2) at 40 °C under argon atmosphere with 2.0 mmol of substrate and monitored by GC. Under the conditions, the **4–6DHBP** ligands were doubly-deprotonated and the **3DHBP** ligand was mono-deprotonated. [b] Calculated based on the generated cyclohexanone in the first 10 min. [c] Calculated based on the generated cyclohexanone in the first 5 min.

Computational Studies

Previously, we demonstrated that $[Cp^*Ir(\mathbf{6DHBP})(OH_2)]^{2+}$ activates an H_2 molecule by a pendent base and a proton relay involving a solvent water molecule resulting in an energetically favorable H_2 heterolysis to generate a hydride complex.[38] However, proposed mechanisms for the hydrogenation of CO_2 consist of two steps: the first being the generation of a hydride complex and the second being the insertion of a CO_2 molecule into the metal–hydide bond to produce a formate complex. Here, we describe the full catalytic cycle for the hydrogenation of CO_2 by $[Cp^*Ir(\mathbf{4DHBP})(OH_2)]^{2+}$ and $[Cp^*Ir(\mathbf{6DHBP})(OH_2)]^{2+}$ complexes obtained via DFT calculations. Details of the computational methods are available in the SI.

CO_2 hydrogenation catalyzed by [Cp*Ir(4DHBP)(OH_2)]$^{2+}$

We started our investigation of the CO_2 hydrogenation mechanism by calculating the free-energy changes (ΔG) associated with deprotonation of the hydroxy groups on the **4DHBP** ligand in the [Cp*Ir(**4DHBP**)(OH_2)] complex. The ΔG values for formation of [Cp*Ir(**4DHBP-H$^+$**)]$^+$ and [Cp*Ir(**4DHBP–2H$^+$**)] from [Cp*Ir(**4DHBP**)]$^{2+}$ are –20.8 and –41.1 kJ/mol, respectively, at pH 8.5. The calculated ΔG values (at standard conditions except for the solution pH) indicate that only the doubly-deprotonated form of [Cp*Ir(**4DHBP**)] will be relevant at pH 8.5, as in the experimental reaction conditions, as both deprotonation steps are found to be energetically favorable. We next considered the possible coordination of a H_2O molecule to [Cp*Ir(**4DHBP–2H$^+$**)] and found it to be energetically unfavorable by 17.1 kJ/mol, indicating that H_2O coordination to the Ir center is unlikely under experimental reaction conditions. This is primarily an entropic effect; the enthalpy of coordination is slightly favorable. However, under the lower entropic conditions that are attained during the crystallization process, the entropic contribution will be less unfavorable and H_2O coordination might be favored. Also crystal packing interactions and hydrogen bonding networks might stabilize H_2O coordination in the crystal structures.

In accordance with this observation, we examined the catalytic mechanism of CO_2 hydrogenation by [Cp*Ir(**4DHBP–2H$^+$**)]. The results involving intermediates with the most stable protonation states are summarized in Figure 5. Starting with [Cp*Ir(**4DHBP–2H$^+$**)], **I**, the first step of the proposed mechanism is the heterolysis of H_2 which occurs via the transfer of a proton to the strongest base in the solution, a bicarbonate anion (HCO_3^-), **I-TS**, with free energy of activation $\Delta G^{\ddagger}$ = 53.1 kJ/mol (Figure 5). The resulting Ir–H intermediate (**II-B**) in which the proton from heterolysis binds to the pendent base oxyanion is slightly more stable than (**II-A**) in

which the proton goes to the solvent. The transition state for the nucleophilic attack of the hydride complex on CO_2, **II-TS**, involves a lower free-energy requirement ($\Delta G^{\ddagger}$ = 36.0 kJ/mol from **II-A**, 41.3 kJ/mol from **II-B**) and generates a formate (HCO_2^-) bound Ir complex, **III**. In the final step of the mechanism, HCO_2^- is released, regenerating the [Cp*Ir (**4DHBP–2H**$^+$)] complex (Figure 5). The calculated free-energy profile indicates that the rate-determining step is the heterolytic H–H bond cleavage assisted by HCO_3^- as the base.

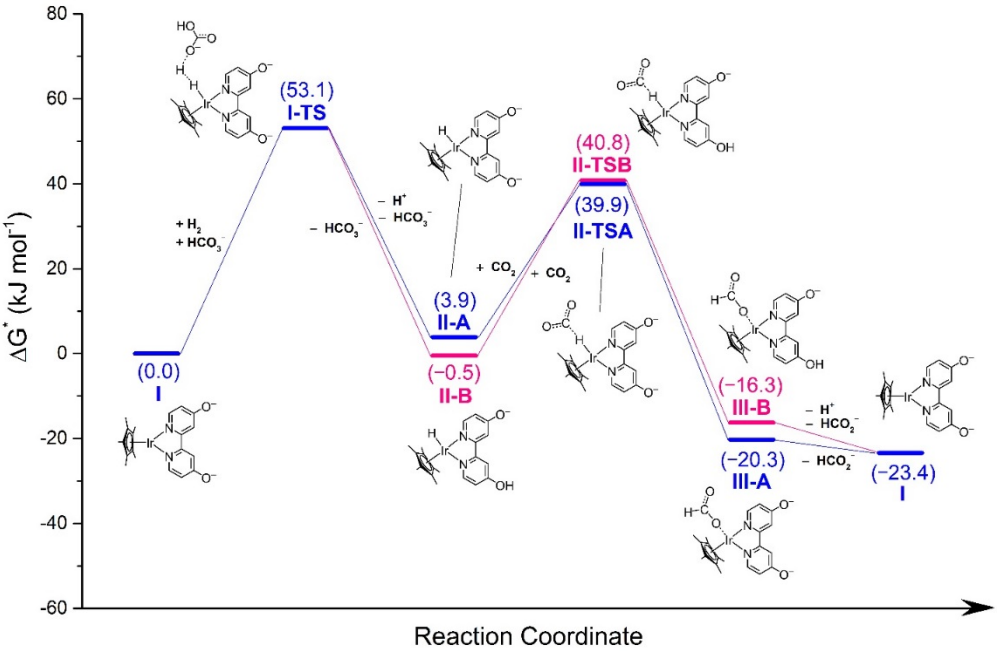

Figure 5. The proposed mechanism for CO_2 hydrogenation by the [Cp*Ir(**4DHBP**)]$^{2+}$ complex at pH 8.5. The relative free energies are reported in units of kJ/mol.

CO_2 hydrogenation process catalyzed by [Cp*Ir(6DHBP)(OH_2)]$^{2+}$

Similar to the case of [Cp*Ir(**4DHBP**)], deprotonation of both hydroxy groups of Cp*Ir(**6DHBP**)] is energetically favorable at pH 8.5; the ΔG values for formation of [Cp*Ir(**6DHBP-H**$^+$)]$^+$ and [Cp*Ir(**6DHBP–2H**$^+$)] from [Cp*Ir(**6DHBP**)]$^{2+}$ are –30.1 and –58.1 kJ/mol, respectively. H_2O coordination to [Cp*Ir(**6DHBP-2H**$^+$)] is also predicted to be unfavorable, although to a smaller extent than in the **4DHBP–2H**$^+$ complex (ΔG = 3.9 kJ/mol).

In contrast to the [Cp*Ir(**4DHBP-2H**$^+$)] catalyst, the presence of basic oxyanion groups in close proximity to the metal center in [Cp*Ir(**6DHBP-2H**$^+$)] (**IV)** enables a proton relay mechanism assisted by a water molecule, as found previously,[38] rather than requiring an external base (e.g., HCO_3^-) in the H_2 heterolysis step. This step proceeds via a proton transfer to an oxyanion group of the **6DHBP-2H**$^+$ ligand assisted by a H_2O molecule, **IV-TS**, and the associated free energy of activation is 40.8 kJ/mol. Nucleophilic attack of the hydride complex on CO_2, **V**, to form transition state **V-TSA**, which occurs with $\Delta G^{\ddagger}$ = 34.0 kJ/mol from **V-A** (or 34.5 kJ/mol from **V-B**), and the release of the product (HCO_2^-) from **VI** completes the catalytic cycle (Figure 6).

Comparison of the activation free energies indicates that in both [Cp*Ir(**4DHBP–2H**$^+$)] and [Cp*Ir(**6DHBP–2H**$^+$)] the H_2 heterolysis to form the iridium hydride intermediate is the rate-determining step, but the presence of the basic oxyanion groups adjacent to the metal center in [Cp*Ir(**6DHBP–2H**$^+$)], **IV**, facilitates the H_2 heterolysis and leads to a faster rate of formate production (Figure 6).

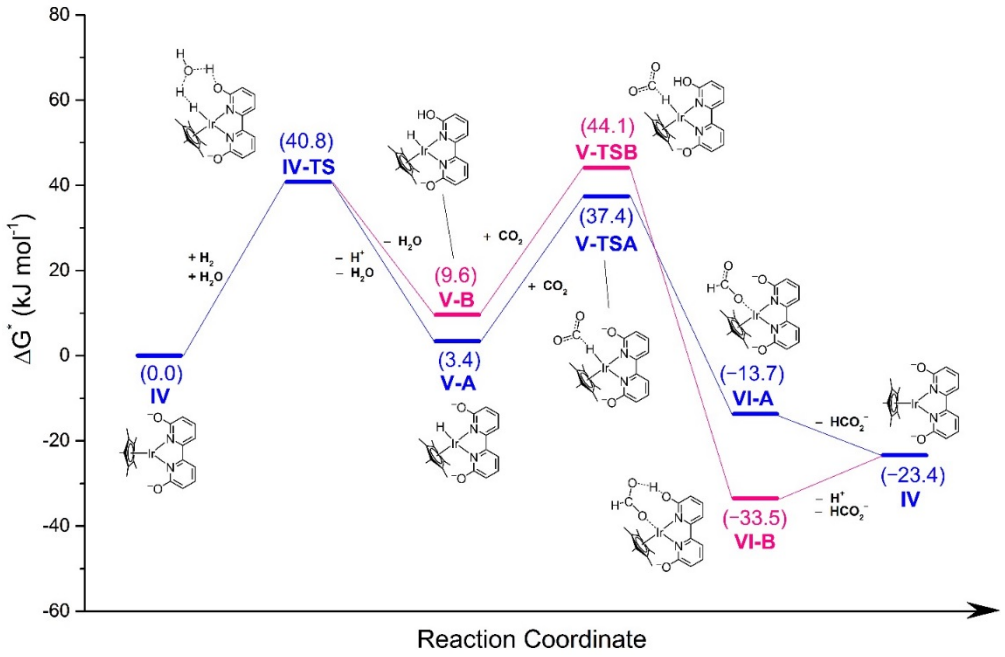

Figure 6. The proposed mechanism for CO_2 hydrogenation by the [Cp*Ir(**6DHBP**)]$^{2+}$ complex at pH 8.5. The relative free energies are reported in units of kJ/mol.

CONCLUSIONS

The positional effects of the hydroxy groups were systematically investigated in half-sandwich Cp*Ir complexes possessing a proton-responsive bipyridine ligand with two hydroxy groups introduced at the 3,3′-, 4,4′-, 5,5′- or 6,6′-positions. Spectroscopic and crystallographic characterization revealed that the position of the hydroxy groups changed the protonation behavior and the electronic properties of the complexes. As shown in Figure 7, the catalytic activities of the **DHBP** complexes under acidic and basic conditions were significantly affected by the position of hydroxy groups. Under acidic conditions, the **4-** and **6DHBP** complexes exhibited high catalytic activity attributed to the electron-donating hydroxy groups. Interestingly, the catalytic performance of the **3DHBP** complex, which has an oxyanion stabilized by an

intramolecular hydrogen bond, was moderately enhanced. On the contrary, no reactions were enhanced to a significant extent by the **5DHBP** complex. Under basic conditions, the resonance structure of the strongly electron-donating oxyanion forms of the **4-** and **6DHBP** complexes, generated by deprotonation of hydroxy groups, significantly increased their catalytic activities. In the CO_2 hydrogenation reaction, the improved activity of the **6DHBP** complex (TOF of 1400 h^{-1}) compared to that of the **4DHBP** (TOF of 650 h^{-1}) was rationalized by DFT calculations. H_2 heterolysis catalyzed by the **4DHBP** complex requires a higher free-energy of activation ($\Delta G^{\ddagger}$ = 53.1 kJ/mol) than that of the nucleophilic attack of Ir–H on CO_2 ($\Delta G^{\ddagger}$ = 36.0 kJ/mol) and involves a HCO_3^- anion as a base. In contrast, H_2 heterolysis proceeds via a proton relay from H_2 to an oxyanion assisted by a water molecule for the **6DHBP** complex, and the associated free-energy of activation is 40.8 kJ/mol, 12.3 kJ/mol lower than that of the **4DHBP** complex. Accordingly, the presence of the ortho-oxyanion as a pendent base in the **6DHBP** complex leads to a faster rate of formate production by facilitating the rate-determining step of H_2 heterolysis.

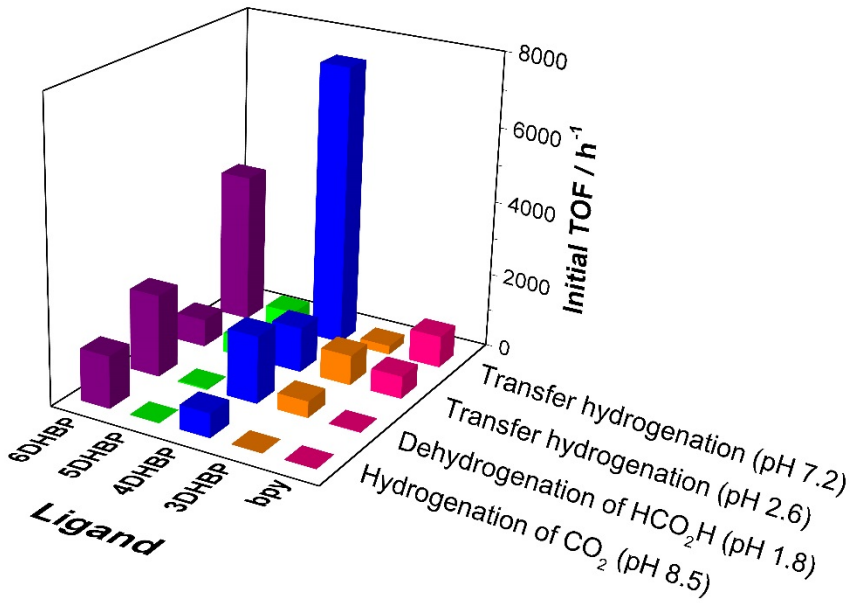

Figure 7. Summary of the catalytic activities of all Cp*Ir(L)$(OH_2)^{2+}$ complexes (L = **bpy**, **3DHBP**, **4DHBP**, **5DHBP** and **6DHBP**).

Supporting Information. UV-vis absorption and ^{1}H NMR spectra, details of crystallographic analysis, CIF files, details of computational methods and Cartesian coordinates of various optimized structures. This material is available free of charge via the Internet at http://pubs.acs.org.

Corresponding Author

*E-mails: (E.F.) fujita@bnl.gov, (Y.H.) himeda.y@aist.go.jp.

Notes

The authors declare no competing financial interest.

ACKNOWLEDGMENT

We thank Dr. Midori Goto (AIST) for X-ray crystal structure determination. Y. H. and W.-H. W. thank the Japan Science and Technology Agency (JST), ACT-C for financial support. The work at BNL was supported by the U.S. Department of Energy, Office of Science, Division of Chemical Sciences, Geosciences & Biosciences, Office of Basic Energy Sciences under contract DE-AC02-98CH10886.

REFERENCES

1. Rothenberg, G., *Catalysis: Concepts and Green Applications*. WILEY-VCH Verlag GmbH & Co. KGaA,: Weinheim, 2008; p 77-125.

2. Crabtree, R. H., *Science* **2010**, *330*, 455-456.
3. Crabtree, R. H., *New J. Chem.* **2011**, *35*, 18-23.
4. Umehara, K.; Kuwata, S.; Ikariya, T., *.J. Am. Chem. Soc.* **2013**, *135*, 6754-6757.
5. Terrade, F. G.; Lutz, M.; van der Vlugt, J. I.; Reek, J. N. H., *Eur. J. Inorg. Chem.* **2013**, 1826-1835.
6. Moore, C. M.; Szymczak, N. K., *Chem. Commun.* **2013**, *49*, 400-402.
7. Lv, R.; Wang, Y.; Zhou, C.; Li, L.; Wang, R., *ChemCatChem* **2013**, *5*, 2978-2982.
8. Deng, J.; Wang, Y.; Pan, T.; Xu, Q.; Guo, Q. X.; Fu, Y., *ChemSusChem* **2013**, *6*, 1163-11637.
9. Kawahara, R.; Fujita, K.; Yamaguchi, R., *J. Am. Chem. Soc* **2012**, *134*, 3643-3646.
10. Fuentes, M. J.; Bognanno, R. J.; Dougherty, W. G.; Boyko, W. J.; Kassel, W. S.; Dudley, T. J.; Paul, J. J., *Dalton Trans.* **2012**, *41*, 12514-12523.
11. Tomas-Mendivil, E.; Diez, J.; Cadierno, V., *Catal. Sci. Technol.* **2011**, *1*, 1605-1615.
12. Nieto, I.; Livings, M. S.; John B. Sacci, I.; Reuther, L. E.; Zeller, M.; Papish, E. T., *Organometallics* **2011**, *30*, 6339-6342.
13. Klein, S.; Dougherty, W. G.; Kassel, W. S.; Dudley, T. J.; Paul, J. J., *Inorg. Chem.* **2011**, *50*, 2754-2763.
14. El Ojaimi, M.; Thummel, R. P., *Inorg. Chem.* **2011**, *50*, 10966-10973.
15. Conifer, C. M.; Taylor, R. A.; Law, D. J.; Sunley, G. J.; White, A. J.; Britovsek, G. J., *Dalton Trans.* **2011**, *40*, 1031-1033.
16. Song, G.; Su, Y.; Periana, R. A.; Crabtree, R. H.; Han, K.; Zhang, H.; Li, X., *Angew. Chem. Int. Ed.* **2010**, *49*, 912-717.
17. Hashiguchi, B. G.; Young, K. J. H.; Yousufuddin, M.; III, W. A. G.; Periana, R. A., *J. Am. Chem. Soc.* **2010**, *132*, 12542-12545.
18. Himeda, Y.; Onozawa-Komatsuzaki, N.; Sugihara, H.; Kasuga, K., *Organometallics* **2007**, *26*, 702-712.
19. Himeda, Y.; Onozawa-Komatsuzaki, N.; Sugihara, H.; Kasuga, K., *J. Photochem. and Photobio. A: Chemistry* **2006**, *182*, 306-309.
20. Himeda, Y.; Miyazawa, S.; Hirose, T., *ChemSusChem* **2011**, *4*, 487-493.
21. Himeda, Y.; Onozawa-Komatsuzaki, N.; Miyazawa, S.; Sugihara, H.; Hirose, T.; Kasuga, K., *Chem. Eur. J.* **2008**, *14*, 11076-11081.
22. Himeda, Y.; Onozawa-Komatsuzaki, N.; Sugihara, H.; Arakawa, H.; Kasuga, K., *Organometallics* **2004**, *23*, 1480-1483.
23. Hull, J. F.; Himeda, Y.; Wang, W. H.; Hashiguchi, B.; Periana, R.; Szalda, D. J.; Muckerman, J. T.; Fujita, E., *Nat. Chem.* **2012**, *4*, 383-388.
24. Himeda, Y., *Green Chemistry* **2009**, *11*, 2018-2022.
25. Himeda, Y.; Onozawa-Komatsuzaki, N.; Sugihara, H.; Kasuga, K., *J. Am. Chem. Soc.* **2005**, *127*, 13118-13119.
26. Greco, C.; Bruschi, M.; Gioia, L. D.; Ryde, U., *Inorg. Chem.* **2007**, *46*, 5911-5921.
27. Nicolet, Y.; Lacey, A. L. d.; Verne`de, X.; Fernandez, V. M.; Hatchikian, E. C.; Fontecilla-Camps, J. C., *J. Am. Chem. Soc.* **2001**, *123*, 1596-1601.
28. Fan, H.-J.; Hall, M. B., *J. Am. Chem. Soc.* **2001**, *123*, 3828-3829.
29. Zhao, B.; Han, Z.; Ding, K., *Angew. Chem. Int. Ed.* **2013**, *52*, 4744-4788.
30. Eisenstein, O.; Crabtree, R. H., *New J.Chem.* **2013**, *37*, 21-27.
31. Rakowski DuBois, M.; DuBois, D. L., *Chem. Soc. Rev.* **2009**, *38*, 62-72.

32. Friedrich, A.; Drees, M.; Gunne, J. S. a. d.; Schneider, S., *J. Am. Chem. Soc.* **2009**, *131*, 17552-17553.
33. Henry, R. M.; Shoemaker, R. K.; DuBois, D. L.; DuBois, M. R., *J. Am. Chem. Soc.* **2006**, *128*, 3002-3010.
34. Lee, D.-H.; Patel, B. P.; Clot, E.; Eisenstein, O.; Crabtree, R. H., *Chem. Commun.* **1999**, 297-298.
35. Chu, H. S.; Lau, C. P.; Wong, K. Y.; Wong, W. T., *Organometallics* **1998**, *17*, 2768-2777.
36. Lough, A. J.; Park, S.; Ramachandran, R.; Morris, R. H., *J. Am. Chem. Soc.* **1994**, *116*, 8356-8357.
37. Jesse C. Lee, J.; Peris, E.; Rheingold, A. L.; Crabtree, R. H., *J. Am. Chem. Soc.* **1994**, *116*, 11014-11019.
38. Wang, W.-H.; Muckerman, J. T.; Fujita, E.; Himeda, Y., *ACS Catal.* **2013**, 856-860.
39. Wang, W.-H.; Hull, J. F.; Muckerman, J. T.; Fujita, E.; Himeda, Y., *Energy & Environ. Sci.* **2012**, *5*, 7923-7926.
40. Fukuda, Y.; Seto, S.; Furuta, H.; Ebisu, H.; Oomori, Y.; Terashima, S., *J. Med. Chem.* **2001**, *44*, 1396-1406.
41. Umemoto, T.; Nagayoshi, M.; Adachi, K.; Tomizawa, G., *J. Org. Chem.* **1998**, *63*, 3379-3385.
42. Hufziger, K. T.; Thowfeik, F. S.; Charboneau, D. J.; Nieto, I.; Dougherty, W. G.; Kassel, W. S.; Dudley, T. J.; Merino, E. J.; Papish, E. T.; Paul, J. J., *J. Inorg. Biochem.* **2014**, *130*, 103-111.
43. Thompson, A. M. W. C.; Jeffery, J. C.; Liard, D. J.; Ward, M. D., *J. Chem. Soc., Dalton Trans.* **1996**, 879-884.
44. Rawson, J. M.; Winpenny, R. E. P., *Coord. Chem. Rev.* **1995**, *139*, 313-374.
45. Giordano, P. J.; Bock, C. R.; Wrighton, M. S., *J. Am. Chem. Soc.* **1978**, *100*, 6960-6965.
46. Ogo, S.; Abura, T.; Watanabe, Y., *Organometallics* **2002**, *21*, 2964-2969.
47. Dadci, L.; Elias, H.; Frey, U.; Hiirnig, A.; Ulrich Koelle; Merbach, A. E.; Paulustd, H.; Schneider, J. S., *Inorg. Chem.* **1995**, *34*, 306-315.
48. Haga, M., *Inorg. Chimi. Acta* **1983**, *75*, 29-35.
49. Mikkelsen, K.; Nielsen, S. O., *J. Phys. Chem.* **1960**, *64*, 632-637.
50. Liu, Z.; Habtemariam, A.; Pizarro, A. M.; Fletcher, S. A.; Kisova, A.; Vrana, O.; Salassa, L.; Bruijnincx, P. C. A.; Clarkson, G. J.; Brabec, V.; Sadler, P. J., *J. Med. Chem.* **2011**, *54*, 3011-3026.
51. Depasquale, J.; Nieto, I.; Reuther, L. E.; Herbst-Gervasoni, C. J.; Paul, J. J.; Mochalin, V.; Zeller, M.; Thomas, C. M.; Addison, A. W.; Papish, E. T., *Inorg. Chem.* **2013**, *52*, 9175−9183.
52. Krezl, A.; Bal, W., *J. Inorg. Biochem.* **2004**, *98*, 161-166.
53. Moret, S.; Dyson, P. J.; Laurenczy, G., *Nat. Commun.* **2014**, *5*, 1-7.
54. Filonenko, G. A.; van Putten, R.; Schulpen, E. N.; Hensen, E. J. M.; Pidko, E. A., *ChemCatChem* **2014**, *6*, 1526-1530.
55. Jeletic, M. S.; Mock, M. T.; Appel, A. M.; Linehan, J. C., *J. Am. Chem. Soc.* **2013**, *135*, 11533-11536.
56. Schmeier, T. J.; Dobereiner, G. E.; Crabtree, R. H.; Hazari, N., *J. Am. Chem. Soc.* **2011**, *133*, 9274-9277.
57. Azua, A.; Sanz, S.; Peris, E., *Chem. Eur. J.* **2011**, *17*, 3963-3967.
58. Tanaka, R.; Yamashita, M.; Nozaki, K., *J. Am. Chem. Soc.* **2009**, *131*, 14168-14169.

59. Ogo, S.; Kabe, R.; Hayashi, H.; Harada, R.; Fukuzumi, S., *Dalton. Trans.* **2006**, 4657-4663.
60. Hayashi, H.; Ogo, S.; Fukuzumi, S., *Chem. Commun.* **2004**, 2714-2715.
61. *New and Future Developments in Catalysis*. Activation of Carbon Dioxide,Elesevier: Sub, S. L., 2013.
62. Olah, G. A.; Prakash, G. K.; Goeppert, A., *J. Am. Chem. Soc.* **2011**, *133*, 12881-12898.
63. Riduan, S. N.; Zhang, Y., *Dalton Trans.* **2010**, *39*, 3347-3357.
64. Joo, F., *ChemSusChem* **2008**, *1*, 805-808.
65. Enthaler, S., *ChemSusChem* **2008**, *1*, 801-804.
66. Sakakura, T.; Choi, J.-C.; Yasuda, H., *Chem. Rev.* **2007**, *107*, 2365-2387.
67. Jessop, P. G.; Joó, F.; Tai, C.-C., *Coord. Chem. Rev.* **2004**, *248*, 2425-2442.
68. Leitner, W., *Angew. Chem. Int. Ed.* **1995**, *34*, 2207-2221.
69. Myers, T. W.; Berben, L. A., *Chem. Sci.* **2014**, *5*, 2771-2777.
70. Manaka, Y.; Wang, W.-H.; Suna, Y.; Kambayashi, H.; Muckerman, J. T.; Fujita, E.; Himeda, Y., *Catal. Sci. Technol.* **2014**, *4*, 34-37.
71. Hsu, S.-F.; Rommel, S.; Eversfield, P.; Muller, K.; Klemm, E.; Thiel, W. R.; Plietker, B., *Angew. Che. Int. Ed.* **2014**, *53*, 7074-7078.
72. Sponholz, P.; Mellmann, D.; Junge, H.; Beller, M., *ChemSusChem* **2013**, 1172-1176.
73. Sordakis, K.; Beller, M.; Laurenczy, G., *ChemCatChem* **2013**, *6*, 96-99.
74. Maenaka, Y.; Suenobu, T.; Fukuzumi, S., *Energ Environ Sci* **2012**, *5*, 7360-7367.
75. Papp, G.; Csorba, J.; Laurenczy, G.; Joo, F., *Angew. Chem. Int. Ed.* **2011**, *50*, 10433-10435.
76. Czaun, M.; Goeppert, A.; May, R.; Haiges, R.; Prakash, G. K. S.; Olah, G. A., *ChemSusChem* **2011**, *4*, 1241-1248.
77. Loges, B.; Boddien, A.; Gärtner, F.; Junge, H.; Beller, M., *Top. Catal.* **2010**, *53*, 902-914.
78. Loges, B.; Boddien, A.; Junge, H.; Beller, M., *Angew. Chem. Int. Ed.* **2008**, *47*, 3962-3965.
79. Fukuzumi, S.; Kobayashi, T.; Suenobu, T., *ChemSusChem* **2008**, *1*, 827-834.
80. Fellay, C.; Dyson, P. J.; Laurenczy, G., *Angew. Chem. Int. Ed.* **2008**, *47*, 3966-3968.
81. Wang, W. H.; Xu, S.; Manaka, Y.; Suna, Y.; Kambayashi, H.; Muckerman, J. T.; Fujita, E.; Himeda, Y., *ChemSusChem* **2014**, *7*, 1976-1983.
82. Wei, Y.; Xue, D.; Lei, Q.; Wang, C.; Xiao, J., *Green Chemistry* **2013**, *15*, 629-634.
83. Robertson, A.; Matsumoto, T.; Ogo, S., *Dalton. Trans.* **2011**, *40*, 10304-10310.
84. Wang, C.; Li, C.; Wu, X.; Pettman, A.; Xiao, J., *Angew. Chem. Int. Ed.* **2009**, *48*, 6524-6528.
85. Joo, F., *Acc. Chem. Res.* **2002**, *35*, 738-745.
86. Menashe, N.; Salant, E.; Shvo, Y., *J. Organomet. Chem.* **1996**, *514*, 97-102.
87. Saidi, O.; Williams, J. M. J., *Top Organomet. Chem.* **2011**, *34*, 77-106.
88. Sandoval, C. A.; Ohkuma, T.; Utsumi, N.; Tsutsumi, K.; Murata, K.; Noyori, R., *Chem. Asian J.* **2006**, *1*, 102-110.
89. Dwars, T.; Oehme, G., *Adv. Synth. & Catal.* **2002**, *344*, 239-260.
90. Noyori, R.; Ohkuma, T., *Angew. Chem. Int. Ed.* **2001**, *40*, 40-73.
91. Soltani, O.; Ariger, M. A.; Va ´ zquez-Villa, H.; Carreira, E. M., *Org. Lett.* **2010**, *12*, 2893-2895.
92. Wu, X.; Li, X.; Zanotti-Gerosa, A.; Pettman, A.; Liu, J.; Mills, A. J.; Xiao, J., *Chem. Eur. J.* **2008**, *14*, 2209-2222.

93. Hamada, T.; Torii, T.; Izawa, K.; Ikariya, T., *Tetrahedron* **2004**, *60*, 7411-7417.
94. Abura, T.; Ogo, S.; Watanabe, Y.; Fukuzumi, S., *J. Am. Chem. Soc.* **2003**, *125*, 4149-4154.
95. Li, X.; Li, L.; Tang, Y.; Zhong, L.; Cun, L.; Zhu, J.; Liao, J.; Deng, J., *J. Org. Chem.* **2010**, *75*, 2981-2988.
96. Kosal, A. D.; Ashfeld, B. L., *Org. Lett.* **2010**, *12*, 44-47.
97. Tsuchiya, Y.; Hamashima, Y.; Sodeoka, M., *Org. Lett.* **2006**, *8*, 4851-4854.
98. Sharma, A.; Kumar, V.; Sinha, A. K., *Adv. Synth. & Catal.* **2006**, *348*, 354-360.
99. Sato, T.; Watanabe, S.; Kiuchi, H.; Oi, S.; Inoue, Y., *Tetrahedron Lett.* **2006**, *47*, 7703-7705.
100. Selvam, P.; Sonavane, S. U.; Mohapatra, S. K.; Jayaram, R. V., *Tetrahedron Lett.* **2004**, *45*, 3071-3075.
101. Sakaguchi, S.; Yamaga, T.; Ishii, Y., *J. Org. Chem.* **2001**, *66*, 4710-4712.

Supporting Information

Positional Effects of Hydroxy Groups on Catalytic Activity of Proton-Responsive Half-Sandwich Cp*Iridium(III) Complexes

Yuki Suna,[†] *Mehmed Z. Ertem,*[‡] *Wan-Hui Wang,*[†,§,#] *Hide Kambayashi,*[†] *Yuichi Manaka,*[†]

James T. Muckerman,[‡] *Etsuko Fujita,*[‡,*] and *Yuichiro Himeda*[†,§,*]

[†] National Institute of Advanced Industrial Science and Technology, Tsukuba Central 5, 1-1-1 Higashi, Tsukuba, Ibaraki, 305-8565, Japan

[§] Japan Science and Technology Agency, ACT-C, 4-1-8 Honcho, Kawaguchi, Saitama, 332-0012 Japan

[‡] Chemistry Department, Brookhaven National Laboratory, Upton, New York 11973, United States

[#] Current address of W.-H. Wang: School of Petroleum and Chemical Engineering, Dalian University of Technology, Panjin 124221, China

Contents

1. General……..... S2

2. UV-vis absorption measurements ……..... S3

3. ^{1}H-NMR Spectra ……..... S5

4. Description of X-ray structures ……..... S7

5. Computational Methods ……..... S21

6. Cartesian Coordinates of Optimized Structures S23

7. References ……..... S48

1. General

^{1}H NMR spectra were recorded at 25 °C on a Bruker Avance operating at 400 MHz, where chemical shifts were determined with respect to sodium 3-(trimethylsilyl)-1-propanesulfonate (DSS) as an internal reference in D_2O. ESI-MS data were collected on a Waters Micromass ZQ Mass Spectrometer with a 2695/2795 HPLC Separations Module. Elemental analysis were performed using a CE Instruments EA1110. UV-vis absorption spectra were recorded using a quartz cell with a 10-mm path length on a JASCO V-550 UV/VIS Spectrophotometer. pH values were measured with a Thermo scientific Orion 3STAR pH portable meter equipped with an Orion 9103BNWP semi-micro Ag/AgCl electrode. Formate concentrations were monitored by a Tosoh HPLC system equipped with an anion-exclusion column (Tosoh TSKgel SCX(H^+)) and a UV detector (λ = 210 nm), using an aqueous H_3PO_4 solution (20 mM) as an eluent. Concentrations of cyclohexanol and cyclohexanone were determined by a Shimadzu GC-2014 system equipped with PEG-HT 5%, Uniport HT 60/80, 2 m packed column and flame ionization detector (FID) using N_2 carrier gas. The flow rate and volume of gas were measured with a HORIBA STEC Film Flow Meter VP-1 and SHINAGAWA Wet Gas Meter W-NK-0.5, respectively.

2. UV-vis absorption measurements

Both acidic and basic solutions containing 0.1 or 0.2 mM complexes were prepared using measuring flasks, the pH values of which were adjusted to 2 or 0.3 with H_2SO_4 and 12 with NaOH. The measurements were started from low pH, then aliquots of the basic solution were directly added into the quartz cell and the resulting pH value was measured. Nonlinear fittings of absorption changes at a single wavelength were performed in Origin 9.0 using a Boltzmann function, and the inflection point was regarded as the average of the two **DHBP** pK_a values (at lower pH) or the pK_a of the aqua ligand (at higher pH).

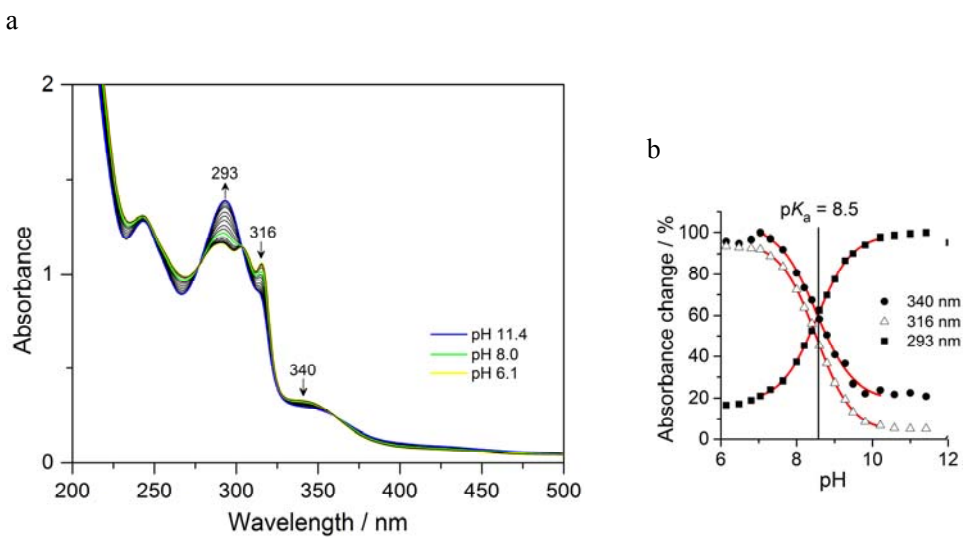

Figure S1. (a) UV-vis absorption spectra of [Cp*Ir(bpy)(OH_2)]SO_4 (0.1 mM) in a pH titration and (b) absorbance changes at single wavelength as a function of pH, Boltzmann fits are depicted in red line.

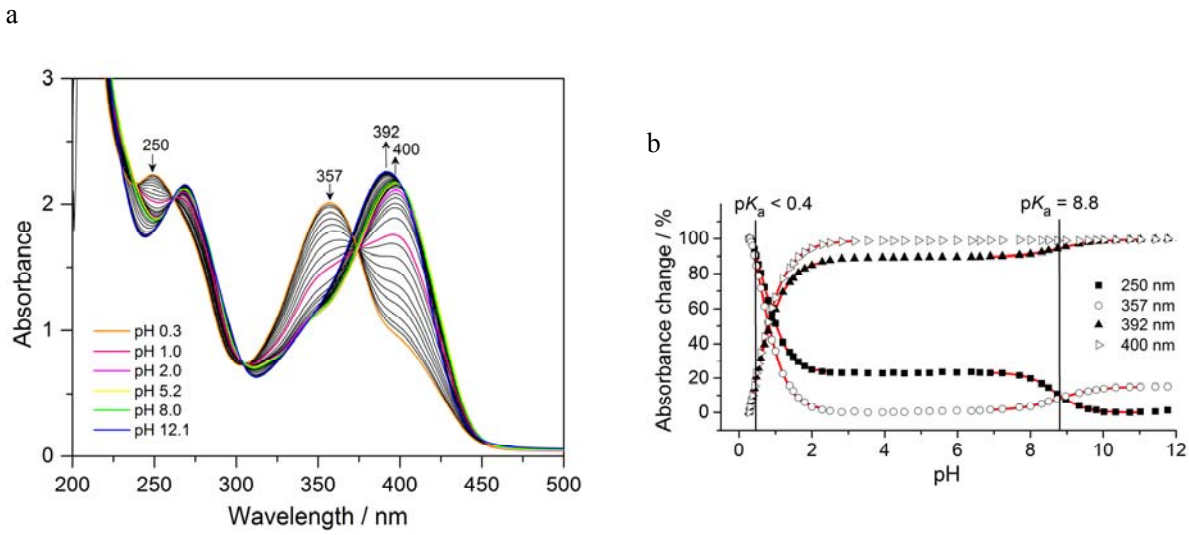

Figure S2. (a) UV-vis absorption spectra of [Cp*Ir(**3DHBP**)(OH_2)]SO_4 (0.1 mM) in a pH titration and (b) absorbance changes at single wavelength as a function of pH, Boltzmann fits are depicted in red line.

a

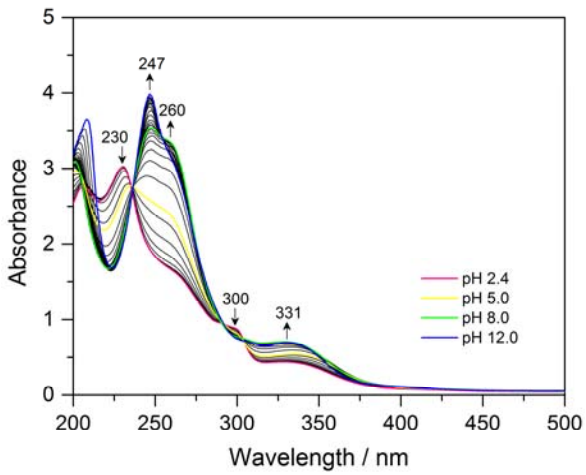

b

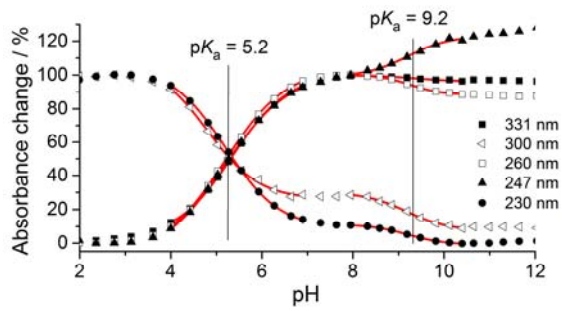

Figure S3. (a) UV-vis absorption spectra of [Cp*Ir(**4DHBP**)(OH_2)]SO_4 (0.1 mM) in a pH titration and (b) absorbance changes at single wavelength as a function of pH with Boltzmann fits are depicted in red lines.

a

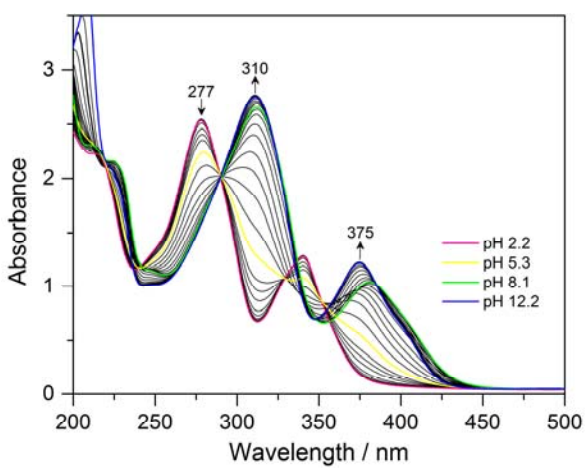

b

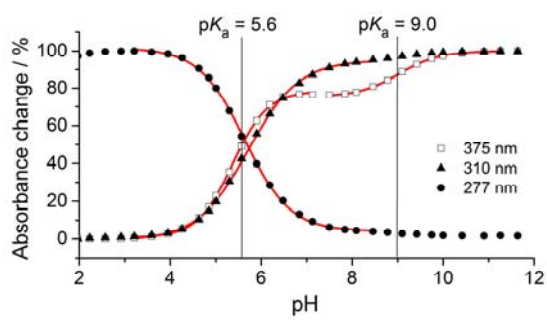

Figure S4. (a) UV-vis absorption spectra of [Cp*Ir(**5DHBP**)(OH_2)]SO_4 (0.1 mM) in a pH titration and (b) absorbance changes at single wavelength as a function of pH with Boltzmann fits are depicted in red lines.

a

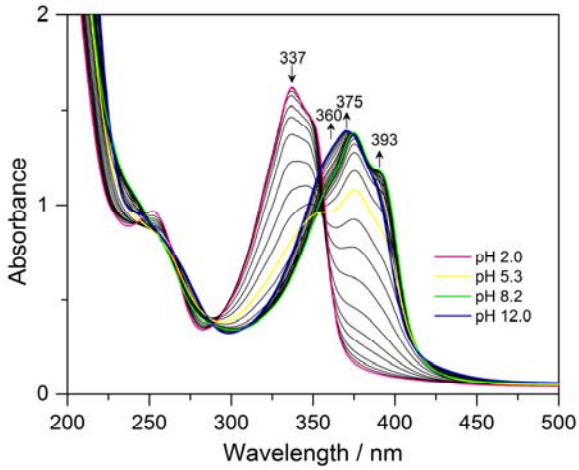

b

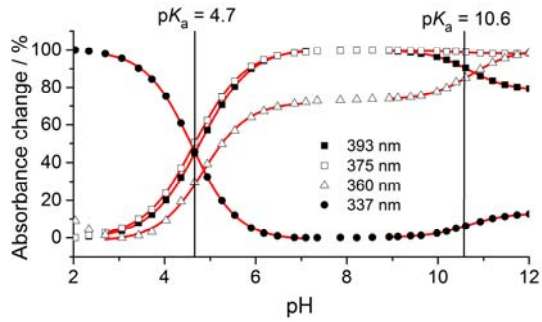

Figure S5. (a) UV-vis absorption spectra of [Cp*Ir(**6DHBP**)(OH_2)]SO_4 (0.1 mM) in a pH titration and (b) absorbance changes at single wavelength as a function of pH with Boltzmann fits are depicted in red lines.

3. ^{1}H-NMR Spectra

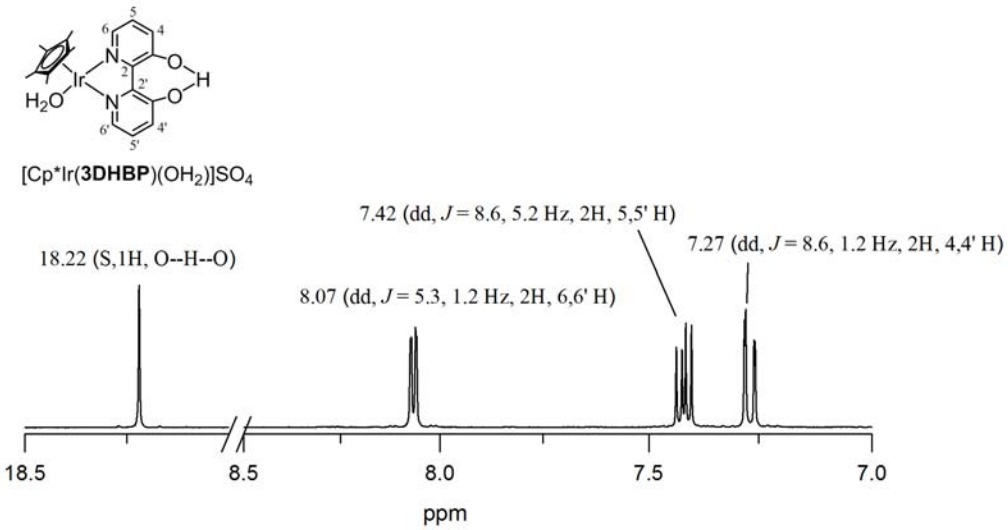

Figure S6. ^{1}H NMR spectrum of **3DHBP** ligand of the Ir complex in DMSO-d_6.

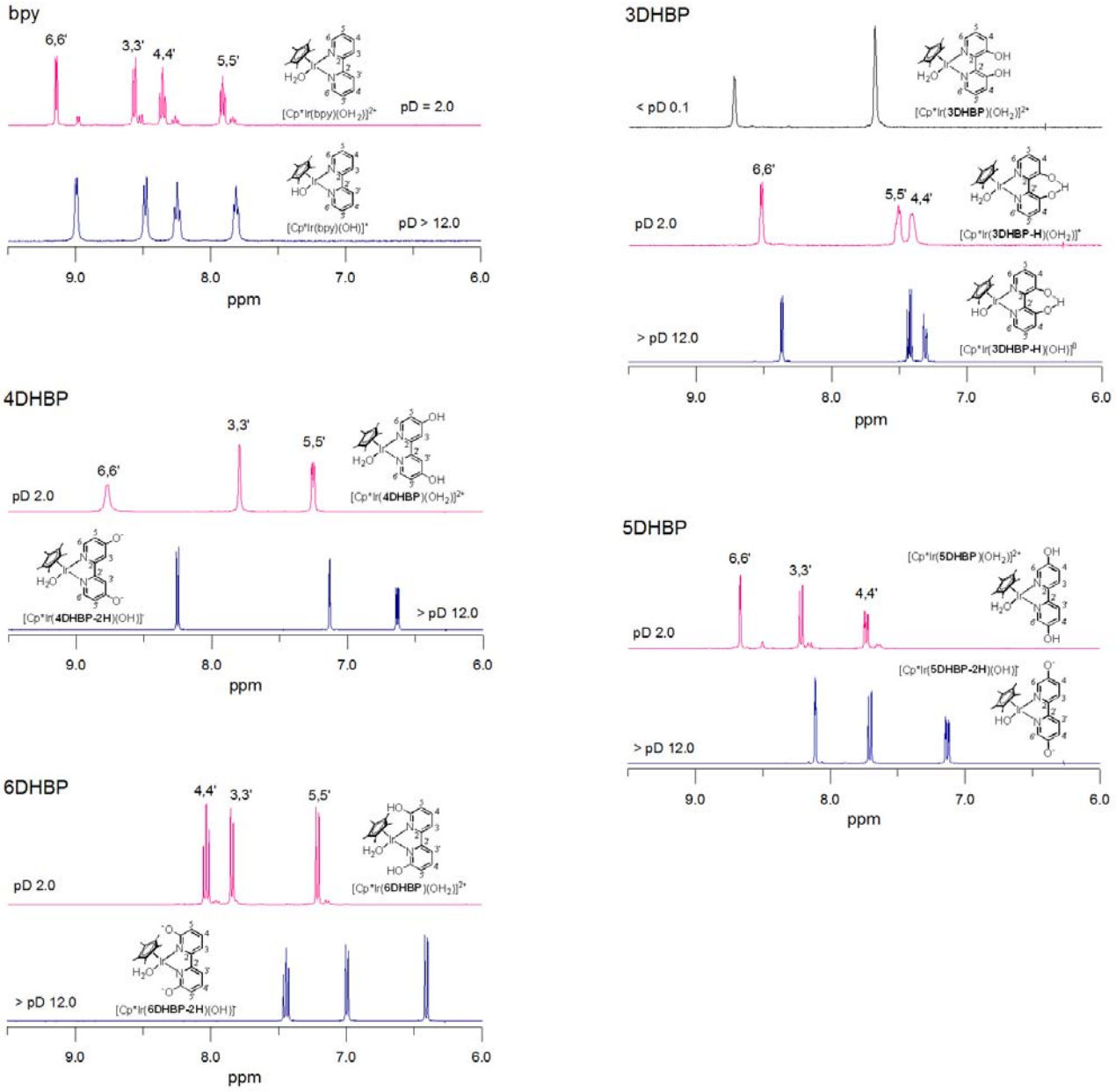

Figure S7. ^{1}H NMR spectra of the bpy and **DHBP** ligands of the complexes in various pD solution.

Table S1. Summary of chemical shifts of the protons of the bpy and **DHBP** ligands in protonated and deprotonated complex.

	3,3′-position	4,4′-position	5,5′-position	6,6′-position
$[Cp^*Ir(bpy)(OH_2)]^{2+}$ [a]	8.57 (d, J = 8.1 Hz, 2H)	8.36 (td, J =7.9, 1.4 Hz, 2H)	7.91 (ddd, J = 7.3, 5.6, 1.3 Hz, 2H)	9.14 (dd, J = 5.9, 1.2 Hz, 2H)
$[Cp^*Ir(bpy)(OH)]^{+}$ [c]	8.48 (d, J = 8.2 Hz, 2H)	8.25 (t, J = 7.9 Hz, 2H)	7.81 (t, J = 6.7 Hz, 2H)	8.99 (d, J = 5.6 Hz, 2H)

[Cp*Ir(**3DHBP**)(OH_2)]$^{2+}$ [b]	–	7.68 (s, 4H)	7.68 (s, 4H)	8.72 (d, *J* = 2.9 Hz, 2H)
[Cp*Ir(**3DHBP–H$^+$**)(OH_2)]$^{+}$ [a]	–	7.41 (d, *J* = 7.6 Hz, 2H)	7.51 (d, *J* = 6.0 Hz, 2H)	8.52 (d, *J* = 5.2 Hz, 2H)
[Cp*Ir(**3DHBP–H$^+$**)(OH)]^{0} [c]	–	7.31 (ddd, *J* = 8.5, 2.4, 1.2 Hz, 2H)	7.42 (dd, *J* = 8.5, 5.2 Hz, 2H)	8.37 (dd, *J* = 5.3, 1.3 Hz, 2H)
[Cp*Ir(**4DHBP**)(OH_2)]$^{2+}$ [a]	7.79 (d, *J* = 2.6 Hz, 2H)	–	7.25 (dd, *J* = 6.5, 2.6 Hz, 2H)	8.77 (s, 2H)
[Cp*Ir(**4DHBP–2H$^+$**)(OH)]$^{-}$ [c]	7.13 (d, *J* = 2.7 Hz, 2H)	–	6.63 (dd, *J* = 6.6, 2.6 Hz, 2H)	8.25 (d, *J* = 6.6 Hz)
[Cp*Ir(**5DHBP**)(OH_2)]$^{2+}$ [a]	8.22 (d, *J* = 9.0 Hz, 2H)	7.73 (dd, *J* = 9.0, 2.6 Hz, 2H)	–	8.67 (d, *J* = 2.6 Hz, 2H)
[Cp*Ir(**5DHBP–2H$^+$**)(OH)]$^{-}$ [c]	7.71 (d, *J* = 9.0 Hz, 2H)	7.13 (dd, *J* = 8.9, 2.7 Hz, 2H)	–	8.11 (d, *J* = 2.6 Hz, 2H)
[Cp*Ir(**6DHBP**)(OH_2)]$^{2+}$ [a]	7.85 (d, *J* = 7.5 Hz, 2H)	8.03 (t, *J* = 8.0 Hz, 2H)	7.21 (d, *J* = 8.3 Hz, 2H)	–
[Cp*Ir(**6DHBP–2H$^+$**)(OH)]$^{-}$ [c]	6.99 (d, *J* = 7.4 Hz, 2H)	7.44 (ddd, *J* = 8.2, 7.3, 0.8 Hz, 2H)	6.41 (dd, *J* = 8.5, 0.9 Hz, 1H)	–

[a] Measured in D_2O/D_2SO_4 (pD 2.0). [b] Measured in D_2O/ D_2SO_4 (pD < 0.1). [c] Measured in D_2O/KOD (pD > 12.0).

4. Description of X-ray crystal structures

Crystal structure determination and refinement of the structure

X-ray single crystal analysis was performed using a Bruker SMART APEX II.[1] A crystal grown in its aqueous solution was mounted on a grass rod and transferred to the diffractometer for the collection of diffraction data. The data were corrected for absorption effects using the multi-scan methods (SADABS).[2] The structure was solved (XS)[3] and refined (XL)[4] using the Bruker SHELXL software package. In the least-squares refinement, anisotropic temperature parameters were used for all the non-hydrogen atoms. Hydrogen atoms attached to the carbon atoms were placed at calculated positions using a riding model, while ones attached to the oxygen atoms of the bpy ligand, aqua ligand and solvent water were determined by difference Fourier maps and refined freely or under constrained conditions. Crystal data and information about the data collection are provided in Table S1–S20.

Table S2. Crystal data and structure refinement for [Cp*Ir(**3DHBP**)(OH_2)]$_2$(HSO_4)$_4$(H_2O)$_2$.

Empirical formula	C40 H60 Ir2 N4 O25 S4
Formula weight	1509.64
Temperature	183(2) K
Wavelength	0.71073 Å
Crystal system	Triclinic

Space group	$P\bar{1}$	
Unit cell dimensions	a = 13.4731(7) Å	α= 106.0120(10)°.
	b = 13.5878(7) Å	β= 98.1890(10)°.
	c = 14.8653(8) Å	γ = 100.2180(10)°.
Volume	2521.1(2) $Å^3$	
Z	2	
Density (calculated)	1.989 Mg/m^3	
Absorption coefficient	5.531 mm^{-1}	
F(000)	1492	
Crystal size	0.30 × 0.20 × 0.10 mm^3	
Theta range for data collection	1.46 to 26.00°.	
Index ranges	$-16 \leq h \leq 16$, $-16 \leq k \leq 16$, $-18 \leq l \leq 18$	
Reflections collected	21715	
Independent reflections	9786 [R(int) = 0.0175]	
Completeness to theta= 26.00°	98.7 %	
Absorption correction	Semi-empirical from equivalents	
Max. and min. transmission	0.6134 and 0.2933	
Refinement method	Full-matrix least-squares on F^2	
Data / restraints / parameters	9786 / 31 / 738	
Goodness-of-fit on F^2	1.045	
Final R indices [I>2sigma(I)]	R1 = 0.0226, wR2 = 0.0572	
R indices (all data)	R1 = 0.0238, wR2 = 0.0584	
Largest diff. peak and hole	1.259 and -1.275 e.$Å^{-3}$	

Table S3. Atomic coordinates (× 10^4) and equivalent isotropic displacement parameters ($Å^2$ × 10^3) for $[Cp^*Ir(\mathbf{3DHBP})(OH_2)]_2(HSO_4)_4(H_2O)_2$. U(eq) is defined as one third of the trace of the orthogonalized U^{ij} tensor.

	x	y	z	U(eq)
C(1)	9608(3)	7627(3)	1402(3)	26(1)
C(2)	9244(3)	7588(3)	475(3)	29(1)
C(3)	8860(2)	6624(2)	-197(2)	27(1)
C(4)	8831(2)	5705(2)	57(2)	25(1)
C(5)	9214(2)	5774(3)	1015(2)	18(1)
C(6)	9272(2)	4912(3)	1443(2)	19(1)
C(7)	8995(3)	3820(3)	1011(2)	27(1)
C(8)	9190(3)	3147(3)	1530(3)	34(1)
C(9)	9608(3)	3538(3)	2485(3)	30(1)
C(10)	9835(3)	4604(3)	2898(3)	26(1)
C(11)	11188(3)	8448(3)	3763(2)	25(1)
C(12)	10900(3)	8023(3)	4492(2)	24(1)
C(13)	11255(3)	7079(3)	4408(2)	23(1)
C(14)	11786(3)	6918(3)	3621(2)	24(1)
C(15)	11747(3)	7760(3)	3230(2)	25(1)
C(16)	11046(4)	9485(3)	3666(3)	39(1)
C(17)	10328(3)	8496(3)	5223(3)	34(1)
C(18)	11191(3)	6467(3)	5109(3)	31(1)

C(19)	12337(3)	6051(3)	3308(3)	32(1)
C(20)	12264(3)	7950(4)	2446(3)	37(1)
C(21)	4715(3)	4523(3)	6692(3)	32(1)
C(22)	4520(3)	3446(3)	6416(3)	36(1)
C(23)	4864(3)	2983(3)	7063(3)	34(1)
C(24)	5388(3)	3589(3)	7976(3)	27(1)
C(25)	5543(3)	4697(3)	8259(2)	22(1)
C(26)	6016(3)	5495(3)	9210(2)	22(1)
C(27)	6320(3)	5327(3)	10093(3)	26(1)
C(28)	6697(3)	6185(3)	10915(3)	29(1)
C(29)	6791(3)	7193(3)	10864(3)	30(1)
C(30)	6488(3)	7324(3)	9987(3)	27(1)
C(31)	4490(3)	7758(3)	8426(2)	23(1)
C(32)	3976(3)	6973(3)	7541(3)	24(1)
C(33)	4547(3)	7130(3)	6814(2)	24(1)
C(34)	5392(3)	8009(3)	7261(2)	23(1)
C(35)	5380(3)	8389(3)	8257(2)	23(1)
C(36)	4123(3)	7942(3)	9346(3)	34(1)
C(37)	3000(3)	6176(3)	7391(3)	36(1)
C(38)	4239(3)	6575(3)	5758(3)	37(1)
C(39)	6171(3)	8453(3)	6774(3)	32(1)
C(40)	6093(3)	9356(3)	8963(3)	33(1)
Ir(1)	10213(1)	6876(1)	3071(1)	17(1)
Ir(2)	5500(1)	6760(1)	7923(1)	16(1)
N(1)	9606(2)	6758(2)	1658(2)	20(1)
N(2)	9693(2)	5271(2)	2399(2)	19(1)
N(3)	5203(2)	5130(2)	7583(2)	23(1)
N(4)	6098(2)	6509(2)	9192(2)	20(1)
O(1)	8611(2)	6780(2)	3163(2)	28(1)
O(2)	8429(3)	4808(2)	-661(2)	46(1)
O(3)	8549(3)	3394(2)	75(2)	49(1)
O(4)	6972(2)	6526(2)	7595(2)	27(1)
O(5)	5774(3)	3112(2)	8586(2)	40(1)
O(6)	6244(3)	4385(2)	10236(2)	47(1)
O(7)	8084(3)	610(3)	1070(2)	59(1)
O(8)	8204(4)	-297(3)	2213(3)	71(1)
O(9)	6546(3)	-279(3)	1409(2)	55(1)
O(10)	7621(3)	1318(2)	2558(3)	54(1)
O(11)	1764(3)	1638(3)	1409(2)	50(1)
O(12)	1129(3)	-58(2)	1570(2)	49(1)
O(13)	788(3)	1473(3)	2623(2)	55(1)
O(14)	5(3)	896(3)	944(3)	63(1)
O(15)	8715(3)	6161(3)	5824(3)	63(1)
O(16)	7669(3)	6034(3)	4356(2)	58(1)
O(17)	6893(2)	6070(2)	5704(2)	41(1)
O(18)	8019(3)	7635(2)	5625(3)	50(1)
O(19)	6789(4)	-331(4)	4545(3)	85(1)
O(20)	6671(4)	1073(4)	3888(3)	92(2)
O(21)	6113(3)	1118(3)	5321(3)	72(1)
O(22)	5183(3)	-186(3)	3862(2)	48(1)
O(16S)	2005(2)	8578(2)	436(2)	36(1)
O(17S)	5125(2)	1157(2)	8069(2)	36(1)
O(18S)	8132(4)	8617(4)	3485(4)	76(1)
S(1)	7595(1)	282(1)	1779(1)	32(1)
S(2)	978(1)	986(1)	1690(1)	30(1)
S(3)	7816(1)	6425(1)	5372(1)	27(1)
S(4)	6224(1)	367(1)	4356(1)	45(1)

Table S4. Crystal data and structure refinement for [Cp*Ir(**3DHBP–H⁺**)(OH_2)](SO_3CF_3).

Empirical formula	C21 H24 F3 Ir N2 O6 S	
Formula weight	681.71	
Temperature	183(2) K	
Wavelength	0.71073 Å	
Crystal system	Monoclinic	
Space group	$P2_1/n$	
Unit cell dimensions	a = 7.9424(3) Å	α= 90°.
	b = 18.4667(7) Å	β= 103.01°.
	c = 16.4824(6) Å	γ = 90°.
Volume	2355.41(15) $Å^3$	
Z	4	
Density (calculated)	1.922 Mg/m^3	
Absorption coefficient	5.824 mm^{-1}	
F(000)	1328	
Crystal size	0.30 × 0.10 × 0.10 mm^3	
Theta range for data collection	1.68 to 27.00°.	
Index ranges	$-10 \leq h \leq 9$, $-23 \leq k \leq 23$, $-21 \leq l \leq 21$	
Reflections collected	21518	
Independent reflections	5129 [R(int) = 0.0202]	
Completeness to theta=27.00°	99.8 %	
Absorption correction	Semi-empirical from equivalents	
Max. and min. transmission	0.5935 and 0.2740	
Refinement method	Full-matrix least-squares on F^2	
Data / restraints / parameters	5129 / 7 / 324	
Goodness-of-fit on F^2	1.062	
Final R indices [I>2sigma(I)]	R1 = 0.0164, wR2 = 0.0408	
R indices (all data)	R1 = 0.0194, wR2 = 0.0416	
Largest diff. peak and hole	1.585 and -0.358 e.$Å^{-3}$	

Table S5. Atomic coordinates (× 10^4) and equivalent isotropic displacement parameters ($Å^2$ × 10^3) for [Cp*Ir(**3DHBP–H⁺**)(OH_2)](SO_3CF_3). U(eq) is defined as one third of the trace of the orthogonalized U^{ij} tensor.

	x	y	z	U(eq)
C(1)	10162(3)	-456(1)	1875(2)	26(1)
C(2)	10600(4)	-1053(1)	1457(2)	31(1)
C(3)	9860(4)	-1135(1)	628(2)	28(1)
C(4)	8691(3)	-620(1)	198(2)	23(1)
C(5)	8245(3)	-27(1)	662(1)	20(1)
C(6)	7040(3)	573(1)	344(1)	20(1)
C(7)	5964(3)	650(1)	-463(2)	24(1)
C(8)	4889(3)	1258(2)	-625(2)	28(1)
C(9)	4878(4)	1769(2)	-24(2)	31(1)

C(10)	5960(4)	1674(1)	751(2)	28(1)
C(11)	9374(3)	1507(2)	3305(2)	27(1)
C(12)	9399(4)	743(2)	3446(2)	29(1)
C(13)	7655(4)	481(2)	3153(2)	33(1)
C(14)	6580(3)	1085(2)	2843(2)	32(1)
C(15)	7640(3)	1727(2)	2928(2)	29(1)
C(16)	10925(4)	1993(2)	3495(2)	39(1)
C(17)	10918(4)	321(2)	3916(2)	45(1)
C(18)	7063(5)	-284(2)	3205(2)	53(1)
C(19)	4653(4)	1072(2)	2536(2)	47(1)
C(20)	7041(4)	2493(2)	2770(2)	41(1)
C(21)	6049(5)	1468(2)	5137(2)	52(1)
F(1)	5707(4)	2020(1)	4613(1)	87(1)
F(2)	4708(4)	1039(2)	4986(2)	104(1)
F(3)	7363(5)	1115(2)	4943(2)	98(1)
Ir(1)	8497(1)	952(1)	2121(1)	19(1)
N(1)	9008(3)	33(1)	1489(1)	21(1)
N(2)	6992(3)	1096(1)	929(1)	23(1)
O(1)	10525(2)	1400(1)	1628(1)	28(1)
O(2)	8079(2)	-700(1)	-604(1)	31(1)
O(3)	5847(3)	182(1)	-1078(1)	35(1)
O(4)	6819(4)	1100(1)	6672(2)	55(1)
O(5)	8090(3)	2200(2)	6258(2)	73(1)
O(6)	5081(3)	2171(1)	6285(2)	57(1)
S(1)	6595(1)	1764(1)	6214(1)	35(1)

Table S6. Crystal data and structure refinement for [Cp*Ir(**3DHBP–H$^+$**)(OH)](H_2O).

Empirical formula	C20 H25 Ir N2 O4	
Formula weight	549.64	
Temperature	183(2) K	
Wavelength	0.71073 Å	
Crystal system	Monoclinic	
Space group	$P2_1/n$	
Unit cell dimensions	a = 7.8579(4) Å	α= 90°.
	b = 14.4489(7) Å	β= 103.00°.
	c = 16.5260(8) Å	γ = 90°.
Volume	1828.23(16) $Å^3$	
Z	4	
Density (calculated)	1.997 Mg/m^3	
Absorption coefficient	7.332 mm^{-1}	
F(000)	1072	
Crystal size	0.20 × 0.15 × 0.10 mm^3	
Theta range for data collection	1.89 to 27.00°.	
Index ranges	$-9 \le h \le 9$, $-18 \le k \le 18$, $-18 \le l \le 21$	
Reflections collected	14807	
Independent reflections	3960 [R(int) = 0.0146]	
Completeness to theta=27.00°	99.5 %	
Absorption correction	Semi-empirical from equivalents	

Max. and min. transmission	0.5281 and 0.3223
Refinement method	Full-matrix least-squares on F^2
Data / restraints / parameters	3960 / 7 / 264
Goodness-of-fit on F^2	1.059
Final R indices [I>2sigma(I)]	R1 = 0.0154, wR2 = 0.0383
R indices (all data)	R1 = 0.0160, wR2 = 0.0387
Largest diff. peak and hole	1.037 and -0.802 e.Å^{-3}

Table S7. Atomic coordinates (× 10^4) and equivalent isotropic displacement parameters (Å^2 × 10^3) for [Cp*Ir(**3DHBP–H$^+$**)(OH)](H_2O). U(eq) is defined as one third of the trace of the orthogonalized U^{ij} tensor.

	x	y	z	U(eq)
C(1)	2450(3)	5592(2)	609(1)	19(1)
C(2)	2498(3)	4915(2)	18(1)	21(1)
C(3)	3603(3)	4176(2)	226(1)	20(1)
C(4)	4679(3)	4105(2)	1030(2)	18(1)
C(5)	4575(3)	4818(2)	1609(1)	14(1)
C(6)	5668(3)	4912(2)	2464(1)	14(1)
C(7)	6824(3)	4237(2)	2921(1)	17(1)
C(8)	7752(3)	4471(2)	3724(1)	20(1)
C(9)	7585(3)	5339(2)	4045(2)	22(1)
C(10)	6439(3)	5966(2)	3577(1)	20(1)
C(11)	979(3)	6753(2)	2394(2)	17(1)
C(12)	1179(3)	7441(2)	1787(1)	17(1)
C(13)	2530(3)	8060(2)	2177(2)	17(1)
C(14)	3218(3)	7759(2)	3014(1)	17(1)
C(15)	2206(3)	6958(2)	3152(1)	17(1)
C(16)	-396(3)	6017(2)	2249(2)	25(1)
C(17)	42(3)	7550(2)	934(2)	25(1)
C(18)	3126(4)	8896(2)	1787(2)	26(1)
C(19)	4563(4)	8273(2)	3643(2)	25(1)
C(20)	2354(4)	6467(2)	3966(2)	24(1)
Ir(1)	3610(1)	6664(1)	2182(1)	12(1)
N(1)	3454(2)	5541(1)	1376(1)	15(1)
N(2)	5482(2)	5750(1)	2821(1)	15(1)
O(1)	5481(2)	7013(1)	1529(1)	19(1)
O(2)	5767(3)	3401(1)	1190(1)	33(1)
O(3)	7044(3)	3408(1)	2639(1)	26(1)
O(1S)	3797(3)	7830(1)	106(1)	36(1)

Table S8. Selected bond lengths [Å] and angles [°] for [Cp*Ir(**3DHBP**)(OH_2)]$_2$$HSO_4$, [Cp*Ir(**3DHBP–H**)($OH_2$)]$SO_3CF_3$ and [Cp*Ir(**3DHBP–H**)(OH)].

	[Cp*Ir(**3DHBP**)(OH_2)]$_2$ (HSO_4)$_4$(H_2O)$_2$	[Cp*Ir(**3DHBP–H$^+$**)(OH_2)] (SO_3CF_3)	[Cp*Ir(**3DHBP–H$^+$**)(OH)] (H_2O)

C(4)-O(2)	1.342(4)	1.309(3)	1.318(3)
C(5)-C(6)	1.487(5)	1.482(3)	1.485(3)
C(7)-O(3)	1.351(4)	1.320(3)	1.311(3)
Ir(1)-N(2)	2.073(3)	2.075(2)	2.072(2)
Ir(1)-N(1)	2.093(3)	2.079(2)	2.080(2)
Ir(1)-O(1)	2.165(3)	2.128(2)	2.086(2)
O(2)-H(2O)	0.822(10)	0.802(10)	0.799(10)
O(3)-H(3O)	0.822(10)	0.802(10)	0.800(10)
N(2)-Ir(1)-N(1)	75.95(11)	76.44(8)	76.29(7)

Table S9. Crystal data and structure refinement for [Cp*Ir(**4DHBP**)$(OH_2)]_2(SO_4)_2(H_2O)_5$.

Empirical formula	C40 H58 Ir2 N4 O19 S2	
Formula weight	1347.4	
Temperature	243(2) K	
Wavelength	0.71073 Å	
Crystal system	Monoclinic	
Space group	C2/c	
Unit cell dimensions	a = 28.6467(11) Å	α = 90°.
	b = 11.0302(4) Å	β = 133.5180(10)°.
	c = 19.8652(7) Å	γ = 90°.
Volume	4551.8(3) $Å^3$	
Z	4	
Density (calculated)	1.963 Mg/m^3	
Absorption coefficient	6.016 mm^{-1}	
F(000)	2652	
Crystal size	0.30 × 0.10 × 0.05 mm^3	
Theta range for data collection	1.96 to 26.00°.	
Index ranges	$-35 \leq h \leq 35$, $-13 \leq k \leq 13$, $-24 \leq l \leq 24$	
Reflections collected	19035	
Independent reflections	4459 [R(int) = 0.0192]	
Completeness to theta=26.00°	100.0 %	
Absorption correction	Semi-empirical from equivalents	
Max. and min. transmission	0.7538 and 0.2666	
Refinement method	Full-matrix least-squares on F^2	
Data / restraints / parameters	4459 / 0 / 309	
Goodness-of-fit on F^2	1.042	
Final R indices [I>2sigma(I)]	R1 = 0.0160, wR2 = 0.0406	
R indices (all data)	R1 = 0.0177, wR2 = 0.0412	
Largest diff. peak and hole	1.110 and -0.699 e.$Å^{-3}$	

Table S10. Atomic coordinates ($\times 10^4$) and equivalent isotropic displacement parameters ($Å^2 \times 10^3$) for [Cp*Ir(**4DHBP**)$(OH_2)]_2(SO_4)_2(H_2O)_5$. U(eq) is defined as one third of the trace of the orthogonalized U^{ij} tensor.

	x	y	z	U(eq)
C(1)	980(1)	3401(3)	7884(2)	26(1)
C(2)	911(1)	4035(3)	8406(2)	27(1)
C(3)	1208(1)	3597(2)	9282(2)	23(1)
C(4)	1582(1)	2544(2)	9607(2)	21(1)
C(5)	1625(1)	1947(2)	9036(2)	19(1)
C(6)	2013(1)	840(2)	9304(2)	20(1)
C(7)	2372(1)	263(2)	10146(2)	23(1)
C(8)	2748(1)	-743(2)	10339(2)	25(1)
C(9)	2752(1)	-1098(2)	9667(2)	29(1)
C(10)	2376(1)	-491(2)	8841(2)	26(1)
C(11)	360(1)	786(3)	6310(2)	28(1)
C(12)	748(1)	-242(3)	6535(2)	28(1)
C(13)	1114(1)	36(2)	6301(2)	25(1)
C(14)	937(1)	1235(2)	5916(2)	26(1)
C(15)	475(1)	1713(3)	5919(2)	27(1)
C(16)	-105(2)	866(4)	6420(3)	48(1)
C(17)	761(2)	-1417(3)	6925(3)	49(1)
C(18)	1535(2)	-824(3)	6337(2)	41(1)
C(19)	1199(2)	1870(3)	5568(2)	41(1)
C(20)	134(2)	2903(3)	5517(2)	42(1)
Ir(1)	1350(1)	1293(1)	7339(1)	18(1)
N(1)	1313(1)	2359(2)	8170(1)	20(1)
N(2)	1998(1)	454(2)	8639(2)	20(1)
O(1)	2159(1)	2427(2)	7934(1)	24(1)
O(2)	1111(1)	4212(2)	9753(1)	32(1)
O(3)	3108(1)	-1364(2)	11129(2)	37(1)
O(4)	1809(1)	6276(2)	6453(2)	32(1)
O(5)	1817(1)	4240(2)	6854(2)	46(1)
O(6)	1040(1)	5650(3)	6516(2)	51(1)
O(7)	2161(1)	5860(2)	7921(2)	46(1)
O(1S)	-42(1)	4228(2)	3560(2)	54(1)
O(2S)	0	2654(5)	2500	112(2)
S(1)	1694(1)	5495(1)	6941(1)	24(1)
O(3S)	1082(6)	8395(11)	8813(7)	308(6)

Table S11. Crystal data and structure refinement for [Cp*Ir(**4DHBP–2H$^+$**)$(OH_2)](H_2O)_4$.

Empirical formula	C20 H31 Ir N2 O7	
Formula weight	603.6596	
Temperature	243(2) K	
Wavelength	0.71073 Å	
Crystal system	Monoclinic	
Space group	C2/m	
Unit cell dimensions	a = 20.2790(9) Å	α= 90°.

	b = 11.6509(5) Å	β= 96.6411(5)°.
	c = 9.7011(4) Å	γ = 90.0°.
Volume	2276.69(17) $Å^3$	
Z	4	
Density (calculated)	1.750 Mg/m^3	
Absorption coefficient	5.906 mm^{-1}	
F(000)	1192	
Crystal size	0.20 × 0.10 × 0.07 mm^3	
Theta range for data collection	2.02 to 27.00°.	
Index ranges	$-25 \leq h \leq 25$, $-14 \leq k \leq 14$, $-12 \leq l \leq 12$	
Reflections collected	9769	
Independent reflections	2557 [R(int) = 0.0266]	
Completeness to theta = 27.00°	98.0 %	
Absorption correction	Semi-empirical from equivalents	
Max. and min. transmission	0.8198 and 0.5894	
Refinement method	Full-matrix least-squares on F^2	
Data / restraints / parameters	2557 / 4 / 159	
Goodness-of-fit on F^2	1.045	
Final R indices [I>2sigma(I)]	R1 = 0.0211, wR2 = 0.0596	
R indices (all data)	R1 = 0.0214, wR2 = 0.0598	
Largest diff. peak and hole	1.875 and -1.183 e.$Å^{-3}$	

Table S12. Atomic coordinates (× 10^4) and equivalent isotropic displacement parameters ($Å^2$ × 10^3) for [Cp*Ir(**4DHBP–2H⁺**)(OH_2)](H_2O)$_4$. U(eq) is defined as one third of the trace of the orthogonalized U^{ij} tensor.

	x	y	z	U(eq)
Ir(1)	-1474(1)	5000	2544(1)	13(1)
O(1)	-3895(1)	8107(2)	634(3)	22(1)
O(1S)	-5000	13169(3)	10000	27(1)
O(2S)	-203(2)	10000	1765(5)	45(1)
O(3)	-1489(2)	5000	356(3)	16(1)
O(3S)	-3511(3)	5000	7188(12)	129(4)
O(4S)	605(9)	0	4205(11)	220(7)
N(1)	-2270(1)	6120(2)	2030(3)	15(1)
C(1)	-2233(2)	7276(3)	2028(3)	17(1)
C(2)	-2760(1)	7976(3)	1590(3)	17(1)
C(3)	-3384(1)	7490(3)	1088(3)	16(1)
C(4)	-3412(1)	6280(3)	1100(3)	18(1)
C(5)	-2861(1)	5632(3)	1554(3)	16(1)
C(6)	-402(2)	5000	3020(4)	18(1)
C(7)	-669(2)	3996(3)	3593(3)	18(1)
C(8)	-1113(2)	4386(3)	4570(3)	22(1)
C(9)	62(2)	5000	1925(5)	24(1)
C(10)	-480(2)	2783(3)	3303(4)	28(1)
C(11)	-1492(2)	3625(4)	5446(4)	38(1)

Table S13. Selected bond lengths [Å] and angles [°] for [Cp*Ir(**4DHBP**)(OH_2)]$_2$(SO_4)$_5$(H_2O) and [Cp*Ir(**4DHBP–2H$^+$**)(OH_2)]$_4$(H_2O).

[Cp*Ir(**4DHBP**)(OH_2)]$_2$(SO_4)$_2$(H_2O)$_5$		[Cp*Ir(**4DHBP–2H$^+$**)(OH_2)](H_2O)$_4$	
C(3)-O(2)	1.329(3)	C(3)-O(1)	1.295(4)
C(5)-C(6)	1.483(4)	C(5)-C(5)	1.473(6)
C(8)-O(3)	1.329(3)	–	–
Ir(1)-N(1)	2.089(2)	Ir(1)-N(1)	2.090(3)
Ir(1)-N(2)	2.091(2)	–	–
Ir(1)-O(1)	2.137(2)	Ir(1)-O(3)	2.120(3)
O(2)-H(2O)	0.830	–	–
O(3)-H(3O)	0.831	–	–
N(1)-Ir(1)-N(2)	75.96(8)	N(1)#1-Ir(1)-N(1)	77.23(14)

Symmetry transformations used to generate equivalent atoms with #1.

Table S14. Crystal data and structure refinement for [Cp*Ir(**5DHBP**)(OH_2)](SO_4)(H_2O)$_3$.

Empirical formula	C20 H31 Ir N2 O10 S	
Formula weight	683.76	
Temperature	153(2) K	
Wavelength	0.71073 Å	
Crystal system	Triclinic	
Space group	$P\bar{1}$	
Unit cell dimensions	a = 10.2412(5) Å	α= 62.404(1)°.
	b = 11.2720(5) Å	β= 81.467(1)°.
	c = 11.5396(5) Å	γ = 81.479(1)°.
Volume	1162.70(9) Å^3	
Z	2	
Density (calculated)	1.953 Mg/m^3	
Absorption coefficient	5.891 mm^{-1}	
F(000)	676.0	
Crystal size	0.20 × 0.20 × 0.04 mm^3	
Theta range for data collection	2.00 to 26.99°.	
Index ranges	$-12 \le h \le 13$, $-14 \le k \le 14$, $-14 \le l \le 14$	
Reflections collected	12919	
Independent reflections	5004 [R(int) = 0.0160]	
Completeness to theta=26.99°	99.0 %	
Absorption correction	Semi-empirical from equivalents	
Max. and min. transmission	0.7987 and 0.3857	
Refinement method	Full-matrix least-squares on F^2	
Data / restraints / parameters	5004 / 0 / 312	
Goodness-of-fit on F^2	0.970	
Final R indices [I>2sigma(I)]	R1 = 0.0170, wR2 = 0.0418	
R indices (all data)	R1 = 0.0173, wR2 = 0.0419	
Largest diff. peak and hole	1.150 and -1.056 e.Å^{-3}	

Table S15. Atomic coordinates ($\times 10^4$) and equivalent isotropic displacement parameters ($Å^2 \times 10^3$) for [Cp*Ir(**5DHBP**)(OH_2)](SO_4)(H_2O)$_3$. U(eq) is defined as one third of the trace of the orthogonalized U^{ij} tensor.

	x	y	z	U(eq)
C(1)	1512(3)	3547(3)	4796(3)	19(1)
C(2)	647(3)	3550(3)	5854(3)	20(1)
C(3)	-577(3)	3051(3)	6078(3)	21(1)
C(4)	-888(3)	2537(3)	5289(3)	20(1)
C(5)	22(2)	2538(2)	4267(2)	17(1)
C(6)	-152(2)	1883(2)	3467(2)	17(1)
C(7)	-1247(3)	1214(3)	3619(3)	20(1)
C(8)	-1263(3)	499(3)	2919(3)	21(1)
C(9)	-161(3)	469(3)	2059(3)	20(1)
C(10)	896(3)	1189(3)	1913(3)	20(1)
C(11)	4502(2)	3417(3)	1703(3)	20(1)
C(12)	2656(2)	4942(3)	974(2)	18(1)
C(13)	2790(3)	4066(3)	362(2)	20(1)
C(14)	3909(3)	3088(3)	840(3)	21(1)
C(15)	3744(2)	4544(3)	1794(2)	18(1)
C(16)	5711(3)	2669(3)	2390(3)	30(1)
C(17)	1676(3)	6149(3)	713(3)	26(1)
C(18)	1944(3)	4185(3)	-646(3)	31(1)
C(19)	4453(3)	2012(3)	437(3)	32(1)
C(20)	4065(3)	5249(3)	2526(3)	25(1)
Ir(1)	2489(1)	2911(1)	2479(1)	14(1)
N(1)	1193(2)	3068(2)	4011(2)	16(1)
N(2)	898(2)	1884(2)	2598(2)	18(1)
O(1)	3033(2)	1050(2)	4083(2)	23(1)
O(2)	937(2)	4028(2)	6646(2)	25(1)
O(3)	-34(2)	-245(2)	1380(2)	26(1)
O(4)	4549(4)	1904(5)	7385(4)	107(2)
O(5)	4210(2)	1019(2)	5954(2)	39(1)
O(6)	5390(5)	2975(3)	5200(4)	105(2)
O(7)	6358(3)	869(3)	6585(4)	74(1)
O(8S)	3275(2)	4812(2)	6042(3)	36(1)
O(9S)	2796(3)	8724(2)	1241(2)	41(1)
O(10S)	7726(2)	9113(3)	1139(2)	41(1)
S(1)	5121(1)	1699(1)	6275(1)	21(1)

Table S16. Selected bond lengths [Å] and angles [°] for [Cp*Ir(**5DHBP**)(OH_2)](SO_4)(H_2O)$_3$.

	[Cp*Ir(**5DHBP**)(OH_2)](SO_4)(H_2O)$_3$
C(2)-O(2)	1.341(3)
C(5)-C(6)	1.465(3)
C(9)-O(3)	1.342(3)
Ir(1)-N(2)	2.089(2)
Ir(1)-N(1)	2.108(2)
Ir(1)-O(1)	2.121(2)
O(2)-H(2A)	0.84
O(3)-H(3A)	0.81
N(2)-Ir(1)-N(1)	76.94(8)

Table S17. Crystal data and structure refinement for [Cp*Ir(**6DHBP**)(OH_2)]$_2$(SO_4)$_2$(H_2O)$_9$.

Empirical formula	C40 H68 Ir2 N4 O23 S2	
Formula weight	1421.56	
Temperature	183(2) K	
Wavelength	0.71073 Å	
Crystal system	Monoclinic	
Space group	C2/c	
Unit cell dimensions	a = 22.0411(11) Å	α= 90°.
	b = 20.1359(11) Å	β= 110.8820(10) °.
	c = 12.8316(7) Å	γ = 90°.
Volume	5320.8(5) Å^3	
Z	4	
Density (calculated)	1.775 Mg/m^3	
Absorption coefficient	5.157 mm^{-1}	
F(000)	2824	
Crystal size	0.30 × 0.10 × 0.10 mm^3	
Theta range for data collection	1.92 to 27.00°.	
Index ranges	$-26 \leq h \leq 28$, $-25 \leq k \leq 25$, $-16 \leq l \leq 15$	
Reflections collected	24289	
Independent reflections	5781 [R(int) = 0.0178]	
Completeness to theta=27.00°	99.5 %	
Absorption correction	Semi-empirical from equivalents	
Max. and min. transmission	0.6274 and 0.3076	
Refinement method	Full-matrix least-squares on F^2	
Data / restraints / parameters	5781 / 0 / 326	
Goodness-of-fit on F^2	1.056	
Final R indices [I>2sigma(I)]	R1 = 0.0163, wR2 = 0.0410	
R indices (all data)	R1 = 0.0178, wR2 = 0.0415	
Largest diff. peak and hole	0.991 and -0.674 e.Å^{-3}	

Table S18. Atomic coordinates (× 10^4) and equivalent isotropic displacement parameters (Å^2 × 10^3) for [Cp*Ir(**6DHBP**)(OH_2)]$_2$(SO_4)$_2$(H_2O)$_9$. U(eq) is defined as one third of the trace of the orthogonalized U^{ij} tensor.

	x	y	z	U(eq)
C(1)	1420(1)	4037(1)	-505(2)	21(1)
C(2)	1500(1)	4272(1)	-1480(2)	26(1)
C(3)	1560(1)	3823(1)	-2244(2)	26(1)
C(4)	1562(1)	3143(1)	-2033(2)	23(1)
C(5)	1476(1)	2939(1)	-1073(2)	18(1)
C(6)	1549(1)	2247(1)	-669(2)	18(1)
C(7)	1632(1)	1702(1)	-1252(2)	25(1)
C(8)	1777(1)	1094(1)	-698(2)	29(1)
C(9)	1865(1)	1052(1)	415(2)	26(1)
C(10)	1774(1)	1623(1)	967(2)	20(1)
C(11)	612(1)	3496(1)	1822(2)	24(1)
C(12)	221(1)	3441(1)	669(2)	23(1)
C(13)	145(1)	2743(1)	379(2)	22(1)
C(14)	449(1)	2370(1)	1401(2)	22(1)
C(15)	753(1)	2826(1)	2276(2)	23(1)
C(16)	835(2)	4126(2)	2469(3)	38(1)
C(17)	-75(1)	4000(1)	-117(3)	37(1)
C(18)	-261(1)	2450(2)	-718(2)	34(1)
C(19)	412(1)	1633(1)	1482(3)	33(1)
C(20)	1138(1)	2657(2)	3467(2)	32(1)
Ir(1)	1151(1)	2967(1)	973(1)	14(1)
N(1)	1378(1)	3382(1)	-339(2)	17(1)
N(2)	1582(1)	2194(1)	412(2)	17(1)
O(1)	2126(1)	3241(1)	1938(1)	22(1)
O(2)	1379(1)	4424(1)	296(1)	27(1)
O(3)	1862(1)	1656(1)	2039(1)	25(1)
O(4)	2729(1)	4380(1)	6754(1)	27(1)
O(5)	1704(1)	4374(1)	5219(2)	30(1)
O(6)	2699(1)	4594(1)	4897(2)	32(1)
O(7)	2474(1)	3490(1)	5408(1)	27(1)
O(1S)	2850(1)	2715(1)	3858(1)	28(1)
O(2S)	2640(2)	4416(1)	2745(2)	57(1)
O(3S)	880(1)	595(2)	4205(3)	93(1)
O(4S)	843(2)	730(3)	6349(4)	131(2)
O(5S)	0	9854(3)	2500	110(2)
S(1)	2401(1)	4204(1)	5553(1)	19(1)

Table S19. Crystal data and structure refinement for [Cp*Ir(**6DHBP–2H**$^+$)(OH_2)](H_2O)$_2$

Empirical formula	C20 H27 Ir N2 O5	
Formula weight	566.45	
Temperature	183(2) K	
Wavelength	0.71073 Å	
Crystal system	Orthorhombic	
Space group	Pnma	
Unit cell dimensions	a = 8.7020(3) Å	α= 90°.
	b = 16.1159(6) Å	β= 90°.
	c = 14.0281(5) Å	γ = 90°.
Volume	1967.31(12) Å^3	
Z	4	
Density (calculated)	1.917 Mg/m^3	
Absorption coefficient	6.821 mm^{-1}	
F(000)	1112	
Crystal size	0.20 × 0.10 × 0.10 mm^3	
Theta range for data collection	1.92 to 24.99°.	
Index ranges	$-10 \le h \le 10$, $-17 \le k \le 17$, $-16 \le l \le 2$	
Reflections collected	16360	
Independent reflections	1706 [R(int) = 0.0404]	
Completeness to theta=24.99°	94.6 %	
Absorption correction	Semi-empirical from equivalents	
Max. and min. transmission	0.5492 and 0.3429	
Refinement method	Full-matrix least-squares on F^2	
Data / restraints / parameters	1706 / 20 / 145	
Goodness-of-fit on F^2	0.704	
Final R indices [I>2sigma(I)]	R1 = 0.0389, wR2 = 0.0983	
R indices (all data)	R1 = 0.0400, wR2 = 0.0998	
Largest diff. peak and hole	2.574 and -1.747 e.Å^{-3}	

Table S20. Atomic coordinates (× 10^4) and equivalent isotropic displacement parameters (Å^2 × 10^3) for [Cp*Ir(**6DHBP–2H**$^+$)(OH_2)](H_2O)$_2$. U(eq) is defined as one third of the trace of the orthogonalized U^{ij} tensor.

	x	y	z	U(eq)
Ir(1)	2159(1)	2500	54(1)	16(1)
O(1S)	5295(6)	4002(3)	9323(4)	33(1)
O(1)	4665(8)	2500	68(4)	20(2)
C(1)	2442(8)	848(4)	1182(5)	26(2)
C(6)	1812(14)	2500	-1474(9)	59(4)
C(7)	1120(10)	1798(6)	-1087(6)	54(3)
C(8)	-10(8)	2938(5)	-427(5)	38(2)
C(10)	-1064(15)	3459(10)	162(9)	90(4)
N(1)	2245(5)	1694(3)	1231(4)	17(1)
C(5)	1690(7)	2048(4)	2040(4)	19(1)

O(2)	3034(6)	509(3)	450(4)	36(1)
C(2)	1938(10)	374(5)	1966(7)	44(2)
C(3)	1305(11)	707(5)	2746(6)	50(2)
C(4)	1184(9)	1584(4)	2805(5)	30(2)
C(11)	1380(19)	912(9)	-1401(12)	119(5)
C(12)	3030(30)	2500	-2219(16)	124(8)

Table S21. Selected bond lengths [Å] and angles [°] for [Cp*Ir(**6DHBP**)(OH_2)]$_2$(SO_4)$_2$(H_2O)$_9$ and [Cp*Ir(**6DHBP–2H$^+$**)(OH)]$_2$(H_2O).

[Cp*Ir(**6DHBP**)(OH_2)]$_2$(SO_4)$_2$(H_2O)$_9$		[Cp*Ir(**6DHBP–2H$^+$**)(OH_2)](H_2O)$_2$	
C(1)-O(2)	1.319(3)	C(1)-O(2)	1.272(9)
C(5)-C(6)	1.474(3)	C(5)-C(5)#1	1.457(13)
C(10)-O(3)	1.321(3)	–	–
Ir(1)-N(2)	2.082(2)	Ir(1)-N(1)#1	2.101(5)
Ir(1)-N(1)	2.095(2)	Ir(1)-N(1)	2.101(5)
Ir(1)-O(1)	2.136(2)	Ir(1)-O(1)	2.181(7)
O(2)-H(2O)	0.7323	–	–
O(3)-H(3O)	0.7493	–	–
N(2)-Ir(1)-N(1)	75.57(7)	N(1)#1-Ir(1)-N(1)	76.3(3)

Symmetry transformations used to generate equivalent atoms with #1.

10. Computational Methods

All geometries were fully optimized at the B3LYP level of density functional theory[5] with SMD aqueous continuum solvation model[6] using the Stuttgart [8s7p6d2f | 6s5p3d2f] ECP60MWB contracted pseudopotential basis set[7] on Ir and the 6-31G(d,p) basis set[8] on all other atoms. Non-analytical integrals were evaluated using the *integral=grid=ultrafine* option as implemented in the Gaussian 09 software package.[9] The nature of all stationary points was verified by analytic computation of vibrational frequencies, which were also used for the computation of zero-point vibrational energies, molecular partition functions (with all frequencies below 50 cm^{-1} replaced by 50 cm^{-1} when computing free energies), and for determining the reactants and products associated with each transition-state structure (by following the normal modes associated with imaginary frequencies). Partition functions were used in the computation of 298 K thermal contributions to free energy employing the usual ideal-gas, rigid-rotator, harmonic oscillator approximation.[10] Following the protocol in our prior

publication,[11] translational entropy contributions were omitted in the final free energies of all species. Free-energy contributions were added to more accurate single-point B3LYP electronic energies computed with the SDD basis set on Ir and the 6-311++G(2d,p) basis set on all other atoms to arrive at final, composite free energies.

Solvation effects associated with water as solvent were accounted for using the SMD aqueous continuum solvation model.[6] A 1 M standard state was used for all species in solution, thus, an adjustment for the 1 atm to 1 M standard-state concentration change of *RT* ln (24.5), or 7.9 kJ/mol was added. In the cases of the water molecule and proton, the experimental solvation free energies of –26.4 kJ/mol and –1112.5 kJ/mol were used, respectively.[12-15] For gaseous species (e.g., H_2 and CO_2) the standard state of 1.0 atm was employed.

Time-dependent density functional theory (TDDFT) calculations were performed to predict the UV/visible electronic excitations of postulated structures. The B3LYP[5] density functional, Stuttgart [8s7p6d2f | 6s5p3d2f] ECP60MWB contracted pseudopotential basis set[7] on Ir and the 6-311+G(d,p) basis set[8] on all other atoms were used for the TDDFT calculations. Non-equilibrium solvation effects were included via the linear response approximation[16] in combination with the SMD aqueous continuum solvation model.[6]

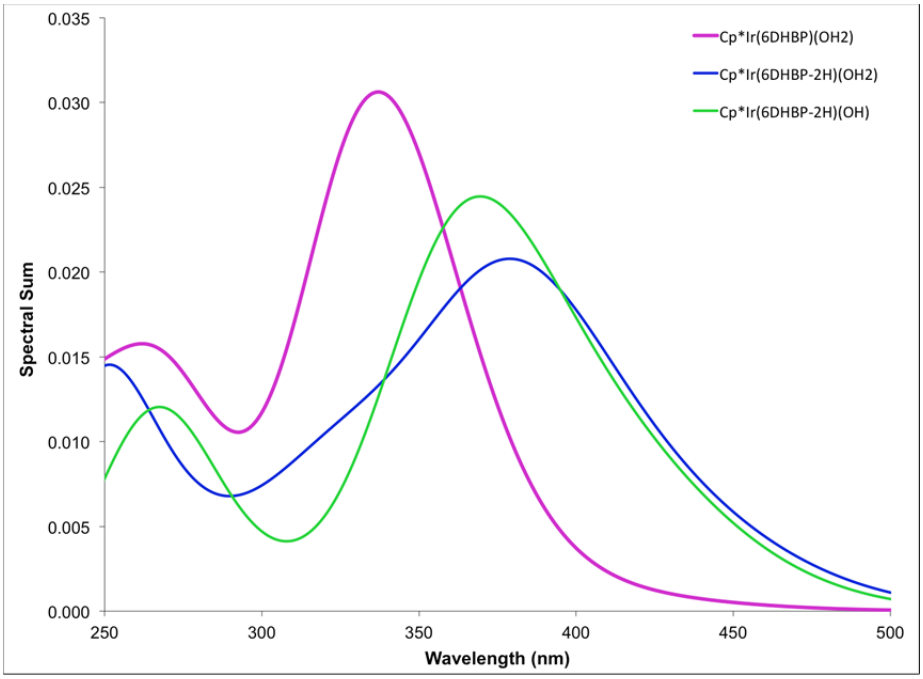

Figure S8. Calculated UV-vis absorption spectra at B3LYP level of theory for [Cp*Ir(**6DHBP**)(OH_2)]$^{2+}$ (magenda), [Cp*Ir(**6DHBP-2H**$^+$)(OH_2)] (blue) and [Cp*Ir(**6DHBP-2H**$^+$)(OH)]$^-$(green).

11. Cartesian Coordinates of Optimized Structures

```
2
H2, Egas = -1.17853935735 a.u.
 H                 0.00000000     0.00000000     0.37139700
 H                 0.00000000     0.00000000    -0.37139700


3
H2O, Egas = -76.4181598319 a.u.
 O                 0.00000000     0.00000000     0.11885400
 H                 0.00000000     0.76018100    -0.47541600
 H                 0.00000000    -0.76018100    -0.47541600


3
CO2, Egas = -188.577569656 a.u.
 C                 0.00000000     0.00000000     0.00000000
 O                 0.00000000     0.00000000     1.16957500
 O                 0.00000000     0.00000000    -1.16957500


4
HCO2, Esol = -189.291234926 a.u.
 C                 0.00000000     0.00000000     0.33530700
 H                 0.00000000     0.00000000     1.45867700
 O                 0.00000000     1.13375900    -0.21690700
 O                 0.00000000    -1.13375900    -0.21690700


5
HCO2H, Esol = -189.764445254 a.u.
 C                 0.12023700     0.37190600    -0.00015600
 H                 0.03030900     1.46871300     0.00017700
 O                 1.17857100    -0.22092500     0.00006800
 O                -1.04957700    -0.28559000    -0.00002600
 H                -1.78368400     0.35197300     0.00042400


5
HCO3,Esol = -264.544604249 a.u.
 C                 0.12023700     0.37190600    -0.00015600
 H                 0.03030900     1.46871300     0.00017700
 O                 1.17857100    -0.22092500     0.00006800
 O                -1.04957700    -0.28559000    -0.00002600
 H                -1.78368400     0.35197300     0.00042400


48
4DHBP,Esol = -1140.18398304 a.u.
 Ir               -0.71826400     0.00247700    -0.19775100
 C                -2.04410900    -0.10197400     1.45818600
 C                -2.38398500    -1.20983400     0.57331900
```

C	-2.74778700	-0.65941800	-0.68881500
C	-2.34389500	1.14006800	0.75305700
C	-2.72914600	0.80420000	-0.57615600
C	-2.28056100	2.50397300	1.36234000
H	-3.19029500	2.66873000	1.95259600
H	-1.42725700	2.60582600	2.03696000
H	-2.22868200	3.28842600	0.60530900
C	-3.11164600	1.75267000	-1.66682800
H	-4.20237700	1.86790200	-1.69093100
H	-2.67219300	2.74066600	-1.51377900
H	-2.79713100	1.38064100	-2.64504900
C	-3.14753400	-1.41347300	-1.91537100
H	-4.24196600	-1.44647400	-1.98522700
H	-2.77515400	-0.92641000	-2.82032500
H	-2.77865200	-2.44082100	-1.89401400
C	-2.38731300	-2.65253700	0.96600900
H	-3.31760200	-2.87130400	1.50429600
H	-2.34483800	-3.31154700	0.09634300
H	-1.55579200	-2.89280700	1.63285100
C	-1.68237300	-0.22034500	2.90188600
H	-1.09458600	0.63657100	3.23801000
H	-2.60017500	-0.25643900	3.50306800
H	-1.11744400	-1.13450600	3.09708700
C	2.18555800	0.74085600	-0.06923400
C	0.86244400	2.66014400	-0.24595700
C	1.96613400	3.48929800	-0.17954400
C	3.23137800	2.90564000	-0.03477700
C	3.33580800	1.50709300	0.01077100
C	2.18624500	-0.73672000	-0.07120000
C	0.87142000	-2.65688600	-0.28436200
C	1.97538200	-3.48427100	-0.20208300
C	3.23563500	-2.89963400	-0.02397600
C	3.33583000	-1.50129400	0.03322400
H	1.84620800	4.56563800	-0.23544500
H	4.31552800	1.05602800	0.10221200
H	1.85840800	-4.56037700	-0.26833100
H	4.31109400	-1.04848400	0.15807800
N	0.95629600	-1.31280000	-0.20747600
N	0.95279600	1.31573700	-0.18079500
H	-0.11973100	-3.06926200	-0.41556900
H	-0.13315200	3.06939100	-0.35601600
O	4.36711000	3.61673800	0.05641500
H	4.17246500	4.56746200	0.01557500
O	4.36971300	-3.60985600	0.09130500
H	4.17652700	-4.56051900	0.04234300

47
4DHBP-H+,Esol = -1139.71842777 a.u.

Ir	0.67443200	0.00665900	-0.08386100
C	2.30177300	0.09952200	1.31977700
C	2.55145900	1.10249000	0.30385800
C	2.64147000	0.42229900	-0.95094200

C	2.33266400	-1.21217100	0.68744700
C	2.52147600	-1.01686800	-0.71165300
C	2.23305000	-2.51059000	1.42456200
H	3.18408100	-2.71137600	1.93261200
H	1.45157600	-2.47936400	2.18847000
H	2.03284500	-3.34633700	0.75214200
C	2.63442700	-2.07635700	-1.76132300
H	3.69149200	-2.29665000	-1.95527200
H	2.15046600	-3.00378500	-1.44775200
H	2.18551600	-1.75269200	-2.70369000
C	2.89260700	1.04634700	-2.28383200
H	3.96861900	1.02133000	-2.49901000
H	2.38316500	0.50128800	-3.08224400
H	2.56903800	2.08883100	-2.30694600
C	2.75685100	2.56413500	0.54909400
H	3.80663500	2.74521100	0.81047200
H	2.53123100	3.15955400	-0.33838000
H	2.14327900	2.92510200	1.37793200
C	2.18817000	0.34882100	2.78713200
H	1.56444600	-0.40510400	3.27274800
H	3.18665400	0.29986300	3.24072500
H	1.77364500	1.33777100	2.99418600
C	-2.25216400	-0.61460600	-0.01935000
C	-0.99776800	-2.58784400	-0.15224000
C	-2.13158500	-3.37433400	-0.11237600
C	-3.37789600	-2.74014500	-0.00349600
C	-3.43095700	-1.34090400	0.03733500
C	-2.18960200	0.86154800	-0.01973300
C	-0.77203900	2.72769700	-0.08916400
C	-1.82700300	3.59806100	-0.07625500
C	-3.18625100	3.11475800	-0.02628400
C	-3.29785300	1.67046100	0.00001300
H	-2.05270600	-4.45483400	-0.16226700
H	-4.39345400	-0.85074300	0.10875300
H	-1.64453400	4.66734000	-0.10464400
H	-4.29453900	1.24558900	0.03011900
N	-0.91024900	1.36948200	-0.06175900
N	-1.03970400	-1.23853000	-0.09580900
H	0.24736500	3.09025400	-0.12757600
H	-0.01561500	-3.03386200	-0.23636500
O	-4.54304300	-3.40960300	0.05688400
H	-4.38191700	-4.36641700	0.02178000
O	-4.19618700	3.87156700	-0.00949900

46
4DHBP-2H+ (I in Figure 5), Esol = -1139.24968821 a.u.

Ir	0.64471000	-0.00006600	-0.07759700
C	2.27395700	0.00817000	1.32752600
C	2.42854900	1.18079600	0.48399800
C	2.57043300	0.72673100	-0.85932600
C	2.42643700	-1.17557400	0.49953900
C	2.56904600	-0.73935500	-0.84965400

C	2.48124700	-2.58071200	1.01319300
H	3.47031400	-2.77130100	1.44724600
H	1.73888200	-2.75374700	1.79667900
H	2.32420200	-3.31079400	0.21662300
C	2.76965200	-1.60249100	-2.05414500
H	3.84115800	-1.68536300	-2.27570200
H	2.38044900	-2.61028100	-1.89458200
H	2.28157900	-1.17779000	-2.93499000
C	2.77353000	1.57345400	-2.07503100
H	3.84568400	1.65515300	-2.29391300
H	2.28934800	1.13572600	-2.95163900
H	2.38198800	2.58269500	-1.93087600
C	2.48524400	2.59250300	0.97895700
H	3.47635700	2.78943900	1.40545100
H	2.32368000	3.31203100	0.17374100
H	1.74676200	2.77522000	1.76386300
C	2.15276500	0.01761500	2.81659100
H	1.62654700	-0.86810900	3.17972500
H	3.15541200	0.01955000	3.26358300
H	1.62798000	0.90850100	3.16898600
C	-2.24021600	-0.74039700	-0.01700500
C	-0.89777600	-2.66429800	-0.11113400
C	-1.98690400	-3.49204000	-0.08931300
C	-3.32447800	-2.95416200	-0.01481800
C	-3.37764200	-1.51021600	0.01430900
C	-2.24034900	0.74032000	-0.01808200
C	-0.89896300	2.66409500	-0.12851700
C	-1.98783800	3.49190600	-0.09825000
C	-3.32447700	2.95414300	-0.00807300
C	-3.37736300	1.51024900	0.02455600
H	-1.84822300	-4.56773800	-0.12904100
H	-4.35590300	-1.04479800	0.05550600
H	-1.84959700	4.56751400	-0.14179200
H	-4.35506200	1.04507400	0.07957000
N	-0.98386100	1.30250200	-0.08290900
N	-0.98308800	-1.30258300	-0.06951300
H	0.10374800	3.06668600	-0.19820900
H	0.10548700	-3.06709000	-0.17058600
O	-4.36483500	-3.67335300	0.01639900
O	-4.36440500	3.67343500	0.03364200

49

4DHBP-2H+(H2O),Esol = -1215.68562106 a.u.

Ir	0.69289100	-0.01041600	-0.20722500
C	1.79767100	-0.08196000	1.62767400
C	2.17087100	1.15210200	0.95320400
C	2.75237400	0.81629100	-0.30451800
C	2.27628800	-1.18820800	0.80649900
C	2.81872100	-0.64408500	-0.39088000
C	2.25746800	-2.62976200	1.20856900
H	3.12639100	-2.83531300	1.84602800
H	1.36262700	-2.88092500	1.78285900

H	2.31549500	-3.29576300	0.34490900
C	3.42434100	-1.40719600	-1.52770600
H	4.51333800	-1.45769300	-1.40404600
H	3.04448000	-2.43021100	-1.57408300
H	3.22596500	-0.92067800	-2.48619800
C	3.30920700	1.76643800	-1.31998600
H	4.38762700	1.89655500	-1.16503300
H	3.16576000	1.39318800	-2.33721000
H	2.84141700	2.75086000	-1.24594800
C	2.00915000	2.52288700	1.52994300
H	2.82907600	2.70883900	2.23486100
H	2.05195900	3.29729500	0.76182700
H	1.07159700	2.62441100	2.08167500
C	1.27740200	-0.19282700	3.02848100
H	0.70201600	-1.11142700	3.16666000
H	2.11171000	-0.20949800	3.74107800
H	0.63644600	0.65466000	3.28328900
C	-2.21211200	-0.72884000	0.02055100
C	-0.90394500	-2.65474300	-0.19257300
C	-2.00167600	-3.47564100	-0.11185600
C	-3.32320300	-2.93093300	0.07113400
C	-3.35719200	-1.49032200	0.11663600
C	-2.20221900	0.75102100	0.00487700
C	-0.86628600	2.64985000	-0.28418500
C	-1.94441800	3.49185400	-0.17371300
C	-3.26773900	2.97474300	0.07013500
C	-3.32840900	1.53571500	0.13690300
H	-1.87466500	-4.55112800	-0.18745300
H	-4.32503100	-1.01185200	0.21801900
H	-1.80069900	4.56394600	-0.26582100
H	-4.29893100	1.07797800	0.29314000
N	-0.95860000	1.29772800	-0.18438100
N	-0.97069700	-1.30024800	-0.10875000
H	0.12892000	3.04036200	-0.46183800
H	0.08801400	-3.06826900	-0.33030500
O	-4.36877300	-3.64450900	0.17161800
O	-4.29212100	3.71225900	0.20741800
O	0.11663300	-0.12281700	-2.46753400
H	-0.55116200	0.56682900	-2.61885900
H	-0.36357700	-0.96026000	-2.57645000

53
I-TS in Figure 5 (389.5 i cm-1), Esol = -1404.97164127 a.u.

Ir	0.43163100	-0.32912100	-0.14871300
C	0.98304000	-0.74680400	-2.26724100
C	0.78858800	-1.99522900	-1.59199600
C	1.75248400	-2.08861500	-0.51094400
C	2.09246800	-0.05631500	-1.62184900
C	2.57181100	-0.90343300	-0.56880900
C	2.73983300	1.20751500	-2.10211100
H	3.57750700	0.96814200	-2.76912100
H	2.04077900	1.82781000	-2.66718900

H	3.13435600	1.79980800	-1.27301800
C	3.75469000	-0.62962900	0.30723700
H	4.63202500	-1.14631700	-0.10173500
H	3.98621000	0.43572300	0.35413600
H	3.59771500	-0.99785800	1.32347000
C	2.01173100	-3.29116600	0.34636600
H	2.74808100	-3.94725100	-0.13495800
H	2.40991300	-3.00608200	1.32336200
H	1.10399400	-3.87828100	0.50395700
C	-0.19697300	-3.05716200	-1.96602800
H	0.28148900	-3.77399700	-2.64469900
H	-0.54353800	-3.61245300	-1.09177800
H	-1.06566900	-2.64047100	-2.48032700
C	0.25119700	-0.26367700	-3.48112000
H	0.14905300	0.82455500	-3.47921400
H	0.80352300	-0.54324800	-4.38675300
H	-0.74703900	-0.70193900	-3.54982600
C	-2.17294700	1.18019800	-0.05835000
C	-0.46405600	2.53111000	-0.90214200
C	-1.32253300	3.58477900	-1.10427200
C	-2.72262100	3.47440000	-0.78267200
C	-3.09206700	2.19499200	-0.23372500
C	-2.50136200	-0.14316200	0.51602300
C	-1.63121000	-2.21087000	1.17255000
C	-2.85437800	-2.64465300	1.62160500
C	-4.02270900	-1.80706600	1.52023400
C	-3.76099200	-0.51292400	0.94415500
H	-0.94046800	4.51596200	-1.51122500
H	-4.12931200	2.04367800	0.04424800
H	-2.94411600	-3.63406900	2.05949000
H	-4.59139300	0.17874300	0.85538400
N	-1.43192000	-0.99161000	0.61235000
N	-0.85493600	1.33395600	-0.39844000
H	-0.75285400	-2.84035900	1.25458700
H	0.58928000	2.62065300	-1.13823100
O	-3.55972800	4.41522900	-0.95941100
H	0.51595100	0.13927900	1.51930600
C	2.62083400	1.75729800	2.67488200
O	2.43809600	0.81865400	3.47639000
O	1.89040500	2.11273600	1.69451400
H	1.00479300	0.83255300	1.28933000
O	-5.17771000	-2.16823100	1.90939900
O	3.75136600	2.54674600	2.82683200
H	4.22374100	2.20275100	3.60176300

47

II-A in Figure 5, Esol = -1139.96810158 a.u.

Ir	-0.68631900	-0.00015500	-0.36283700
C	-2.00926800	0.70729800	1.40196100
C	-2.00969400	-0.70729900	1.40192700
C	-2.50631400	-1.16581000	0.10419800
C	-2.50582400	1.16603500	0.10424100

C	-2.86800200	0.00021200	-0.65913500
C	-2.85416200	2.58687400	-0.23309700
H	-3.86718300	2.82640500	0.11663700
H	-2.17319800	3.29508800	0.24630100
H	-2.82674800	2.76572900	-1.31122600
C	-3.58968500	0.00043400	-1.97494300
H	-4.67397600	0.00055700	-1.80412000
H	-3.34808000	0.88585900	-2.56785300
H	-3.34831400	-0.88493200	-2.56803900
C	-2.85493400	-2.58658600	-0.23304800
H	-3.86732800	-2.82647300	0.11826100
H	-2.82919400	-2.76503500	-1.31128300
H	-2.17304800	-3.29482700	0.24501500
C	-1.60269900	-1.61714700	2.52208200
H	-2.48671100	-2.01082500	3.03945200
H	-1.03563900	-2.47705800	2.15211200
H	-0.98833000	-1.09779400	3.26176400
C	-1.60136900	1.61682500	2.52207300
H	-1.03599500	2.47762200	2.15161500
H	-2.48482200	2.00908700	3.04146700
H	-0.98489800	1.09763800	3.26012800
C	2.22275300	0.73995800	-0.09847700
C	0.90804200	2.65684900	-0.26896400
C	1.99981800	3.48489700	-0.15081900
C	3.32470900	2.94681500	0.01156800
C	3.36563900	1.50944800	0.02234400
C	2.22285800	-0.73986300	-0.09842400
C	0.90840500	-2.65701600	-0.26781900
C	2.00039900	-3.48487300	-0.15026000
C	3.32531300	-2.94652000	0.01100400
C	3.36595400	-1.50913400	0.02166700
H	1.86188100	4.56161100	-0.18327200
H	4.33454500	1.03480500	0.13165800
H	1.86258800	-4.56161200	-0.18242000
H	4.33486400	-1.03431900	0.13020100
N	0.98275500	-1.30287400	-0.23681700
N	0.98263900	1.30271200	-0.23766800
H	-0.08510800	-3.06963500	-0.40031900
H	-0.08544300	3.06926200	-0.40221200
O	4.36771900	3.66906400	0.13247100
O	4.36861000	-3.66849500	0.13104800
H	-0.35335500	-0.00100300	-1.94067800

48

II-B in Figure 1,Esol = -1140.44555820 a.u.

Ir	0.70108900	-0.01870600	-0.35654200
C	2.01134800	-0.75407000	1.40532700
C	2.06625500	0.65891100	1.38919400
C	2.56303400	1.08128000	0.07788400
C	2.48007200	-1.24698300	0.11012300
C	2.87882900	-0.10744700	-0.67239700
C	2.76757500	-2.68424300	-0.21342200

H	3.77281300	-2.95971800	0.13177800
H	2.06373900	-3.35915600	0.28059400
H	2.72534200	-2.87350600	-1.28919200
C	3.58627300	-0.14819800	-1.99481400
H	4.67139500	-0.17604000	-1.83262000
H	3.31362400	-1.03519800	-2.57147900
H	3.36439600	0.73519400	-2.59814400
C	2.95857000	2.48369200	-0.28196100
H	3.98414900	2.68745300	0.05302500
H	2.92446200	2.65007800	-1.36175100
H	2.31077600	3.22234700	0.19723700
C	1.71257500	1.59747600	2.50295400
H	2.62116400	1.96791500	2.99407400
H	1.16688200	2.47074100	2.13236500
H	1.09915400	1.10915600	3.26400100
C	1.57196200	-1.63587600	2.53543600
H	0.97073100	-2.47629100	2.17413200
H	2.44143600	-2.05938100	3.05364100
H	0.97968400	-1.08608500	3.27095400
C	-2.23078800	-0.62798400	-0.09480100
C	-0.98673500	-2.59607000	-0.24487800
C	-2.11762100	-3.38547300	-0.13704800
C	-3.36063600	-2.75373500	-0.00294700
C	-3.41034500	-1.35841500	0.01432700
C	-2.17682300	0.84579000	-0.09718400
C	-0.78792400	2.70430100	-0.26929500
C	-1.84754500	3.57287000	-0.15036900
C	-3.19337600	3.08990900	0.01552000
C	-3.29206900	1.65373600	0.02508800
H	-2.03412700	-4.46673100	-0.16379600
H	-4.36912500	-0.86493400	0.11025100
H	-1.66736000	4.64318700	-0.18168300
H	-4.27808500	1.21688400	0.13739800
N	-0.91515400	1.35462200	-0.23811300
N	-1.02285100	-1.24758100	-0.21947800
H	0.22035100	3.07818700	-0.40285100
H	-0.01088400	-3.04761700	-0.36611700
O	-4.52820300	-3.42958600	0.10644700
H	-4.35934200	-4.38468500	0.08023300
O	-4.20359400	3.85322500	0.14082200
H	0.36962300	-0.02666700	-1.93378900

50

II-TSA in Figure 5 (486.0 i cm-1),Esol = -1328.53334216 a.u.

Ir	0.69740500	0.03214500	0.04104600
C	1.98017300	0.45580700	-1.77717600
C	2.20261700	-0.89732400	-1.34897900
C	2.70935700	-0.88272100	0.00042600
C	2.37335800	1.32542600	-0.68169100
C	2.82695400	0.51163400	0.40386800
C	2.44058400	2.82057300	-0.75660300
H	3.39113800	3.12072600	-1.21572500

H	1.63759900	3.23407300	-1.37158100
H	2.39340900	3.28195200	0.23266400
C	3.43666300	0.99352300	1.68649400
H	4.52866700	1.04230600	1.58810800
H	3.08122800	1.99231800	1.95078700
H	3.21025600	0.32011200	2.51651700
C	3.20559900	-2.06266400	0.78355600
H	4.27761400	-2.22168800	0.60841600
H	3.06374900	-1.91485600	1.85731400
H	2.68602500	-2.98103800	0.49793100
C	2.01912000	-2.11342200	-2.20517000
H	2.90461700	-2.24747100	-2.83898600
H	1.90469200	-3.01942000	-1.60703500
H	1.15323600	-2.02082600	-2.86566100
C	1.57760000	0.90113800	-3.15086500
H	0.99988600	1.82897200	-3.11933000
H	2.46296500	1.08724700	-3.77323900
H	0.97369200	0.14317800	-3.65654200
C	-2.20537300	0.78734900	-0.19462800
C	-0.90823100	2.68318800	0.20279800
C	-2.00342900	3.51190500	0.15194500
C	-3.32036500	2.98728700	-0.10103800
C	-3.35044600	1.55784700	-0.26162300
C	-2.19472400	-0.68605600	-0.32255600
C	-0.86222200	-2.60065500	-0.26293000
C	-1.94700600	-3.42776600	-0.42882200
C	-3.27537900	-2.89007700	-0.57491900
C	-3.33022000	-1.45473300	-0.49519000
H	-1.87538400	4.57892000	0.30771100
H	-4.31328900	1.09006900	-0.43554600
H	-1.80310000	-4.50387800	-0.44830800
H	-4.30295300	-0.98114100	-0.56915100
N	-0.94930900	-1.24661100	-0.22924000
N	-0.97060900	1.34013000	0.02034800
O	-1.39918700	-0.51892500	3.02460000
C	-0.20971700	-0.61461800	3.09167100
O	0.80539700	-0.87599700	3.66758400
H	0.30069800	-0.10275500	1.65382400
H	0.07750200	3.08480700	0.40324200
H	0.13455400	-3.00971900	-0.14385000
O	-4.30851800	-3.61278100	-0.75007400
O	-4.36482700	3.71201300	-0.16977000

51

II-TSB in Figure 5 (503.9 i cm-1), Esol = -1329.00953604 a.u.

Ir	-0.71236200	0.01762500	0.04502500
C	-1.92742500	0.19656700	-1.86165000
C	-2.34481100	1.21385400	-0.92026700
C	-2.84104900	0.57321400	0.26181400
C	-2.18919000	-1.08216100	-1.24792600
C	-2.74149800	-0.86795800	0.06063200
C	-1.99883100	-2.40756800	-1.91860300

H	-2.84728200	-2.59810300	-2.58754600
H	-1.09057900	-2.43006500	-2.52660100
H	-1.95801600	-3.22788100	-1.19921400
C	-3.27785300	-1.91763700	0.98813800
H	-4.34507200	-2.08893000	0.79697400
H	-2.76111800	-2.87172700	0.85648000
H	-3.17354000	-1.61754500	2.03359600
C	-3.48242800	1.24022500	1.44228700
H	-4.57136300	1.27483200	1.31079000
H	-3.27788200	0.69612900	2.36768200
H	-3.12857000	2.26653200	1.56569900
C	-2.36583200	2.68417900	-1.20433600
H	-3.26111900	2.92493600	-1.79127300
H	-2.40475200	3.27711800	-0.28802400
H	-1.49714000	2.99950000	-1.78761900
C	-1.47290600	0.43175700	-3.27044400
H	-0.84212700	-0.38562500	-3.62924300
H	-2.33478700	0.50561100	-3.94677900
H	-0.90681400	1.36291900	-3.35810500
C	2.20751300	-0.60159300	-0.26557600
C	0.94775700	-2.56306800	-0.14231600
C	2.06746100	-3.35752100	-0.30620300
C	3.31066900	-2.73206000	-0.47115000
C	3.37547800	-1.33705900	-0.43837300
C	2.16767900	0.86946900	-0.17603400
C	0.80056300	2.71970000	0.18160500
C	1.86606100	3.58519200	0.11792300
C	3.20208700	3.10692600	-0.12837000
C	3.28721100	1.67430000	-0.25694000
H	1.97594300	-4.43838300	-0.30659500
H	4.33504000	-0.84751000	-0.54558700
H	1.69925600	4.64919600	0.25506800
H	4.26739700	1.23911100	-0.41703300
N	0.91274000	1.37740100	0.02306000
N	0.99691400	-1.21503600	-0.14111100
O	1.26948100	-0.35511800	3.13265200
C	0.07647600	-0.45281300	3.14167200
O	-0.95859400	-0.68765000	3.69596400
H	-0.36059200	-0.04399400	1.68071100
H	-0.02922100	-3.00761000	-0.00523300
H	-0.20001000	3.08829300	0.37188200
O	4.21507900	3.86915200	-0.21674600
O	4.46275400	-3.41480100	-0.65536500
H	4.28411400	-4.36879400	-0.65794400

50

III-A in Figure 5,Esol = -1328.56672396 a.u.

Ir	-0.66813500	-0.09133700	0.06836300
C	-1.84210300	0.47177000	-1.67033400
C	-2.53879200	0.95318600	-0.48703800
C	-2.88625400	-0.19927000	0.30028800
C	-1.76452900	-0.96360100	-1.59298900

C	-2.41092800	-1.38377900	-0.35950100
C	-1.20797500	-1.88075300	-2.63826200
H	-2.01333700	-2.22407200	-3.29934400
H	-0.45956900	-1.37830500	-3.25536500
H	-0.74615700	-2.76491800	-2.19213000
C	-2.69277800	-2.79574500	0.05996700
H	-3.69583500	-3.09599400	-0.26891200
H	-1.98349800	-3.49862300	-0.38302700
H	-2.65495100	-2.91022500	1.14662100
C	-3.64490500	-0.18026000	1.59140200
H	-4.71587900	-0.30342500	1.38660300
H	-3.33964900	-0.99874600	2.24797400
H	-3.51168700	0.76206600	2.12524800
C	-2.99204500	2.36095800	-0.24042100
H	-4.00217000	2.50811800	-0.64373100
H	-3.02224500	2.59486300	0.82588000
H	-2.33849800	3.08681300	-0.73031900
C	-1.38889500	1.32269500	-2.81680000
H	-0.58735900	0.84189400	-3.38219300
H	-2.22656000	1.49709000	-3.50337000
H	-1.03121600	2.29778800	-2.47728800
C	2.27530900	-0.71257000	-0.00757800
C	1.02998000	-2.67158100	0.22108000
C	2.16118300	-3.45025300	0.28476100
C	3.47211400	-2.86119600	0.19292900
C	3.45456100	-1.42894300	0.04759200
C	2.21109900	0.76095200	-0.13764500
C	0.79671000	2.61528400	-0.21333300
C	1.85209500	3.48353200	-0.35451600
C	3.20882000	3.00193500	-0.40277800
C	3.32076200	1.57205500	-0.27781800
H	2.06673200	-4.52481900	0.40888300
H	4.40799300	-0.91584700	-0.01276300
H	1.66259500	4.54991000	-0.43196900
H	4.31452100	1.13863000	-0.30173500
N	0.94147400	1.27036800	-0.11192400
N	1.05369900	-1.32481600	0.06715500
O	-0.09529100	-0.08094400	2.18596800
C	-0.39013700	0.89173300	2.98080500
H	-0.03357200	0.72023300	4.01575100
O	-0.99499900	1.94133800	2.71261200
H	-0.22084300	2.98479300	-0.17374200
H	0.04604100	-3.11851000	0.30200200
O	4.55115000	-3.53415200	0.24174600
O	4.21734100	3.76481400	-0.54438900

51
III-B in Figure 5,Esol = -1329.04223942 a.u.

Ir	-0.68698900	-0.10285700	0.07514800
C	-1.85341000	0.33440000	-1.70037700
C	-2.56515300	0.87161500	-0.54863100
C	-2.90540100	-0.23623900	0.30044900

C	-1.76363800	-1.09253900	-1.54014400
C	-2.40646000	-1.45024700	-0.28598800
C	-1.19227300	-2.05964300	-2.53023400
H	-1.99120700	-2.42642200	-3.18642700
H	-0.43203500	-1.59058300	-3.15878000
H	-0.74679700	-2.92690800	-2.03725500
C	-2.66751400	-2.83765700	0.21912900
H	-3.66599700	-3.17186800	-0.08998500
H	-1.94802400	-3.55659200	-0.17944600
H	-2.62881300	-2.88247500	1.31071300
C	-3.67418000	-0.15407000	1.58232400
H	-4.73886400	-0.32325300	1.37771400
H	-3.35058400	-0.91812600	2.29336500
H	-3.57351000	0.82513700	2.05280600
C	-3.03527800	2.28509600	-0.38147900
H	-4.05871000	2.38624300	-0.76446800
H	-3.04128300	2.58853200	0.66767000
H	-2.41024200	2.98614000	-0.93913800
C	-1.40365400	1.12546700	-2.89014400
H	-0.59745900	0.61994900	-3.42664300
H	-2.24058700	1.25726800	-3.58685600
H	-1.05292900	2.11937600	-2.60133100
C	2.27834800	-0.60303900	-0.01941600
C	1.11054000	-2.60541000	0.24710000
C	2.27861800	-3.34492900	0.29839400
C	3.49947200	-2.66856100	0.17479400
C	3.49217800	-1.27980500	0.01861800
C	2.15938600	0.86213900	-0.15529000
C	0.67783100	2.65639300	-0.24869800
C	1.70252900	3.56277400	-0.37803900
C	3.07781600	3.13565200	-0.40553100
C	3.24266200	1.70895100	-0.28048200
H	2.24257900	-4.42051700	0.43468300
H	4.43236800	-0.75005800	-0.06487000
H	1.47325800	4.62081000	-0.45969700
H	4.25262200	1.31407300	-0.28724300
N	0.87039000	1.31822500	-0.14357000
N	1.09557100	-1.26865800	0.08097600
O	-0.09340900	-0.04409200	2.17734000
C	-0.40328700	0.93735100	2.95796500
H	-0.02855800	0.79500900	3.99036100
O	-1.03824300	1.96374700	2.67458000
H	-0.35240500	2.98862400	-0.22127900
H	0.14814000	-3.08920500	0.34950900
O	4.69695800	-3.29356800	0.20623500
H	4.56765100	-4.24841200	0.32247700
O	4.05757000	3.93517200	-0.52691000

48
6DHBP, Esol = -1140.18405574 a.u.

Ir	0.47908600	-0.00421800	-0.27289100
C	1.38339400	0.02809900	1.64547100

C	1.90753200	1.17825400	0.91782100
C	2.56184800	0.69133800	-0.25053000
C	1.85966300	-1.17662700	0.97538800
C	2.53445800	-0.77523500	-0.21466800
C	1.69332600	-2.56112700	1.51419200
H	2.38859300	-2.68973900	2.35296000
H	0.68360000	-2.72565600	1.89828100
H	1.91574900	-3.32249200	0.76713500
C	3.19034600	-1.65964400	-1.22607100
H	4.27247900	-1.68083200	-1.04695100
H	2.81680700	-2.68307200	-1.17057700
H	3.03316500	-1.28438900	-2.24078200
C	3.24151200	1.50033300	-1.30821000
H	4.32262700	1.51229100	-1.12172000
H	3.08496300	1.06657400	-2.29954600
H	2.88760300	2.53236200	-1.31814100
C	1.80665300	2.59358600	1.38736100
H	2.52136300	2.73487000	2.20768500
H	2.04829000	3.30514000	0.59848800
H	0.81183100	2.82076800	1.77773000
C	0.70055600	0.07367700	2.97346000
H	0.05338600	-0.79412600	3.11788500
H	1.45478500	0.06872100	3.77072500
H	0.10278800	0.98119400	3.08236000
C	-2.42681400	-0.72214000	0.03016100
C	-1.20639700	-2.62859300	-0.56238600
C	-2.30849300	-3.45756300	-0.30663000
C	-3.47996200	-2.87407100	0.14259100
C	-3.55427700	-1.48535600	0.29718000
C	-2.41439600	0.75190500	0.03491300
C	-1.17304000	2.63837000	-0.57712100
C	-2.25732700	3.48508000	-0.30491000
C	-3.42818800	2.92135200	0.17043500
C	-3.52212900	1.53406800	0.32788000
H	-2.22305500	-4.52506600	-0.47715700
H	-4.34793700	-3.49001500	0.35190900
H	-4.48074500	-1.01762100	0.60270700
H	-2.15801500	4.55077200	-0.47944700
H	-4.28096700	3.55178900	0.39825100
H	-4.44727000	1.08196400	0.65943800
N	-1.23281500	1.31549700	-0.35833700
N	-1.24898600	-1.30431100	-0.34779100
O	-0.01584000	3.07968100	-1.08938400
H	-0.03327100	4.04757000	-1.17068600
O	-0.04819700	-3.08881100	-1.05557200
H	-0.08104400	-4.05571400	-1.14338600

51
6DHBP(H2O), Esol = -1216.62900916 a.u.

Ir	-0.48965900	-0.00713700	-0.21274900
C	-1.27244500	0.02553200	1.77609200
C	-1.79590300	-1.16911200	1.13044500

C	-2.54081300	-0.76295400	-0.01948700
C	-1.83114400	1.17626900	1.08248300
C	-2.56037000	0.70082800	-0.05045900
C	-1.69090300	2.59190100	1.54323800
H	-2.38155000	2.74853800	2.38130300
H	-0.68267300	2.80088000	1.90861500
H	-1.94043500	3.30696500	0.75984400
C	-3.31684800	1.52341000	-1.04617900
H	-4.37723500	1.55885400	-0.76767400
H	-2.94540100	2.54887600	-1.08842700
H	-3.25514800	1.09045000	-2.04801600
C	-3.27386500	-1.64577000	-0.98006600
H	-4.33794700	-1.67721800	-0.71561600
H	-3.20117600	-1.26592000	-2.00244600
H	-2.89159600	-2.66773200	-0.96229300
C	-1.61174500	-2.55946500	1.64949000
H	-2.28792800	-2.69899600	2.50209600
H	-1.84929900	-3.31452300	0.90069000
H	-0.59373800	-2.72583100	2.00995900
C	-0.51293100	0.06151900	3.06633000
H	0.10605300	0.95884600	3.13781000
H	-1.21039500	0.06635700	3.91320400
H	0.13314100	-0.81325300	3.17019600
C	2.39060000	0.75714700	0.15344500
C	1.16053200	2.62643500	-0.52200200
C	2.24194500	3.47872800	-0.25600700
C	3.40459100	2.92768500	0.25499700
C	3.49537100	1.54517000	0.44672500
C	2.40654400	-0.71653900	0.14866300
C	1.20004700	-2.61520300	-0.49033900
C	2.30795500	-3.44206300	-0.25236800
C	3.47411800	-2.86289900	0.21686700
C	3.53855600	-1.47831500	0.40433700
H	2.14675300	4.53967200	-0.45994600
H	4.25349000	3.56401300	0.48094300
H	4.41566500	1.09853500	0.79902300
H	2.23019800	-4.50565300	-0.44956000
H	4.34512500	-3.47858600	0.41398200
H	4.46162000	-1.00966900	0.71904300
N	1.23254200	-1.29659500	-0.24259700
N	1.21478200	1.31120000	-0.26525600
O	-0.23500400	-0.09604100	-2.49540200
H	0.59959700	-0.53957500	-2.71911000
H	-0.12307100	0.81823200	-2.80186400
O	0.04411700	-3.07535800	-0.99218800
H	0.09110400	-4.03827500	-1.11157400
O	0.01008800	3.05716200	-1.06254800
H	0.03395600	4.02239100	-1.16970400

47
6DHBP-H+,Esol = -1139.72546361 a.u.

Ir	-0.46068900	-0.02074100	-0.25759800

C	-1.41912100	0.01553900	1.63018300
C	-1.90254700	-1.17014900	0.93205600
C	-2.53825300	-0.73387900	-0.26682700
C	-1.90501100	1.18666300	0.90777600
C	-2.54133300	0.73361200	-0.27981100
C	-1.77626100	2.59235200	1.40201200
H	-2.48387500	2.73665200	2.22787700
H	-0.77518300	2.79439000	1.79089000
H	-2.00588100	3.32199200	0.62597400
C	-3.18996500	1.57034700	-1.33681100
H	-4.27546500	1.59015300	-1.17834700
H	-2.82665500	2.59911500	-1.31730200
H	-3.01226000	1.15714100	-2.33341100
C	-3.18980300	-1.58968100	-1.30554200
H	-4.27439100	-1.60572100	-1.13998700
H	-3.01755400	-1.19330900	-2.30986400
H	-2.82451600	-2.61679700	-1.26940300
C	-1.79520600	-2.56556300	1.45853300
H	-2.53502500	-2.69347000	2.25864200
H	-1.99336100	-3.31005100	0.68821000
H	-0.80978300	-2.75966100	1.88906800
C	-0.77139100	0.03173800	2.97697300
H	-0.15577900	0.92392600	3.11147500
H	-1.54532100	0.03620400	3.75521100
H	-0.14778000	-0.85201300	3.12898300
C	2.43403500	0.70466800	0.03462300
C	1.21080100	2.61392500	-0.55453800
C	2.30358500	3.44616100	-0.28449700
C	3.47285700	2.86401900	0.17980300
C	3.55202500	1.47723000	0.32690800
C	2.41927500	-0.76814000	0.02390800
C	1.10168000	-2.67917800	-0.60185100
C	2.24795100	-3.49988200	-0.30009800
C	3.42650800	-2.94101100	0.12370500
C	3.53732100	-1.54107100	0.26984400
H	2.21682600	4.51375100	-0.45380800
H	4.33408300	3.48395100	0.40570600
H	4.47333900	1.01129800	0.65057300
H	2.14382300	-4.56923300	-0.44983900
H	4.28750000	-3.57008600	0.33055500
H	4.47959400	-1.08906200	0.54989700
N	1.21789800	-1.32133500	-0.33515300
N	1.25596000	1.28700800	-0.34578700
O	0.04018400	-3.14623500	-1.09472400
O	0.05441000	3.07157700	-1.06040700
H	0.08406800	4.03926400	-1.13652700

46
6DHBP-2H+ (IV) in Figure 6,Esol = -1139.26412751 a.u.

Ir	-0.42158200	-0.00000700	-0.19041500
C	-1.60492000	-0.00059300	1.57865600
C	-1.99863900	-1.17878200	0.81963400

C	-2.49627000	-0.73359100	-0.43527200
C	-1.99863900	1.17819800	0.82050900
C	-2.49639800	0.73400800	-0.43465300
C	-1.95579400	2.57627700	1.35246100
H	-2.80319300	2.71994400	2.03442100
H	-1.04184100	2.76385000	1.92156100
H	-2.02689000	3.31895400	0.55863300
C	-3.04048300	1.57832900	-1.54251600
H	-4.13729600	1.57114700	-1.50709700
H	-2.70474900	2.61304800	-1.46309800
H	-2.74183100	1.18983500	-2.52012100
C	-3.04043400	-1.57708000	-1.54374000
H	-4.13723400	-1.57030900	-1.50795600
H	-2.74222500	-1.18759100	-2.52109100
H	-2.70429600	-2.61175400	-1.46538300
C	-1.95599000	-2.57726200	1.35054900
H	-2.80351900	-2.72137100	2.03226000
H	-2.02701500	-3.31934100	0.55616500
H	-1.04214100	-2.76535200	1.91964900
C	-1.10106500	-0.00107500	2.98659600
H	-0.49844400	0.88609400	3.19460100
H	-1.95069300	-0.00075500	3.68171900
H	-0.49933400	-0.88891300	3.19430900
C	2.45512000	0.73739500	0.06141500
C	1.14221800	2.66304500	-0.54014900
C	2.30014000	3.47428000	-0.26827200
C	3.48240300	2.90487400	0.13319700
C	3.58288600	1.50594800	0.28204700
C	2.45510300	-0.73711900	0.06158000
C	1.14264500	-2.66280000	-0.54080600
C	2.30028700	-3.47404700	-0.26777500
C	3.48224900	-2.90461800	0.13455500
C	3.58268500	-1.50566400	0.28315800
H	2.20431900	4.54291700	-0.42853100
H	4.35464100	3.52668200	0.31480500
H	4.52732800	1.04627100	0.54181500
H	2.20454200	-4.54270900	-0.42791100
H	4.35430600	-3.52643200	0.31701500
H	4.52691900	-1.04595600	0.54363200
N	1.24729300	-1.30268300	-0.26409300
N	1.24714400	1.30292700	-0.26364900
O	0.07962000	-3.13843700	-1.02336400
O	0.07872800	3.13871300	-1.02167500

49
6DHBP-2H+(H2O),Esol = -1215.70792199 a.u.

Ir	0.48844500	0.01631400	-0.24498500
C	1.11029300	0.49687800	1.73205500
C	1.89017200	1.36775000	0.85698500
C	2.65821700	0.54318600	-0.00982700
C	1.51249000	-0.87302000	1.45035900
C	2.43802200	-0.85214800	0.35605300

C	1.06525700	-2.07999600	2.21385800
H	1.75125600	-2.24546800	3.05396400
H	0.06323800	-1.94595200	2.62725000
H	1.07190300	-2.97896100	1.59472000
C	3.17428400	-2.02285400	-0.22133200
H	4.16591400	-2.11006900	0.24078900
H	2.64144100	-2.95940100	-0.04714600
H	3.32378000	-1.90993900	-1.29841800
C	3.58934900	1.00541100	-1.08626900
H	4.61416800	1.05302200	-0.69719600
H	3.59240300	0.31490000	-1.93356100
H	3.32218200	1.99983400	-1.45023900
C	1.94081200	2.86048500	0.95436100
H	2.64184400	3.13715700	1.75228000
H	2.28962200	3.31944800	0.02819000
H	0.96794400	3.28531100	1.20868100
C	0.25221400	0.95321100	2.87263400
H	-0.51361300	0.21283000	3.11571500
H	0.86512200	1.11027800	3.76887100
H	-0.24474600	1.89808400	2.63945100
C	-2.33455000	-0.78630900	0.19115400
C	-1.02227800	-2.63336800	-0.58913900
C	-2.07839900	-3.51072300	-0.19042000
C	-3.22675700	-3.00078300	0.37961100
C	-3.38955800	-1.61273400	0.54621800
C	-2.38930400	0.68830400	0.12023900
C	-1.21940300	2.58530300	-0.77339400
C	-2.37335700	3.38193100	-0.45095700
C	-3.48425400	2.81785100	0.13199700
C	-3.51812600	1.43698600	0.40883200
H	-1.95843800	-4.57173600	-0.38181400
H	-4.03167200	-3.67138600	0.66708500
H	-4.32110600	-1.20078000	0.91306200
H	-2.33891600	4.43510500	-0.70982400
H	-4.35198200	3.43192200	0.35722400
H	-4.40946400	0.96911000	0.80719500
N	-1.25232300	1.25761100	-0.38562500
N	-1.15625000	-1.30524200	-0.25886200
O	0.51153000	-0.67004300	-2.50777300
H	-0.32599400	-0.41533100	-2.92484500
H	0.38036700	-1.61456400	-2.20057100
O	-0.21374700	3.04855300	-1.38928400
O	0.01268700	-3.01080400	-1.24215600

48
6DHBP-2H+(OH),Esol = -1215.22660649 a.u.

Ir	0.47027200	-0.00765300	-0.25684200
C	1.26295500	0.10373000	1.77939700
C	1.82374700	1.20816400	1.02871700
C	2.56833900	0.68225400	-0.07428100
C	1.74472900	-1.11712900	1.16719800
C	2.52185300	-0.77526400	0.01223900

C	1.52693500	-2.48788400	1.73239000
H	2.23387900	-2.65142200	2.55560300
H	0.51952900	-2.60010600	2.14128100
H	1.68536100	-3.27065300	0.99039000
C	3.27479200	-1.71682200	-0.87947000
H	4.32418200	-1.78628700	-0.56582400
H	2.85044300	-2.72257800	-0.85180200
H	3.26669400	-1.37405200	-1.91804900
C	3.36748600	1.46487600	-1.07255000
H	4.40443200	1.57923200	-0.73137600
H	3.39645600	0.95931800	-2.04177900
H	2.95291100	2.46424800	-1.22363300
C	1.71010100	2.64694800	1.43138800
H	2.40617500	2.83751800	2.25835100
H	1.96240400	3.32338100	0.61495900
H	0.70653100	2.89152300	1.78772700
C	0.51927700	0.20590900	3.07853300
H	-0.15890400	-0.64046800	3.21689100
H	1.21476100	0.21465800	3.92817200
H	-0.07199800	1.12417600	3.12865400
C	-2.39289700	-0.71853600	0.14861400
C	-1.12725300	-2.63561700	-0.54151900
C	-2.27418800	-3.44373100	-0.23241100
C	-3.43485400	-2.87438000	0.24106500
C	-3.52098500	-1.48149900	0.41542300
C	-2.38297900	0.75885300	0.12945600
C	-1.10949100	2.64615200	-0.62495500
C	-2.24338900	3.47233100	-0.30942200
C	-3.39763700	2.92817900	0.20577500
C	-3.49330200	1.54047900	0.41462600
H	-2.19673300	-4.51048200	-0.41590200
H	-4.29894100	-3.49738100	0.45633000
H	-4.44969300	-1.01585500	0.71896100
H	-2.15705500	4.53445500	-0.51475900
H	-4.24813200	3.56606600	0.43148700
H	-4.41453600	1.09274800	0.76427300
N	-1.20676100	1.30195400	-0.30202400
N	-1.21293700	-1.28776100	-0.23270500
O	0.25298100	-0.16403500	-2.38477000
H	0.22701400	-1.12805700	-2.47165400
O	-0.06215300	3.10452800	-1.17175500
O	-0.07673900	-3.10825600	-1.07343200

51
IV-TS in Figure 6 (922.4 i cm-1),Esol = -1216.87366840 a.u.

Ir	-0.44358600	-0.12040400	-0.25775800
C	-1.06352200	-0.26172500	1.86117400
C	-1.36703800	-1.52176900	1.22425200
C	-2.29989100	-1.28352000	0.16112200
C	-1.90216700	0.74880600	1.23897200
C	-2.64082500	0.13552700	0.18459800
C	-2.03725000	2.15654900	1.73005000

H	-2.68035000	2.15801600	2.61941600
H	-1.07398600	2.57972100	2.02420700
H	-2.49292800	2.80905600	0.98476300
C	-3.68117200	0.79017400	-0.67397600
H	-4.67505600	0.65776600	-0.22796300
H	-3.50177000	1.86289600	-0.77528700
H	-3.70990100	0.34991300	-1.67403100
C	-2.97456800	-2.32356900	-0.68321200
H	-3.90596400	-2.65089500	-0.20397600
H	-3.23153200	-1.93123000	-1.67027100
H	-2.34111500	-3.20217000	-0.81885300
C	-0.83663400	-2.85036200	1.66548900
H	-1.44541500	-3.21452200	2.50257100
H	-0.87666200	-3.59227100	0.86816800
H	0.19457700	-2.77591400	2.01909400
C	-0.22042100	-0.06729300	3.08622300
H	0.20078600	0.94050600	3.12459200
H	-0.82028700	-0.20846900	3.99431600
H	0.60481900	-0.78304300	3.12076400
C	2.27015900	1.00436000	0.15070600
C	0.74029800	2.76914800	-0.34128500
C	1.73701300	3.70244900	0.07599000
C	2.96681600	3.26832300	0.51932700
C	3.25923000	1.89568900	0.53812700
C	2.48735300	-0.44647600	0.00310400
C	1.47420600	-2.46305600	-0.82435200
C	2.73580300	-3.11880900	-0.61327500
C	3.82088800	-2.43390900	-0.11846100
C	3.71671800	-1.06266100	0.17815200
H	1.49174300	4.75674600	0.00910900
H	3.72070800	3.98589300	0.82973700
H	4.23761300	1.54108300	0.83479100
H	2.79758300	-4.16894300	-0.87893900
H	4.76936400	-2.94422900	0.02493700
H	4.57924900	-0.49968300	0.51019000
N	1.38789500	-1.13735100	-0.42388000
N	1.01886100	1.42637900	-0.21278400
O	0.48031800	-3.04499700	-1.34956100
O	-0.38208200	3.16513100	-0.82514800
H	-0.83791900	2.39742800	-2.03540800
H	-0.37424000	-0.23594800	-1.96071100
O	-1.05903400	1.77977700	-2.83273300
H	-2.02807200	1.74859200	-2.88597000
H	-0.71597000	0.64107100	-2.14805200

47

V-A in Figure 6,Esol = -1139.98555173 a.u.

Ir	0.43442500	-0.02689400	-0.33910200
C	1.53147300	-0.16761800	1.71504400
C	1.84300400	1.07522900	1.08171700
C	2.47451400	0.81414600	-0.19376600
C	1.96733300	-1.22184800	0.82388900

C	2.56685200	-0.63057100	-0.33708300
C	1.96792200	-2.67856800	1.18372200
H	2.78192500	-2.87478400	1.89364100
H	1.03470900	-2.97843800	1.66856800
H	2.12315000	-3.31697800	0.31359600
C	3.30851100	-1.36076300	-1.41992400
H	4.36131400	-1.49916500	-1.14054000
H	2.88204400	-2.35041500	-1.60141000
H	3.28851500	-0.80618900	-2.36151500
C	3.16743800	1.82506900	-1.06257000
H	4.20846000	1.96164600	-0.74008900
H	3.18671200	1.50757200	-2.10860300
H	2.67770100	2.79955500	-1.01582200
C	1.63610300	2.43059900	1.69052500
H	2.52981000	2.72107100	2.25760200
H	1.45745300	3.19259500	0.93099100
H	0.79158800	2.43517500	2.38469800
C	0.97252500	-0.36596700	3.09410200
H	0.34580300	-1.26121000	3.14771300
H	1.77561000	-0.48832200	3.83361400
H	0.36586900	0.48697100	3.41036700
C	-2.44636400	-0.68203300	0.10829900
C	-1.24368300	-2.63670300	-0.57956700
C	-2.41740600	-3.40593300	-0.27354100
C	-3.56220100	-2.80221300	0.19552300
C	-3.60089800	-1.40894800	0.36964500
C	-2.39881200	0.79287000	0.10665500
C	-1.07884400	2.66908200	-0.59063400
C	-2.19366200	3.51186100	-0.26265000
C	-3.36611400	2.98390400	0.22875700
C	-3.49360700	1.59583000	0.40042100
H	-2.37184800	-4.47427900	-0.45829800
H	-4.44680900	-3.39705700	0.40722000
H	-4.51381100	-0.91357400	0.67327500
H	-2.07799900	4.57629300	-0.43956200
H	-4.20282300	3.63610200	0.46474000
H	-4.42687500	1.16259500	0.73524700
N	-1.20614100	1.31551500	-0.30740800
N	-1.28046000	-1.28240700	-0.27424500
O	-0.01753400	3.12342000	-1.11630000
O	-0.21358700	-3.15255100	-1.10869700
H	0.22944900	-0.07160300	-1.94443600

48
V-B in Figure 6,Esol = -1140.45396993 a.u.

Ir	0.44089300	-0.01224300	-0.33681200
C	1.54418400	-0.18238700	1.71687700
C	1.84284100	1.07138900	1.10787400
C	2.46226300	0.83566500	-0.18269100
C	1.98019500	-1.21950300	0.80224900
C	2.57256400	-0.60532300	-0.34906800
C	1.98044000	-2.68216500	1.13446600

H	2.78573400	-2.88576600	1.85199500
H	1.04230800	-2.99372200	1.60153500
H	2.15195400	-3.30316500	0.25495000
C	3.31983900	-1.30596500	-1.44683800
H	4.37952200	-1.41164800	-1.18030800
H	2.92342700	-2.30795700	-1.62853800
H	3.27047100	-0.74630400	-2.38409300
C	3.14936700	1.86455200	-1.03399100
H	4.19385600	1.98483100	-0.71704200
H	3.15635800	1.57292400	-2.08749500
H	2.66640300	2.84007000	-0.95609300
C	1.62806200	2.41673400	1.73379400
H	2.53395800	2.71924600	2.27441900
H	1.41389600	3.17988100	0.98459700
H	0.80576000	2.39924500	2.45357900
C	0.98542300	-0.41373200	3.09030200
H	0.34403000	-1.29956400	3.11880500
H	1.79050400	-0.57316300	3.82005800
H	0.39624400	0.44011100	3.43487100
C	-2.45732000	-0.65421500	0.10638700
C	-1.30978800	-2.59056900	-0.51281600
C	-2.43345000	-3.38647700	-0.26116000
C	-3.58530200	-2.77300700	0.20830800
C	-3.60983100	-1.38882600	0.37532200
C	-2.40077100	0.81660200	0.09967800
C	-1.07201400	2.68627700	-0.58792300
C	-2.19069700	3.53002200	-0.26703800
C	-3.36776600	3.00583300	0.21278400
C	-3.49833900	1.61664600	0.38282200
H	-2.38422500	-4.45339000	-0.45004200
H	-4.47056300	-3.36444800	0.41715400
H	-4.51766500	-0.89125500	0.69003600
H	-2.07035700	4.59440800	-0.44037100
H	-4.20544300	3.65863400	0.44195100
H	-4.43532400	1.18486000	0.70824200
N	-1.20287800	1.33279500	-0.30761200
N	-1.29640000	-1.26706500	-0.27533400
O	-0.00857500	3.14135100	-1.10294100
O	-0.17388900	-3.09312000	-1.03325700
H	-0.25559800	-4.05488500	-1.13645600
H	0.25120100	-0.04149300	-1.94304500

50

V-TSA in Figure 6 (460.4 i cm-1),Esol = -1328.55322749 a.u.

Ir	0.44878700	0.03487000	0.05115900
C	1.40220500	0.33040400	-1.97779700
C	1.89053800	-0.90327500	-1.40017200
C	2.57270500	-0.59912100	-0.17864700
C	1.81592200	1.40225200	-1.10774200
C	2.52184600	0.84584300	0.01166700
C	1.63069600	2.85913000	-1.40763000
H	2.41704200	3.18536700	-2.10017200

H	0.67015400	3.05386300	-1.89158800
H	1.69564500	3.47335000	-0.50961800
C	3.24929800	1.61044700	1.07830000
H	4.28475500	1.80791700	0.77149800
H	2.77279500	2.57231800	1.27839000
H	3.28565900	1.04920400	2.01571900
C	3.34235400	-1.56038800	0.67753200
H	4.39108700	-1.60072100	0.35545300
H	3.33186300	-1.25729900	1.72707000
H	2.93516100	-2.57190400	0.61186700
C	1.80825700	-2.23826300	-2.07783900
H	2.56296700	-2.28281700	-2.87336900
H	1.99482000	-3.06255900	-1.38939400
H	0.83244100	-2.39462200	-2.54529500
C	0.75081000	0.47375600	-3.32114600
H	0.12281500	1.36742400	-3.36885300
H	1.50559300	0.55843500	-4.11445100
H	0.12549300	-0.39186000	-3.55686400
C	-2.38874500	0.86859100	-0.24731400
C	-1.09777900	2.61185900	0.77938500
C	-2.21675300	3.48930300	0.57735900
C	-3.37485500	3.04073400	-0.01626300
C	-3.48830400	1.69816000	-0.41759200
C	-2.40867200	-0.58696400	-0.48831600
C	-1.15588700	-2.59813200	-0.11698100
C	-2.31000300	-3.33662500	-0.54904300
C	-3.46796800	-2.69280500	-0.92174800
C	-3.54267100	-1.28984400	-0.86977700
H	-2.11724200	4.51003500	0.93187700
H	-4.21437300	3.71692000	-0.15401000
H	-4.41365700	1.31803600	-0.83061200
H	-2.23853700	-4.41934700	-0.53913300
H	-4.33708100	-3.26710100	-1.23134600
H	-4.46736100	-0.77428400	-1.09410100
N	-1.22915500	-1.21523100	-0.20366800
N	-1.20662400	1.32968700	0.25933600
O	-1.19436300	-1.15383400	3.12134100
O	-0.11190200	-3.16150000	0.32922600
O	-0.05305600	2.96802700	1.40343100
C	-0.00300100	-1.11772100	3.02538800
O	1.09922500	-1.36312600	3.41804800
H	0.25465000	-0.23709500	1.69192800

51
V-TSB in Figure 6 (478.8 i cm-1),Esol = -1329.01987833 a.u.

Ir	0.45010400	0.02245700	0.03096000
C	1.40255700	0.34237900	-1.99566500
C	1.82741900	-0.92674500	-1.45985800
C	2.52018200	-0.69467500	-0.22196500
C	1.87247900	1.36874600	-1.09310800
C	2.55245200	0.74651100	0.00290700
C	1.75817200	2.83847200	-1.36297600

H	2.48254400	3.11116500	-2.14066900
H	0.76593500	3.10774300	-1.73455700
H	1.97366800	3.43755900	-0.47839400
C	3.30137300	1.43617800	1.10463200
H	4.35861900	1.55246200	0.83386000
H	2.89751700	2.43158200	1.30254900
H	3.26043000	0.86122000	2.03328100
C	3.25056600	-1.71659000	0.59713800
H	4.29687500	-1.78227300	0.27186600
H	3.25001300	-1.45422200	1.65761200
H	2.80610500	-2.70830800	0.49243200
C	1.67381000	-2.23816400	-2.16779800
H	2.45038100	-2.31746300	-2.93907200
H	1.78083400	-3.08529200	-1.49092300
H	0.70634200	-2.31601600	-2.67034400
C	0.75199700	0.56934500	-3.32717400
H	0.13873000	1.47447700	-3.32372700
H	1.50894600	0.68740900	-4.11389000
H	0.11356800	-0.27202900	-3.60946200
C	-2.42583600	0.80119400	-0.25387900
C	-1.20094200	2.59392500	0.61015300
C	-2.28787800	3.46216100	0.45903900
C	-3.45990400	2.96270200	-0.08880200
C	-3.54337300	1.61249200	-0.43022100
C	-2.41800500	-0.65830200	-0.44459100
C	-1.12535200	-2.63330900	-0.03366600
C	-2.27539300	-3.40197200	-0.42893800
C	-3.44962200	-2.79048300	-0.79887800
C	-3.54714700	-1.38672100	-0.78406500
H	-2.19460500	4.49430300	0.77891400
H	-4.31646300	3.61430000	-0.22560100
H	-4.46673500	1.19954000	-0.81457400
H	-2.18327000	-4.48247300	-0.39382900
H	-4.31333800	-3.38700100	-1.07890600
H	-4.48420800	-0.89382500	-1.00706300
N	-1.22236200	-1.25486600	-0.15851200
N	-1.24507500	1.31294900	0.20657400
O	-1.09365400	-1.01065200	3.23286000
O	-0.06851600	-3.16810000	0.41113800
O	-0.04779200	2.97618700	1.18992700
H	-0.09192800	3.91997000	1.41439400
C	0.09068800	-0.88765700	3.11216800
O	1.20974100	-0.98454300	3.52466100
H	0.26639900	-0.22865500	1.68037600

50
VI-A in Figure 6,Esol = -1328.58074070 a.u.

Ir	0.41264900	-0.07343700	-0.07080300
C	0.85489300	-0.33564100	2.01722800
C	1.64269200	0.79452900	1.56522300
C	2.53769700	0.34772200	0.54862200
C	1.35928200	-1.51298300	1.33056300

C	2.34200200	-1.09290500	0.38327700
C	0.96047100	-2.91747200	1.66372300
H	1.48361700	-3.21775700	2.58074000
H	-0.11133800	-3.00132400	1.85811900
H	1.22702000	-3.62111600	0.87573800
C	3.15016000	-1.97202200	-0.52312200
H	4.12286800	-2.20002600	-0.06891400
H	2.64231700	-2.91882600	-0.71900300
H	3.33920600	-1.48304200	-1.48249400
C	3.64771800	1.15744000	-0.05111100
H	4.50421600	1.16641700	0.63587300
H	3.98626700	0.74083100	-0.99983100
H	3.34824700	2.19433400	-0.21957600
C	1.57609500	2.16771700	2.15843800
H	2.14992700	2.17827800	3.09391300
H	1.99731500	2.92251700	1.49437000
H	0.54971100	2.45319700	2.40155100
C	-0.10833300	-0.32964000	3.16727000
H	-0.85187900	-1.12508200	3.07234300
H	0.42248200	-0.48370200	4.11553100
H	-0.63791200	0.62394400	3.23758500
C	-2.53041900	-0.46025200	0.00219800
C	-1.43122200	-2.47164400	-0.71396900
C	-2.68731400	-3.15297200	-0.55403300
C	-3.81183300	-2.48078300	-0.13362100
C	-3.75472800	-1.09970500	0.12934500
C	-2.35116800	1.00341700	0.09873000
C	-0.78454300	2.77323500	-0.32345100
C	-1.84952900	3.70582700	-0.07252300
C	-3.11482300	3.27057200	0.24652300
C	-3.39242400	1.89315200	0.31706300
H	-2.71363700	-4.20979300	-0.79909200
H	-4.75519100	-3.00965600	-0.02710300
H	-4.64607200	-0.54867400	0.39984900
H	-1.61686000	4.76154900	-0.16642100
H	-3.91086300	3.98907000	0.42278800
H	-4.39678800	1.53855800	0.50889000
N	-1.07614700	1.42964300	-0.14653300
N	-1.39353600	-1.14013000	-0.32893500
O	0.20878600	-0.01747300	-2.25471600
O	0.37156900	3.13907500	-0.68970500
O	-0.39950800	-3.03855700	-1.18083200
C	1.05782400	0.43579900	-3.10870600
H	0.69914300	0.34246600	-4.15437700
O	2.17003400	0.94139600	-2.89553800

51
VI-B in Figure 6,Esol = -1329.06052983 a.u.

Ir	0.40850700	-0.18127500	-0.08712500
C	0.86223100	-0.48403800	1.99779000
C	1.76495600	0.54886500	1.51931800
C	2.56265300	0.00413800	0.47040900

C	1.20215800	-1.71219500	1.29868900
C	2.20355900	-1.40567500	0.32537700
C	0.64955600	-3.06197600	1.63211100
H	1.18950400	-3.45029300	2.50504900
H	-0.40896200	-3.01216200	1.89735100
H	0.77212800	-3.77096600	0.81398600
C	2.86665700	-2.36484900	-0.61444400
H	3.81379100	-2.71815100	-0.18810500
H	2.23739600	-3.23572000	-0.80793600
H	3.09450500	-1.88613600	-1.57088400
C	3.69571900	0.67652900	-0.24302700
H	4.64257400	0.42869500	0.25340700
H	3.77228100	0.34374500	-1.28049900
H	3.59042600	1.76300400	-0.23735500
C	1.87758600	1.91722200	2.11455500
H	2.44898000	1.84274900	3.04839400
H	2.39887500	2.61103900	1.45516600
H	0.89945100	2.33497900	2.36455100
C	-0.05620100	-0.36588600	3.17706000
H	-0.88656300	-1.07289500	3.10864100
H	0.48674600	-0.57953900	4.10651300
H	-0.47005200	0.64223800	3.25915700
C	-2.56637900	-0.20570900	-0.01787700
C	-1.72211600	-2.31850100	-0.78142800
C	-3.05915900	-2.83649700	-0.64936100
C	-4.09348700	-2.03862600	-0.22275600
C	-3.86269500	-0.68289000	0.08160300
C	-2.20848500	1.21341000	0.15537200
C	-0.50898300	2.79558500	-0.20630500
C	-1.36692100	3.84078800	0.17375800
C	-2.65942400	3.53585800	0.56399600
C	-3.10076500	2.20923200	0.53296400
H	-3.21536800	-3.87630300	-0.91708500
H	-5.09795000	-2.44389300	-0.13751900
H	-4.67933000	-0.03025300	0.36131900
H	-0.99753600	4.85852300	0.13338900
H	-3.33836100	4.32689000	0.86529300
H	-4.12166200	1.96305900	0.79450200
N	-0.90656800	1.50710300	-0.15047400
N	-1.52047500	-1.00875300	-0.37474500
O	0.42588500	-0.19094900	-2.30459500
O	0.72312200	3.08989600	-0.61774600
O	-0.76526900	-3.00566700	-1.24037100
C	1.06535000	0.67313900	-2.99237000
H	1.12965300	0.43996800	-4.06973200
O	1.60558900	1.72789700	-2.58684700
H	1.08424500	2.39422300	-1.26859200

12. References

1. *APEX2*, Version 2009/9 (Bruker AXS Inc.).
2. *SADABS*, Version 2008/1 (Sheldrick, Bruker AXS Inc.).
3. *XS*, Version 2008/1 (George M. Sheldrick, Acta Cryst. 2008, A64, 112).
4. *XL*, Version 2008/4 (George M. Sheldrick, Acta Cryst. 2008, A64, 112).
5. Becke, A. D., *J. Chem. Phys.* **1993**, *98*, 5648-5652.
6. Marenich, A. V.; Cramer, C. J.; Truhlar, D. G., *J. Phys. Chem. B* **2009**, *113*, 6378-6396.
7. Andre, D.; Haussermann, U.; Dolg, M.; Stoll, H.; Preuss, H., *Theoretica. Chemica. Acta.* **1990**, *77*, 123-141.
8. Hehre, W. J.; Rodam, L.; Schleyer, P. V. R.; Pople, J. A., *Ab Initio Molecular Orbital Theory*. Wiley: New York: 1986.
9. Frisch, M. J.; Trucks, G. W.; Schlegel, H. B.; Scuseria, G. E.; Robb, M. A.; Cheeseman, J. R.; G. Scalmani; Barone, V.; Mennucci, B.; Petersson, G. A.; Nakatsuji, H.; Caricato, M.; Li, X.; Hratchian, H. P.; Izmaylov, A. F.; Bloino, J.; Zheng, G.; Sonnenberg, J. L.; Hada, M.; Ehara, M.; Toyota, K.; Fukuda, R.; Hasegawa, J.; Ishida, M.; Nakajima, T.; Honda, Y.; Kitao, O.; Nakai, H.; Vreven, T.; J. A. Montgomery, J.; Peralta, J. E.; Ogliaro, F.; Bearpark, M.; Heyd, J. J.; Brothers, E.; Kudin, K. N.; Staroverov, V. N.; Kobayashi, R.; Normand, J.; Raghavachari, K.; Rendell, A.; Burant, J. C.; Iyengar, S. S.; Tomasi, J.; Cossi, M.; Rega, N.; Millam, J. M.; Klene, M.; Knox, J. E.; Cross, J. B.; Bakken, V.; Adamo, C.; Jaramillo, J.; Gomperts, R.; Stratmann, R. E.; Yazyev, O.; Austin, A. J.; Cammi, R.; Pomelli, C.; Ochterski, J. W.; Martin, R. L.; Morokuma, K.; Zakrzewski, V. G.; Voth, G. A.; Salvador, P.; Dannenberg, J. J.; Dapprich, S.; Daniels, A. D.; Farkas, Ö.; Foresman, J. B.; Ortiz, J. V.; Cioslowski, J.; Fox, D. J. *Gaussian 09*, C. 01; Gaussian, Inc., Wallingford CT: 2009.
10. Cramer, C. J., *Essentials of Computational Chemistry: Theories and Models; 2nd ed.* wiley & Sons: Chichester: 2004.
11. Wang, W.-H.; Muckerman, J. T.; Fujita, E.; Himeda, Y., *ACS Catal.* **2013**, 856-860.
12. Michael D.Tissandier; Cowen, K. A.; Feng, W. Y.; Gundlach, E.; Cohen, M. H.; Earhart, A. D.; Coe, J. V., *J. Phys. Chem. A* **1998**, *102*, 7787-7794.
13. Camaioni, D. M.; Schwerdtfeger, C. A., *J. Phys. Chem. A* **2005**, *109*, 10795-10797.
14. Kelly, C. P.; Cramer, C. J.; Truhlar, D. G., *J. Phys. Chem. B* **2006**, *110*, 16066-16081.
15. Bryantsev, V. S.; Diallo, M. S.; III, W. A. G., *J. Phys. Chem. B* **2008**, *2008*, 9709-9719.
16. Scalmani, G.; Frisch, M. J.; Mennucci, B.; Tomasi, J.; Cammi, R.; Barone, V., *J. Chem. Phys.* **2006**, *124*, 094107.